A THESIS

entitled

A MULTINUCLEAR MAGNETIC RESONANCE STUDY OF VANADIUM(V) COMPLEXES AND EQUILIBRIA

by

Aidan Timothy Harrison, B.Sc.(Hons.)

Submitted to the University of Warwick in fulfilment of the requirements for the award of the degree of Doctor of Philosophy.

Department of Chemistry

March 1986

TABLE OF CONTENTS

LIST OF FIGURES

LIST OF TABLES

DECLARATION

To the best of my knowledge, the work described in this thesis is original. Parts of this work have been published in the scientific literature, with the following references:

A. T. Harrison and O. W. Howarth
"High-Field Vanadium-51 and Oxygen-17 Nuclear Magnetic Resonance Study of Peroxovanadates(V)"
J. Chem. Soc., Dalton Trans., 1985, 1173

A. T. Harrison and O. W. Howarth
"Oxygen Exchange and Protonation of Polyanions: A Multinuclear Magnetic Resonance Study of Tetradecavanadophosphate (9-) and Decavanadate (6-)"
J. Chem. Soc., Dalton Trans., 1985, 1953

ACKNOWLEDGEMENTS

I wish to express my gratitude to my supervisor, Dr. O. W. Howarth, for his encouragement and guidance during the course of this project.

Throughout the research towards this thesis, I received encouragement and support from my friends, especially, Dr. E. H. Curzon, Dr. D. P. Leworthy (Shell Research Ltd., Sittingbourne), Colin Moore and Tony Parker. All their efforts are gratefully recognised.

I thank Dr. P. Moore for the use of his non-linear regression analysis program.

I, also, acknowledge the use of the facilities in the Department of Chemistry, the help of the Electrical, Glassblowing and Mechanical Workshops, and a Science and Engineering Research Council maintenance award.

ABSTRACT

The use of high-field n.m.r. spectroscopy to study the aqueous chemistry of vanadium(V) has yielded information not only about the species present but, also, a qualitative understanding of the ^{17}O n.m.r. chemical shifts in polyanions. The peroxo and sulphido complexes of vanadium(V) are reported as well as the interaction of vanadate with ADP and ATP, and oxygen exchange in the polyanion tetradecavanadophosphate(9-) ($[PV_{14}O_{42}]^{9-}$).

In general, peroxovanadate complexes tend to contain two peroxide ligands per vanadium, although some mono-, tri- and tetraperoxovanadates are found. The mono- and diperoxovanadates undergo a change in co-ordination from octahedral to tetrahedral on removal of their final proton ($\sim$ pH 14). Four new dimeric species have been observed, three of which are unsymmetrical.

The pH-dependent differential rates of oxygen exchange of tetradecavanadophosphate(9-) can be explained in terms of the stabilisation of the anion by the two pentaco-ordinate VO caps with respect to the "equator" of the Keggin type structure. The four half-hemisphere units resist exchange. Bulk distortions of this anion and decavanadate(6-) can be deduced from the observation of their ^{17}O chemical shifts with pH.

The three known sulphido and oxosulphido-vanadium(V) species $[VS_4]^{3-}$, $[VOS_3]^{3-}$ and $[VO_2S_2]^{3-}$ have been identified by high-field vanadium-51 n.m.r., together with the previously unobserved ions $[VO_3S]^{3-}$, $[V_2S_7]^{4-}$, $[O_3VSVO_3]^{4-}$, $[SO_2VSVO_2S]^{4-}$ and the protonated monomers. No equilibria between monomeric species are observed other than for protonation.

Vanadate complexes with the polyphosphate chain in both ATP and ADP, probably as $[VO_2]^+$ bridging two adjacent phosphates. Exchange with species containing $[VO_3]^-$ bound to the terminal phosphate and, in ATP only, "$[VO]^{3+}$" bound to all the phosphates may occur.

SYMBOLS AND ABBREVIATIONS

Physical

Å	Angstrom
B_0	magnetic field strength
δ_X	n.m.r. chemical shift of nucleus X
$\Delta\nu_{\frac{1}{2}}$	width of a peak at half-height
e.m.f.	electromotive force
e.s.r.	electron spin resonance spectroscopy
e.g.	*exempli gratis* (for instance)
et al.	*et alii* (and others)
F.I.D.	free induction decay
HOMO	highest occupied molecular orbital
Hz	units of frequency
i.r.	infra-red spectroscopy
i.e.	*id est* (that is)
J	coupling constant
LUMO	lowest unoccupied molecular orbital
n.m.r.	nuclear magnetic resonance spectroscopy
pKa	acid dissociation constant
pKc	formation constant
p.p.m.	parts per million
rf.	radiofrequency
T_1	spin-lattice relaxation time
u.v./vis	ultra-violet/visible spectroscopy

Chemical

acac	acetylactonate
ADP	adenosine 5'-diphosphate
AMP	adenosine 5'-monophosphate
ATP	adenosine 5'-triphosphate
bipy	bipyridyl
Co^n	Cobalt in the n^{th} oxidation state
Cr^n	Chromium in the n^{th} oxidation state

DSS	2,2-dimethyl-2-silapentane-5-sulphonate
$[edta]^{4-}$ or $[H_2edta]^{2-}$	ethylenediamine tetraacetate
en	ethylenediamine
nta	nitrilotriacetate
(OO)	complexed peroxide
ox	oxalate
pda	2,6-pyridinediacetate
phen	1,10-phenanthroline
PPP_i	inorganic tripolyphosphate
(*Pn*)	peroxovanadate species n
PV_{14}	tetradecavanadophosphate(9-) ($[PV_{14}O_{42}]^{9-}$)
SB	Schiff's base
(*Sn*)	sulphidovanadate species n
Ti^n	titanium in the n^{th} oxidation state
TSS	3(trimethylsilyl)-1-propane sulphonic acid
V^n	vanadium in the n^{th} oxidation state
V_{10} or HV_{10} or H_2V_{10}	decavanadate(6-) and its protonated forms

To my parents

To know non-knowledge
is the highest good.
Not to know what knowledge is
is a kind of suffering.
Only if one suffers from this suffering
does one become free of suffering.
If the Man of Calling does not suffer
it is because he suffers from this suffering:
therefore he does not suffer.

Tao Te Ching, Chapter 71
Lao Tzu

1. INTRODUCTION

1.1 AIMS

The aim of this project was to investigate the aqueous chemistry of vanadium in its highest oxidation state of +5. Information about the complexes formed, their equilibria and co-ordination sphere was sought as little is known about these. In addition an insight into the factors affecting vanadium-51 and oxygen-17 n.m.r. chemical shifts is expected. Together with other transition metals vanadium exhibits variable valence, i.e., it shows a range of oxidation states (from -1 to +5 for V). Those in the first row ranging from Ti to Mn (including V) are of greater interest in their higher oxidation states because of the uses and range of compounds.[1] The chemistry of vanadium(V) [V^V] is described here. That of its other oxidation states can be found in references 1-3.

1.2 VANADIUM(V) CHEMISTRY

1.2.1 Complexes with only Oxo Ligands

1.2.1.1 Oxo Species

A number of oxovanadium(V) salts are known. Their anions can be summarised as metavanadate $[VO_3]^-$, orthovanadate $[VO_4]^{3-}$, pyrovanadate $[V_2O_7]^{4-}$, cyclic

tetramer $[V_4O_{12}]^{4-}$ and decavanadate(6-) $[V_{10}O_{28}]^{6-}$ (V_{10}). In addition, vanadium(V) oxide $[V_2O_5]$ has been characterised. Perhaps the most studied of these is the V_{10} anion. Crystal structures[4-8] have shown it to be composed of 6 octahedra in a planar 3 x 2 edge sharing arrangement with 4 "capping" V-O units (Fig. 1.1).

As would be expected for an early transition metal in its highest oxidation state V^V forms various oxo species in aqueous solution. Early attempts[10-13] to elucidate the structures and equilibria identified monomeric, dimeric and V_{10} anions, and gave some evidence of intermediate polymeric species. Complexes of nominal formulae were $[VO_4]^{3-}$, $[HVO_4]^{2-}$, $[H_2VO_4]^{-}$, $[V_2O_7]^{4-}$, $[V_{10}O_{28}]^{6-}$, $[HV_{10}O_{28}]^{5-}$ and $[H_2V_{10}O_{28}]^{4-}$ with $[HV_2O_7]^{3-}$, $[V_3O_9]^{3-}$, $[V_4O_{12}]^{4-}$ and $[VO_2]^{+}$ postulated.

Firstly, the low pH region. Between pH 2 and 6.5 only the V_{10} isopolyanion is present in solution[14]. Below pH 2 the cation $[VO_2]^{+}$ is formed on breakdown of V_{10}. Protonation of V_{10} has been studied in this pH range by ^{51}V and ^{17}O n.m.r. spectroscopy. Howarth and Jarrold[14] found pKa's of 5.5 and 3.6 and suggested terminal oxygens O_f and O_g to be the most likely sites of protonation, although Klemperer and Shum[15] favoured bridging sites O_c and O_b. Evans and Pope[8] suggest O_c from empirical bond length/bond order calculations to find valence deficient O atoms from the crystal structure of HV_{10}. The exact sites of protonation have yet to be resolved.

Fig. 1.1 Structure of V_{10}, $[V_{10}O_{28}]^{6-}$.
From ^{17}O $\{^{51}V\}$ n.m.r. experiments[9]
$\delta_V(V_{(1)}) < \delta_V(V_{(2)}) < \delta_V(V_{(3)})$

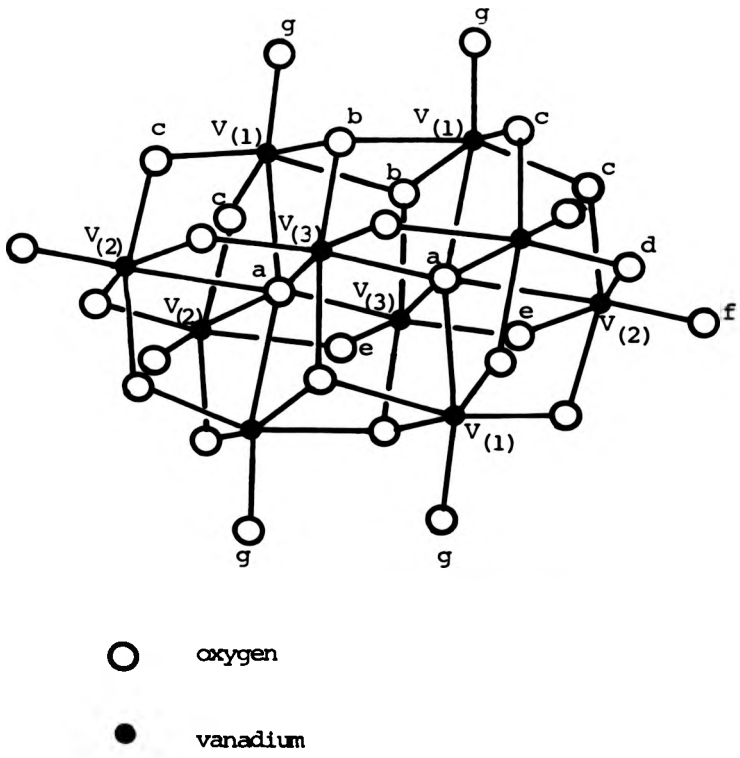

Oxygen exchange[15,16] between those in V_{10} and solvent water has been found to occur at a single rate. An intermediate model of a cyclic V_4 unit bonded to a V_6 unit via an oxygen bridge formed by partial dissociation of V_{10} accounts for this observation. Dissociation of the V_{10} anion has been studied in both acid[17] (forming $[VO_2]^+$) and basic[18,19] solution (giving various isopolyvanadates) revealing it to be dependent on pH and solution composition. Reduction of V_{10} has been reported with 6 species claimed to be formed with retained structure; $[V_8{}^{V}V_2{}^{IV}O_{28}]^{8-}$, $[V_7{}^{V}V_3{}^{IV}O_{28}]^{9-}$, $[V_6{}^{V}V_4{}^{IV}O_{28}]^{10-}$, $[V_5{}^{V}V_5{}^{IV}O_{28}]^{11-}$, $[V_4{}^{V}V_6{}^{IV}O_{28}]^{12-}$ and $[V_3{}^{V}V_7{}^{IV}O_{28}]^{13-}$. The complexes of $V^V:V^{IV}$ in ratios of 7:3 and 3:7 predominate. However, the redox chemistry of polyvanadates has not been as extensively studied as the molybdenum and tungsten isopoly and heteropoly complexes (including V as a heterometallate)[21,22].

Under extreme acid conditions[23] (concentrated perchloric and sulphuric acid media) a cationic dimer is found with the proposed formula $[V_2O_3]^{4+}$ (or $[V_2O_4]^{2+}$). This has been studied by spectroscopy, large angle x-ray scattering and cyclic voltammetry. The x-ray data indicated the complex to have a non-linear oxygen bridge and a V-V distance of 3.25 Å.

A general trend of increasing size of polymeric species is observed with decreasing pH, ending with the formation of V_{10} at pH 7. At high pH the major

species is monomer, with small amounts of dimer present. On decreasing the pH various polymers are formed, however until recently the composition of the species in solution was the subject of conflicting views[12]. Even the major polymeric species of notional formula $[VO_3]_n^{n-}$ had not been unambiguously defined with some suggesting n to be 3 and others 4. Two studies[24,25] based on ^{51}V and ^{17}O n.m.r. spectroscopy measurements concluded that n = 3 and/or 4[24] and that n = 4,[25] with various other polymeric species present. Heath and Howarth[25] employed ^{51}V n.m.r. at 105.2 MHz in their investigation rather than at 23.66 MHz as used by Habayeb and Hileman[24] giving better resolution and sensitivity. A resonance due to $[V_4O_{12}]^{4-}$ was assigned after unambiguous preparation[24], but not for $[V_3O_9]^{3-}$. Evidence for the existence of $[V_4O_{12}]^{4-}$ rather than $[V_3O_9]^{3-}$ presented by Heath and Howarth[25] is based on a better standard deviation to the equilibrium constant (eqn. 1.1), between the tetramer and monomer (log K = -10.004 ± 0.074) than the monomer and trimer (log K = -9.865 ± 0.099).

$$n[H_2VO_4]^- \rightleftharpoons [V_nO_{3n}]^{n-} + nH_2O \qquad 1.1$$

In addition, formation of the next higher oligomeric species gives a better fit for the tetramer → pentamer (log K = -0.015 ± 0.029) rather than trimer → tetramer (log K = -0.061 ± 0.035). If both $[V_4O_{12}]^{4-}$ and $[V_3O_9]^{3-}$ were present with coincident resonances badly fitting equilibrium constants would be measured.

Other polymeric species were assigned using similar techniques. Also 2 groups[26,27] have observed the species $[H_3VO_4]$ using e.m.f. measurements.

A summary of the various vanadate species found in aqueous solution is shown in Table 1.1, together with their n.m.r. data, and formation and acid dissociation constants.

The aqueous chemistry[1] of the oxo species of titanium, chromium and manganese in their highest oxidation states shows some speciation. $[TiO]^{2+}$, $[TiO(OH)]^{+}$, $[Ti(OH)_2]^{2+}$ and $[Ti(OH)_3]^{+}$ cations have been observed together with $[Ti(OH)_3(HSO_4)]$ and $[Ti(OH)_2(HSO_4)]^{+}$ in sulphuric acid, and colloidal TiO_2 at higher pH. Various protonated Cr^{VI} species of $[CrO_4]^{2-}$ have been shown to exist. Above pH 6 $[CrO_4]^{2-}$ is formed, between 2 and 6, $[HCrO_4]^{-}$ and below pH 1, $[H_2CrO_4]$. Of these $[HCrO_4]^{-}$ is in equilibrium with the dichromate anion $[Cr_2O_7]^{2-}$. Derivatives of tri-, $[Cr_3O_{10}]^{2-}$, and tetrachromates, $[Cr_4O_{13}]^{3-}$ are known and have been shown to contain corner-sharing CrO_4 tetrahedra. Only two monomeric manganese(VII) oxide species are found in aqueous solution, the $[MnO_4]^{-}$ and $[MnO_3]^{+}$ ions. The latter is formed by reaction of small amounts of $KMnO_4$ with concentrated H_2SO_4. Further addition of $KMnO_4$ forms the explosive dimer Mn_2O_7.

Various other vanadate species have been claimed to be formed, but have received little

TABLE 1.1 REPORTED AQUEOUS VANADATE SPECIES AND THEIR N.M.R. CHEMICAL SHIFTS

#	Species	δ_V/p.p.m.	$\Delta\nu_{\frac{1}{2}}$(V)/Hz	δ_O/p.p.m.	$\lvert {}^1J_{VO}\rvert$ Hz	K or pKa	Ref
1	$[VO_4]^{3-}$	-541.2	< 5	+565	62.6		25
2	$[HVO_4]^{2-}$	-538.8	100	+573	34	pKa ≈ 12	25
3	$[H_2VO_4]^-$	-560.4	200			pKa = 7.1	25
4	$[H_3VO_4]$	Observed from e.m.f. measurements					26,27
5	$[VO_2]^+$	-545					38
6	$[V_2O_7]^{4-}$	-561.0	130	+405(br), +695(t)	31(t)	$\log_{10}('6'/2^2)^* = 1.39$	25
7	$[HV_2O_7]^{3-}$	-563.5	180			pKa = 8.9	25
8	$[H_2V_2O_7]^{2-}$	-572.7	150			pKa = 7.2	25
9	$[V_2O_3]^+$	-640	5000				23
10	$[V_3O_{10}]^{5-}$	-556.3,-590.4	< 400,350	+438(br),+721(t),+852		$\log_{10}('10'/2^3.H)^*$	25
11	$[HV_3O_{10}]^{4-}$?	ca. -570				pKa = 8.9	25
12	$[V_4O_{13}]^{6-}$	-569.1,ca.-585				$\log_{10}$ $('12'/15.H^2)^* = 16.5$	25
13	$[HV_4O_{13}]^{5-}$	-560 to -590				pKa ≈ 9	25
14	$[H_2V_4O_{13}]^{4-}$?	-597,-605	< 300				25
15	$[V_4O_{12}]^{4-}$	-577.6	130	+472(br),+928(t)		$\log_{10}$ $('15'/2^4.H^4)^* = 40.01$	25
16	$[V_5O_{16}]^{7-}$?	-570					25
17	$[V_5O_{15}]^{5-}$	-586.0	150	+472(br),+928(t)		$\log_{10}$ $('17'^4/'15'^5)^* = 0.14$	25
18	$[V_6O_{18}]^{6-}$	-589.4	150			$\log_{10}$ $('18'^5/'17'^6)^* \approx -7$	25
19	$[V_{10}O_{28}]^{6-}$)						
20	$[HV_{10}O_{28}]^{5-}$)	3 resonances		6 resonances			
21	$[H_2V_{10}O_{28}]^{4-}$)	between		between			14,15
22	$[H_3V_{10}O_{28}]^{3-}$)	-420 and -530		0 and 1200			

*The numbers in parentheses represent concentrations of species as numbered in column 1, and H = $[H^+]$.

attention. A mixed valence[28] $[V_8^{V}V_2^{IV}O_{26}]^{4-}$ complex has been prepared and characterised using spectroscopic methods. The crystal structure[29] has shown it to consist of a planar cyclic structure containing 8 corner sharing V^{V} tetrahedra with the two pentaco-ordinate V^{IV} tetragonal pyramids sited above and below the plane. A range of large polymeric compounds have been prepared[30] by rapid quenching and slow cooling of melts containing mixtures of M_2CO_3 and $[NH_4]VO_3$ or V_2O_5; for instance $K_2V_8O_{21}$, $K_3V_5O_{14}$, $K_{32}V_{18}O_{61}$ and $K_2V_{12}O_{30}$. X-ray scattering and i.r. spectroscopy have been used in the analysis of these melts.

1.2.1.2 Oxoperoxo Species

Note: Peroxide ligands are written as (OO) for visual clarity.

A number of halooxoperoxovanadium(V) and other heteroligand complexes have been prepared and characterised. These will be described later.

Many transition metal compounds in their higher oxidation states are known for their ability to catalyse the epoxidation of olefins by hydrogen peroxide. Molybdenum, titanium, niobium and vanadium are of particular importance. The intermediates in these reactions are metal peroxide species formed by the interaction of H_2O_2 and ROOH with the transition metal species. These reactions have been recently reviewed[31], and the role of peroxovanadates in catalytic oxidation processes described[32].

Several species are formed on complexation of H_2O_2 with Ti^{IV} and Cr^{VI}[33]. For instance, Ti forms[34] $[Ti(OO)(OH)aq]^+$ below pH 1. On increasing the pH higher polymers are produced until a hydrated peroxo complex is precipitated. The only stable oxoperoxochromate(VI) is $[Cr(O)(OO)_2]$, decomposition of this species[34] was studied and $[Cr_2(OO)]^{4+}$ and $[Cr_3(OO)_2]^{5+}$ were later identified as intermediates in the reduction of Cr^{VI} to Cr^{III}. This would indicate that aqueous peroxide can complex with vanadate species to form a variety of complexes.

Connor and Ebsworth[35] reviewed the chemistry of peroxovanadates in 1965, and the species reported can be summarised as $[VO(OO)]^+$, $[VO(OO)_2]^-$, $[HVO(OO)_3]^{2-}$, $[VO(OO)_3]^{3-}$, $[HVO_2(OO)_2]^{2-}$, $[V(OO)_4]^{3-}$ and the dimeric species $[H\{VO(OO)_2\}_2O]^{3-}$, mainly based on the work of Chauveau[36,37] using spectrophotometry and cryoscopy. In 1979, Howarth and Hunt[38] examined the aqueous complexation of peroxovanadates using ^{51}V n.m.r. spectroscopy. The species that they observed are those described in the review[35] plus $[HVO_3(OO)]^{2-}$, $[VO_3(OO)]^{3-}$, $[H_2VO_2(OO)_2]^-$ and a dimer assigned $[\{V(OH_2)(OO)_2\}_2O]$. Table 1.2 contains all these species, their ^{51}V n.m.r. data and pKa's.

Generally, V^V prefers to complex with two peroxide ligands, however under appropriate conditions the mono-, tri- and tetraperoxo complexes are produced.

TABLE 1.2 PEROXOVANADATES ALREADY KNOWN[38]
(See Table 1.1 for Vanadate Data)

Peroxo ligand per V	1	2	3	4
Formula[a]		$[VO_2(OO)_2]^{3-}$?	$[VO(OO)_3]^{3-}$	$[V(OO)_4]^{3-}$
δ_V[b]		-760	-845	-734
Width/Hz[c]		250	380	480
Colour		Yellow	yellow?	purple
Formula[a]	$[HVO_2(OO)]^{2-}$	$[HVO_2(OO)_2]^{2-}$	$[HVO(OO)_3]^{2-}$	
δ_V[b]	-622.8	-765.6	-733.2	
Width/Hz[c]	85	240	160	
Colour	Colourless or yellow	yellow	yellow	
pKa[d]	v.large	>14	ca. 13	
Formula[a]		$[H\{VO(OO)_2\}O]^{3-}$		
δ_V[b]		-757		
Width/Hz[c]		650		
Colour		yellow?		
pKa[d]		6.8		
Formula[a]	$[H_2VO_2(OO)]^-$?	$[H_2VO_2(OO)_2]^-$		
δ_V[b]	-621	-696		
Width/Hz[c]		260		
Colour		yellow		
pKa[d]	<7.7	7.9		
Formula[a]		$[\{V(OH_2)(OO)_2\}_2O]$?		
δ_V[b]		-650		
Width/Hz[c]		700		
Colour		red/brown		
Formula[a]	$[VO(OO)]^+$			
δ_V[b]	-543			
Width/Hz[c]	340			
Colour	red/brown			

[a] May omit coordinated water. Query indicates tentative identification.

[b] Downfield from internal $VOCl_3$ capillary.

[c] At half-height.

[d] Approximate value (for loss of one proton) based on n.m.r. integrals.

Howarth and Hunt's investigations showed that at approximately neutral pH in the presence of two equivalents of H_2O_2 the diperoxo dimer $[H\{VO(OO)_2\}_2O]^{3-}$ and the diperoxo monomer (with the mono- and diprotonated species in equilibrium) are formed together with a small amount of the triperoxo species. As the pH is lowered slightly, the second protonation of the diperoxo monomer $[HVO_2(OO)_2]^{2-}$ is completed and the dimer is disfavoured. Further addition of acid forms a dimer with speculative formula[38] $[\{V(OH_2)(OO)_2\}_2O]$ and then $[VO(OO)]^+$ cation. Lowering the peroxide concentration allows the formation of the appropriate amount of vanadate species. No other peroxovanadate species are formed by varying the peroxide concentration. On increasing the pH in the presence of 2 equivalents of H_2O_2, the species $[HVO_2(OO)_2]^{2-}$ is favoured, the diperoxo dimer remains until pH 9 and some mono- and triperoxo species are formed. Deprotonation of the diperoxo species is found at high pH. Increase or decrease in the H_2O_2 concentration favours the formation of species with higher or lower V:(OO) ratios respectively and the formation of the appropriate vanadate species in the latter case.

Information concerning the coordination sphere of V in these aqueous complexes has not been reported. Asymmetrical dimers should logically be present, however these could be in such small proportions to be undetected as yet.

Data concerning the protonation/deprotonation

of the monoperoxo species are somewhat speculative. Howarth and Hunt[38] suggested $[H_2VO_3(OO)]^-$ is formed from $[HVO_3(OO)]^{2-}$ on lowering the pH to 8 on the evidence of a very small change (1.8 p.p.m.) in the ^{51}V chemical shift (*cf.* the chemical shift difference between $[HVO_4]^{2-}$ and $[H_2VO_4]^-$ is 21.6 p.p.m., and that for the second protonation of the diperoxo monomer is 69.6 p.p.m.). Also they found no evidence of $[VO_3(OO)]^{3-}$, but proposed a disproportionation reaction giving $[VO_4]^{3-}$ and $[VO_2(OO)_2]^{3-}$.

Of the peroxovanadates mentioned above, the diperoxo dimer $[H\{VO(OO)_2\}_2O]^{3-}$ has been extensively studied. The unprotonated form of this anion has been examined crystallographically[39,40], by i.r. spectroscopy[41,42,43] (together with the protonated form) and by thermal decomposition[44]. The x-ray and i.r. data indicate an oxo (or hydroxy) bridge, with a postulated[39,40] peroxide O-V weak bridging bond. Information concerning the co-ordination polyhedron of these peroxovanadates has been gained using i.r. spectroscopy in the 660-490 cm^{-1} region ($V-O_{peroxide}$ stretching). Thermal decomposition leads to formation of $K[VO_3]$ and $K_3[VO(OO)_2CO_3]$ from $K_4[V_2O_3(OO)_4].2H_2O$ and $K_3[HV_2O_3(OO)_4].H_2O$ in the presence of atmospheric CO_2. However, according to the preparative method given[40], the unprotonated dimer is precipitated at approximately pH 9, whilst Howarth and Hunt[38] found no evidence for this species at this pH in their solution study.

Work on the monoperoxo species, $[VO(OO)]^{+}$, has been limited to studies of its formation[45] ($K = 3.7 \pm 0.4 \times 10^{4}$ dm^{3} mol^{-1} for the equilibrium between H_2O_2 with $[VO_2]^{+}$ and $[VO(OO)]^{+}$), its interconversion with the diperoxo anion $[H_2VO_2(OO)_2]^{-}$[45,46,47] ($K = 0.6 \pm 0.1$ mol dm^{-3}), and its oxidation[48,49] to the radical cation $[VO(OO)]^{2+\cdot}$ by HSO_5^{-}, Co^{3+} and $S_2O_8^{2-}$, which decomposes to form VO_2^{+} and O_2.

1.2.2 Complexes Containing Phosphorus

1.2.2.1 Tetradecavanadophosphate$^{(9-)}$ $[PV_{14}]$

A wide range of isopoly and heteropolyanions with molybdenum, tungsten and mixed vanadium/tungsten/molybdenum metallates and with silicon, germanium, phosphorus and arsenic heteroatoms have been prepared[50,51]. The importance of the heteropolyanions can be seen by their applications. Gravimetric or colourimetric analysis for molybdenum can be undertaken by the formation of $[XMo_{12}O_{40}]^{n-}$ (where X = P, As, Si or Ge). Complexes with $[PMo_{12}O_{40}]^{3-}$ and $[SiMo_{12}O_{40}]^{4-}$ form the basis of the determination of elements such as Ti, Zr, Hf, Th, Nb, Ce and Sb. The biochemist can use "phosphotungstic acids" for the precipitation of proteins or as a non-specific electron stain for electron microscopy. They have also been used as catalysts for oxidation, reduction, epoxidation, polymerisation and hydrosulphurisation. Other applications include ion-exchange materials, thin-

layer chromatography and ion-selective membranes. Because of the importance of this large range of compounds, those comprising solely of vanadium (as the metallate) are discussed separately.

Various polyanions containing V^V and phosphorus have been postulated[52]. Recently[53,54], these have been shown to be due to only one, the PV_{14} polyanion (the arsenic analogue is also described). X-ray crystallography[53] has shown that both anions comprise an α-Keggin structure with two "$[VO]^{3+}$" capping units of penta-coordinate vanadium (although the arsenic analogue is highly distorted). Kato *et al.*[53] suggested that the presence of the caps is to decrease the overall charge of the anion. Fig. 1.2 shows the structure of PV_{14} and Fig. 1.3 a polyhedral model of the anion. Limited n.m.r. data for this anion is available. ^{51}V and ^{31}P n.m.r.[53] of a mixture of the reactants and the product anion shows the chemical shifts to be pH dependent, but resonances from the reactants overlap those from the product hindering observation. An oxygen-17 n.m.r. spectrum[54] (pH undisclosed) shows the large chemical shift range typically found for these types of species[15,55] and their dependence on co-ordination number[56], bond length[57] and π bond order[58] that have already been found. Fedotov, *et al.*[54] assigned the ^{17}O n.m.r. spectrum of PV_{14} by the relative intensities of the peaks, and used the inverse correlation between ^{17}O n.m.r. chemical shift

Fig. 1.2 Structure of the PV_{14} anion[53], $[PV_{14}O_{42}]^{9-}$.

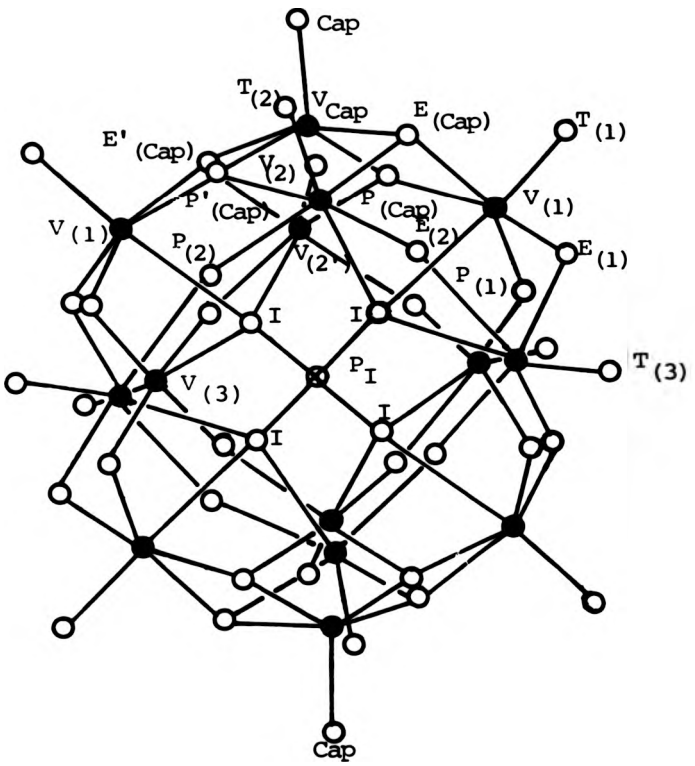

Fig. 1.3 Polyhedral model of PV_{14}.

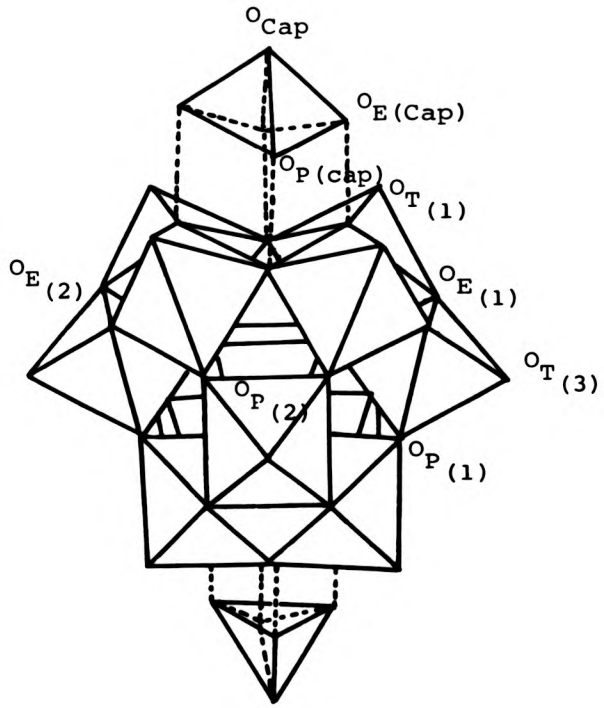

and V-O bond length for those of equal areas. No evaluations of its redox or catalytic behaviour have been reported.

1.2.2.2 Phosphate and Polyphosphate Species

Firstly, complexes of V^V with orthophosphate. These generally have a V:P ratio of 1:1. Compounds with the formula $VOPO_4$ have been synthesised[59,60], eg, α_I-$VOPO_4$, α_{II}-$VOPO_4$, β-$VOPO_4$ and $VOPO_4.2H_2O$. A crystal structure[59] of the latter shows it to exist as infinite sheets of VO_6 octahedra and PO_4 tetrahedra linked by shared oxygen atoms, with water of crystallisation interlinking the sheets. The other $VOPO_4$ structures are based on a layered construction, formed by reaction of vanadate with approximately 3 mol dm^{-3} H_3PO_4.

In addition, 2 V^V-phosphate complexes have been studied spectrophotometrically[61] at low pH and found to contain species with V:P ratios of 2:1 and 1:3. These have been suggested to be $[H(PO_2(VO_3)_2)]$ and $[H(V(HPO_4)_3)]$ respectively.

Examination of the interactions of vanadate with polyphosphate have been concentrated on those with tripolyphosphate (PPPi). Spectrophotometric studies[62] in the pH range 0-4 indicated 3 complexes are formed; $[VO_2(H_2PPPi)]^{2-}$, $[VO_2(HPPPi)]^{3-}$ and $[VO_2(HPPPi)_2]^{7-}$ having stability constants $(3.95 \pm 1.09) \times 10^4$ dm^3 mol^{-1}, $(1.34 \pm 0.49) \times 10^8$ dm^3 mol^{-1} and $(8.05 \pm 1.13) \times 10^{12}$ dm^6 mol^{-2} respectively. At slightly higher pH[63] (in the range 2-8) the V^V (PPPi) species prepared by oxidation of the V^{IV}(PPPi) species

has been shown to have tetrahedral V from the characteristic u.v. absorbance at 255 nm. This leads to 3 possible species, (i) with $[VO]^{3+}$ bound to all 3 phosphates, (ii) $[VO_2]^{+}$ bound to 2 adjacent phosphates, and (iii) $[VO_3]^{-}$ bound to 1 phosphate (Fig. 1.4). Since then[64] three complexes have been suggested ($[VO(PPPi)]^{2-}$, $[(VO)_2(PPPi)]^{3-}$ and $[VO(PPPi)_2]^{7-}$) in the study of (PPPi) hydrolysis in the presence of vanadate by u.v./vis monitoring of phosphomolybdenum blue complexes. Data from this study indicated that hydrolysis of (PPPi)[64] occurs when the vanadate species is bound only to the terminal phosphate group (structure (iii), Fig. 1.4), then ligated $[OH]^{-}$ or $[H_2O]$ can attack this phosphorus atom creating pentaco-ordinate phosphorus intermediates. Structure (i) (Fig. 1.4) is inferred to be the most inert complex from the data in the study, with the formula $[VO(PPPi)]^{2-}$.

1.2.2.3 ATP and ADP

The interactions of metal ions with nucleoside di- and triphosphates has been extensively studied[65-69] with regard to strength, structure of coordination and effects on phosphate reactivity. The role of V in biological systems has been recently reviewed[70] and includes a report of the presence of vanadate in natural ATP. Measurement of rates of hydrolysis of ATP by vanadate species have been undertaken[63,64] and some information concerning the intermediate species gained[64]. A 1:1 V:ATP complex ($K_f \approx 18$ dm^3 mol^{-1}) is

has been shown to have tetrahedral V from the characteristic u.v. absorbance at 255 nm. This leads to 3 possible species, (i) with $[VO]^{3+}$ bound to all 3 phosphates, (ii) $[VO_2]^{+}$ bound to 2 adjacent phosphates, and (iii) $[VO_3]^{-}$ bound to 1 phosphate (Fig. 1.4). Since then[64] three complexes have been suggested ($[VO(PPPi)]^{2-}$, $[(VO)_2(PPPi)]^{3-}$ and $[VO(PPPi)_2]^{7-}$) in the study of (PPPi) hydrolysis in the presence of vanadate by u.v./vis monitoring of phosphomolybdenum blue complexes. Data from this study indicated that hydrolysis of (PPPi)[64] occurs when the vanadate species is bound only to the terminal phosphate group (structure (iii), Fig. 1.4), then ligated $[OH]^{-}$ or $[H_2O]$ can attack this phosphorus atom creating pentaco-ordinate phosphorus intermediates. Structure (i) (Fig. 1.4) is inferred to be the most inert complex from the data in the study, with the formula $[VO(PPPi)]^{2-}$.

1.2.2.3 ATP and ADP

The interactions of metal ions with nucleoside di- and triphosphates has been extensively studied[65-69] with regard to strength, structure of coordination and effects on phosphate reactivity. The role of V in biological systems has been recently reviewed[70] and includes a report of the presence of vanadate in natural ATP. Measurement of rates of hydrolysis of ATP by vanadate species have been undertaken[63,64] and some information concerning the intermediate species gained[64]. A 1:1 V:ATP complex ($K_f \approx 18$ dm^3 mol^{-1}) is

Fig. 1.4 A diagramatic representation of the three possible vanadate complexes with PPPi: (i) with "$[VO]^{3+}$" bound to all three phosphates, (ii) $[VO_2]^+$ bound to two adjacent phosphates and (iii) $[VO_3]^-$ bound to one phosphate.

(i)

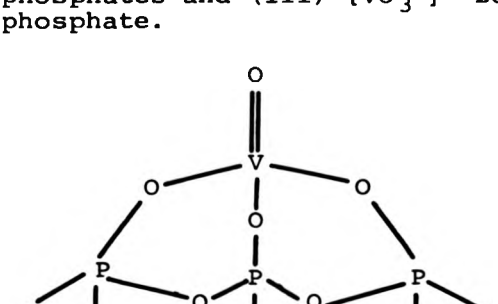

(ii)

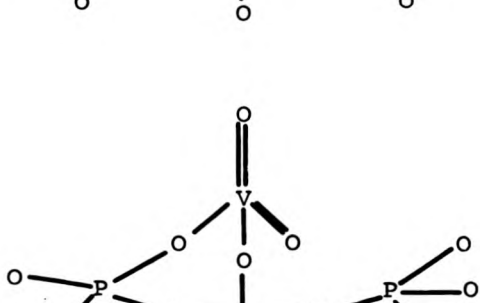

(iii)

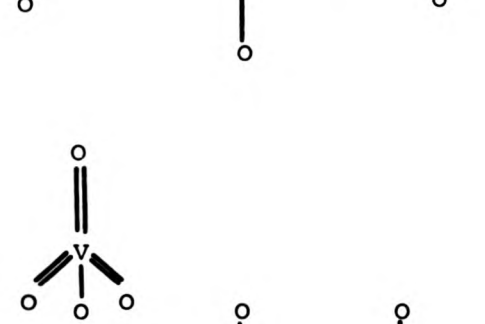

involved in the hydrolysis of ATP to ADP by vanadate species, $[VO_2]^+$ produced by pH jump from "$[VO_4]^{3-}$". The rate constants for the hydrolysis of (PPPi), ATP and ADP are similar ($k_{obs} \approx 10^5\ s^{-1}$) suggesting corresponding mechanisms, possibly when vanadate is bound to the terminal phosphate only (Section 1.2.2.2).

1.2.3 V^V Sulphur, Selenium and Tellurium Complexes

A recent review[71] of the thiometallates of transition metals in their highest oxidation states reported only three V^V sulphide complexes ($[VS_4]^{3-}$, $[VOS_3]^{3-}$ and $[VO_2S_2]^{3-}$) and their selenium analogues. All of these can be prepared either by reaction of the elements or by the reaction of H_2S (or H_2Se) with aqueous vanadate species.

Very little is known of the selenium and tellurium complexes. The u.v./vis spectra of all the selenium containing anions have been measured[72,73]. The thallium and copper salts of $[VSe_4]^{3-}$ have been prepared[74,75] and the i.r. spectrum obtained[76]. The only tellurium complex known is $Cu_3[VTe_4]$[75]. These all show a tetrahedral configuration of ligands around the central vanadium. Solid state ^{51}V n.m.r.[76] spectra of $Cu_3[VSe_4]$ (1710 p.p.m.), $Cu_3[VTe_4]$ (3880 p.p.m.) and $Tl_3[VSe_4]$ (2570 p.p.m.) have been obtained and are the highest ^{51}V chemical shifts reported for V^V complexes.

However, the three V^V sulphide complexes

have received slightly more attention. The crystal structures of the copper[77], potassium[78] and ammonium[79] salts and the i.r. spectrum[74] of $[VS_4]^{3-}$ show the anion to have a tetrahedral configuration about vanadium. U.v./vis spectra[80-83] have been measured for the sulphide and oxosulphide complexes in solution. There are no reported data on solution equilibria. As for the monosulphide species of notional formula $[VO_3S]^{3-}$ no direct evidence for its existence has appeared in the literature. Ranade, *et al.*[80] have postulated its electronic spectrum and suggested that it may be formed by reaction of solid Na_3VO_4 with solid Na_2S on addition of a few drops of methanol. The only polymeric V^V sulphide reported[84] is non-crystalline V_2S_5, which is prepared from the thermal decomposition of $[NH_4]_3[VS_4]$.

Similar monomeric molybdenum and tungsten sulphide species are known[71,85], as well as a number of polymeric species[85].

1.2.4 V^V Species with Oxo, Peroxo and Halogen Ligands

1.2.4.1 Halo Oxo Complexes

The bromo and chloro compounds $VOBr_3$, VO_2Cl and $VOCl_3$ have been prepared[86]. Anionic complexes[87,88] $VOCl_4^-$ and $VO_2Cl_2^-$ have been studied using ^{51}V n.m.r. and showed a decrease of metal shielding with increasing number of chloro ligands; $[VO_2Cl_2]^-(\delta_V = -359$ p.p.m.) > $VOCl_3$ ($\delta_V = 0$ p.p.m.) > $[VOCl_4]^-$ ($\delta_V = +45$ p.p.m.).

Mixed chlorofluorovanadate anions[87] have been characterised by both ^{51}V and ^{19}F n.m.r. Their $^{1}J_{V-F}$ coupling constants have been recorded, and range from 20-100 Hz.

In addition, reactions of $VOCl_3$ have been reported. Schiff base complexes[89] have been synthesised by reaction of $VOCl_3$ with various azomethanes. Complexes containing one or two bases have been prepared with formulae $[(VOCl_2)(SB)]$ and $[(VOCl)(SB)_2]$, where SB = Schiff's base. On characterisation by i.r., ^{1}H n.m.r. and u.v. spectroscopy, together with magnetic susceptibility measurements, distorted trigonal bipyramidal and octahedral geometries are proposed respectively. Reactions of $VOCl_3$ with alcohols[90,91], amines[92], acids[93] and $(NSCl)_3$[88] have also been undertaken. Stepwise replacement of the chlorine by alcohols and amines give a number of tetrahedral species of general formulae $[VOCl_{3-n}(O-R)_n]$ and $[VOCl_{3-n}(N-R')_n]$, together with mixed alkoxide and amino compounds. The tris carboxylate complex $[VO(OOCR)_3]$ (formed by reaction of $VOCl_3$ with either the acid or silver carboxylate) is heptaco-ordinate with the formation of bonds to each carboxylate oxygen. Hydrolysis of this compound yields a polymeric material $[VO_2(OOCR)]_n$. Various cyclic thiazene complexes of V^V have been prepared; $[VCl_2(N_3S_2)]_\infty$ and $[VCl_2(N_3S_2).NSCl]_2$ together with $(AsPh_4)_2[VCl_3(N_3S_2)]_2$. In each case octahedral co-ordination is found, from

i.r. data for the first two and x-ray crystallography for the latter.

Some alkoxohalide, aminohalide and alkoxo-amine species have been used in the study of ^{51}V shielding[94]. Linear progressions exist between the ^{51}V chemical shift and substituent parameters such as electronegativity, Pearson's hardness parameter, and Taft's electronic and steric constants.

The oxytrifluoro complex (VOF_3) has been prepared and its crystal structure[95] determined to consist of chains of VOF_5 octahedra with 2 cis bridging fluorides. The hexa fluoride, $[VF_6]^-$, and tetrafluoride, $[VOF_4]^-$, anions have been made[96] and characterised. ^{51}V n.m.r. data of the reaction product of V_2O_5 and 48% HF has been interpreted as being the species $[VOF_4]^-$. The crystal structure[98] of the caesium salt showed the anion to have a tetragonal pyramid structure with the oxygen at the apex. Recently, the structure of this ion in solution was suggested[99,100] from the ^{51}V and ^{19}F n.m.r. spectra, and the e.s.r. of the reduced species to be that of $[VO_2F_4]^{3-}$ which has been independently synthesised. It has also been proposed that $[VO_2F_4]^{3-}$ is formed by the hydrolysis of $[VOF_4]^-$, and $[VOF_4]^-$ exists only in aqueous free environments[100]. Other oxy fluoro complexes that are known[101] are $A_3VO_2F_4$ (A = Na, K), $A_2VO_2F_3$ (A = K, Rb, Cs), $A_3V_2O_4F_5$ (A = Rb, Cs) and $A_2A'VO_2F_4$ (A = K, Rb, Cs; A' = Na, K, Rb) all of

which contain cis oxygens, and the polymer, fluorine bridges. The crystal structure[102] of $K_2VO_2F_3$ shows chains of $[VO_2F_4]$ octahedra with cis oxygens in the same plane as the two cis bridging fluorine ligands.

1.2.4.2 Halo Oxoperoxo Complexes

Most of the species reported are fluoro complexes. However, two chloro anions[103] have been synthesised by reacting V_2O_5, the alkali chloride and H_2O_2 in the appropriate concentration to form $A_2[VO(O_2)_2Cl]$ and $A_2[V(O_2)_3Cl]$ (where A = Na, K, $[NH_4]^+$). These have been characterised by elemental analysis, magnetic susceptibility measurements and i.r. spectroscopy. The reversible conversion of $[VO(O_2)_2Cl]^{2-}$ to $[V(O_2)_3Cl]^{2-}$, shown in this study, provides evidence for the relative ease of diperoxy-triperoxy interconversion.

As for the fluoro complexes, studies of the $[VO(O_2)_2F]^{2-}$ anion predominate. Crystal structures of the potassium[104], caesium[105] and ammonium[106] salts show a pentagonal pyramid configuration about the vanadium with apical oxygen (assuming peroxide to be bidentate). A distorted pentagonal bipyramid is found in the ammonium salt due to interaction of V with the apical oxygen in a neighbouring anion. The thermal decomposition[107,108] of the potassium salt has been examined until KVO_3 and KF are formed, with decomposition starting at 423 K for loss of peroxide oxygen. Isothermal decomposition studies[107]

showed the activation energy for the first (OO) loss to be 108 kJ mol^{-1} and 53 kJ mol^{-1} for the second. The potassium and ammonium salts[109] can be formed from mixtures of MVO_3-(MF,HF)-H_2O_2-H_2O together with the dimeric products $M_3[HV_2O_2(OO)_3F_4].2H_2O$ and $(NH_4)_3[V_2O_2(OO)_4F].nH_2O$ ($n \approx 2$). Raman and i.r. spectra show these anions contain V-[μ(OO)]-V[109,110] and V-F-V[109] bridges respectively. Oxo and fluoro bridges have been repeatedly observed in polymeric V^V complexes, but $M_3[HV_2O_2(OO)_3F_4].2H_2O$ contains the only reported peroxide bridge. The polymeric material $K_6[V_4O_4(OO)_6F_6]$ has been identified (by vibrational spectroscopy and x-ray analysis) as an intermediate in the thermal decomposition[111] of the dimer $K_3[HV_2O_2(OO)_3F_4].2H_2O$ and is the largest V^V polymer containing peroxide ligands.

The crystal structure[112] of $(NH_4)_3[VO(OO)_2F_2]$ shows the ligands form a pentagonal bipyramid around V with the two (OO) ligands in the same plane as an F, and O and the other F occupying the apical sites. A fluoro triperoxo species $A_2[V(OO)_3F]$ (where A = Na, K and $[NH_4]^+$) has been synthesised and characterised[113] in a similar manner to the analogous chloro compound[103], although in the solid state it may be polymeric with weak fluorine bridges.

1.2.5 Mixed Ligand Complexes

1.2.5.1 Complexes without Oxo Ligands

(p-Tolyl imido) vanadium(V) trichloride has been prepared[114] and characterised by ^{51}V n.m.r. giving a resonance at δ_V = +305 p.p.m. Gradual substitution of the chloride ligands by potassium t-butoxide, under mild conditions, gives a range of haloimidoalkoxide complexes. Analogous compounds[115], t-butylimino vanadium(V) trichloride and tribromide have been prepared and characterised by n.m.r. spectroscopy. These undergo the same substitution reactions.

1.2.5.2 Complexes with Oxygen Bound to V

V^V alkoxides have already been described (Sections 1.2.4.1 and 1.2.5.1). Characterisation[116] of the mono-, di- and triisopropoxide and tri(t-butoxide) complexes have been undertaken using i.r., Raman, ^1H and ^{13}C n.m.r. spectroscopy. In the case of the tri(t-butoxide) complex rotamers are observed. Alkoxide complexes can be used to prepare various amino V^V monomeric[117] species (e.g. $[VO(OR)_2[NR'(SiMe_3)]]$ and $[VO(OR)[NR'(SiMe_3)]_2]$) and imino V^V compounds (e.g. $[R'N=V(OSiMe_3)_3]$, $[R'N=V(OSiMe_3)_2(OR)]$ and $[R'N=V(OR)_2Cl]$) by reaction with $LiNR'(SiMe_3)$ and $HNR'(SiMe_3)$ respectively.

V^V xanthate and thioxanthate derivatives have been made from calcium alkylxanthate and sodium metavanadate using a two phase system of water and dichloromethane between 0 and 5°C (water at pH 5-6).

A number of complexes of V^V with polydentate ligands have been prepared; e.g. with adamantyl hydroxamic acid[119], 2-pyrilideniminobenzohydroxamic acid[120] (used for V^V determination spectrophotometrically), an N,N'-ethylene-bis(salicylidene iminato) V^V complex[121] (which contains a three coordinate Cu in the CuCl salt), tetraphenylporphine[91] and dipicolinato V^V complexes[122]. All of these species contain penta- or hexaco-ordinate V centres. The tetraphenylporphine derivative does not have the V in the centre of the porphine ring, but has two $VOCl_3$ units bonded to nitrogen diagonally opposite each other on the porphine ring. The protonated dipicolinato complex[122] forms a polymer with μ-hydro bridges, which could be di-, tri- or tetrameric.

$K[CH_3PVO_5].H_2O$ has been shown[123] to consist of polyhedral corner sharing V-O- and CH_3-P-O- chains. The V polyhedron is a distorted trigonal bipyramidal structure with two terminal oxygen atoms.

1.2.5.3 Complexes Containing Peroxide

The formation[124] of the Na, K, and $[NH_4]^+$ salts of $M[VO(OO)_2L].nH_2O$ (where L = (bipy) and (phen); and $2 \leq n \leq 6$) and $M_3[VO(OO)_2(ox)].2H_2O$, under the appropriate conditions, have been reported and studied by i.r. spectroscopy and molar conductance measurements which indicated the presence of 1:1 and 1:3 electrolytes respectively. Dimeric species $M'[V_2O_2(OO)_4L_2].6H_2O$ (where M' = (H_2bipy) and (H_2phen); and L = (bipy) and (phen) respectively) were, also, found in the presence

of large excesses of bidentate nitrogen ligands. Crystal structures of $K_3[VO(OO)_2(ox)].H_2O_2$[125], $(NH_4)[VO(OO)_2(bipy)].4H_2O$[125,126] and $(C_{10}H_9N_2)[VO(OO)_2(bipy)].(3 + x)H_2O_2.(2 - x)H_2O$ (where x = 0.4)[127] indicated that all contain a pentagonal bipyramidal anion (assuming peroxide to be bidentate) with both peroxide ligands in the same plane and the oxo ligand in the apical site.

Novel compounds[128] with the formula $[VO(OO)(O\text{-}N)LL']$, where O-N can be pyridine-2-carboxylate and pyrazine-2-carboxylate; and LL' are H_2O, MeOH, mono- or bidentate ligands, have been synthesised. These have been studied by i.r. spectroscopy and x-ray crystallography showing them to have a pentagonal bipyramid structure, with hydrogen bonding between the peroxide and equatorial water ligands. The catalytic ability to oxidise olefins to epoxides, alkanes to alcohols and ketanes, and aromatic hydrocarbons to phenols of these compounds were noted.

Dipicolinato[122], nitrilotriacetate (nta)[129,130], 2,6-pyridenedicarboxylic acid[130,131] (pda), iminodiacetic acid[132] and dipicolinato alkyl[133] peroxide complexes have been prepared, all of which have structures based on the pentagonal bipyramid. Mechanisms[129,130] of formation of the (nta) and (pda) complexes have been investigated. Rate constants have been calculated for the reactions via proposed associative mechanisms. In addition, the catalytic behaviour of the dipicolinato alkyl peroxide complexes is similar to that of the pyridine-2-carboxylate and pyrazine-2-carboxylate[128] complexes mentioned earlier.

In this section of mixed ligand complexes, the central V^V has been shown to prefer to be penta- or heptaco-ordinate, forming mainly pentagonal bipyramidal structures in peroxide complexes, with some tetrahedra in alkoxo, amino or alkoxo amino complexes. To date those species mentioned in this section have been prepared and characterised by various methods, with little further investigation except for some formation and catalytic behavioural studies.

1.2.6 Redox Reactions of V^V

V^V is well known as an oxidising agent. The ability for catalytic oxidation by V^V peroxide complexes has been discussed earlier (Sections 1.2.1.2 and 1.2.5.3). Vanadate redox chemistry has, also, been described (Sections 1.2.1.1 and 1.2.2.1). Two other examples of this type of chemistry will be briefly examined here.

Reaction of vanadate species with $[Co(NH_3)_5L]^{2+}$ complexes[134] (where L = α-hydroxy acids, e.g. mandelic, lactic or glycolic acids) have both one and two equivalent V^V-induced electron transfer pathways, forming V^{IV}, Co^{II} and a carbonyl compound. Both mechanisms are of equal importance, with each forming a 1:1 V^V-Co^{III} complex intermediate that can be monitored spectrophotometrically but only the slow 1 equivalent pathway forms a second intermediate which is a radical cation.

The kinetics of oxidation of phenylphosphinic acid[135] by vanadate species has been investigated and

shown to occur via an acid-independent pathway (considered to be due to the reaction of VO_2^+ and $C_6H_5P:(OH)_2$ the active form of phenylphosphinic acid which is in equilibrium with the inactive form in aqueous acidic solution), and an acid-dependent pathway (between $V(OH)_3^{2+}$ and $C_6H_5P(O)(OH)H$, the inactive form). Both pathways form phenylphosphonic acid and V^{IV} as products.

The sections above have shown the range and uses of V^V complexes, and similarities to other transition metals in their highest oxidation states. The aqueous equilibria of isopoly vanadate species (together with various mixed ligand complexes prepared by specific methods) have been extensively studied. However, the sulphido species has received little attention by comparison. In this study, it was proposed to examine the peroxo species by both ^{51}V and ^{17}O n.m.r. to resolve the anomalies mentioned in Section 1.2.1.2; the sulphido species in solution; the polyanions V_{10} and PV_{14} by ^{17}O n.m.r. for further information about these species, especially the reason for changes in ^{17}O chemical shifts with pH, and the complexation of vanadate with ATP and ADP in phosphate hydrolysis which has yet to be determined.

2. MATERIALS AND METHODS

2.1 METHODS OF INVESTIGATION

Recently, various methods of investigating isopoly and heteropolyanions in solution have been compared[136], with n.m.r. seemingly the most utilised. In this section a summary of the methods previously used to study vanadate and peroxovanadate equilibria is given.

Some of these methods are of limited value in the study of equilibria in solution, but are more important for solutions containing a single polyanion. Methods of determining molecular weight (e.g., salt cryoscopy, diffusion coefficient measurements and ultracentrifugation) can be classed as such, although some have been used to study vanadate equilibria. Thus, Jander and Jahr[137] preferred the cyclic tetramer for the major vanadate species between pH 7 and 9 (Section 1.2.1.1) from their diffusion coefficient measurements. Also, Naumann and Hallada[138] agreed with the earlier findings[137] using the same technique, and Chauveau[36,37] used salt cryoscopy (in conjunction with spectrophotometry) in her examination of peroxovanadate equilibria, and her findings were the major source of information concerning these species until 1979 when Howarth and Hunt[38] published their study (Section 1.2.1.2). In addition, no information

about the protonation sites in these polyanions has been gained from these non-n.m.r. methods, apart from the suggestion of O_c in V_{10} by Evans and Pope[8] from X-ray data.

Further success in studying the vanadate equilibria was attained using potentiometric titration[26,139,140,141] (which has, also, been used to study isopolyniobate[142] and isopolymolybdate[143] equilibria), and spectroscopy[144,145,146] (in particular n.m.r. spectroscopy[10,24,25,26,38]). Potentiometric titrations require the precise measurement of the hydrogen ion concentration (via e.m.f.) as a function of added acid (or base) and total metal ion concentration. The data is then analysed to find values for p,q and $\beta_{(p,q)}$ (Eqn. 2.1).

$$pH^+ + qMo_4^{n-} \rightleftharpoons [(H^+)_p(Mo_4)_q] \qquad (2.1)$$

$\beta_{(p,q)}$ = formation const

The "correctness" of the postulated equilibria is then determined by statistical analysis, and by comparison with data from other methods if available.

Direct observation of the metal and its associated oxo ligands is possible via n.m.r. spectroscopy, with a wide variety of metals already used, e.g. ^{51}V, ^{93}Nb, ^{95}Mo, ^{181}Ta and ^{183}W. Spectral

interpretation and identification of equilibria relies on metal-ion concentration-dependence, effect of pH changes, unambiguous preparation and peak integral ratios. Statistical analysis of the data determines the "correctness" of the postulated equilibria in an analogous manner to that used for the potentiometric titration data.

As can be seen n.m.r. spectroscopy was a major analytical tool in the elucidation of vanadate equilibria. In the present project this technique was used to study complexation of vanadate with hydrogen peroxide, hydrogen sulphide and polyphosphate derivatives in addition to examining the V_{10} and PV_{14} polyanions. By observing different nuclei (^{51}V, ^{17}O, ^{31}P, ^{1}H and ^{13}C) information about the complexation, equilibria, protonation sites and coordination spheres of the metallates could be gained.

2.2 N.M.R. SPECTROSCOPY

Detailed n.m.r. theory will not be presented here as this can easily be found elsewhere[147,148,149]. A brief discussion of various factors affecting the use of n.m.r. in this study will provide an insight into particular problems.

2.2.1 Quadrupolar Effects

The presence of a nuclear electric quadrupole

moment can cause the rapid relaxation of the nucleus under observation, with signal broadening in excess of that caused by inhomogeneities in B_0. All nuclei of spin ≥ 1 have electric quadrupole moments. In this study most of the data obtained are from observation of quadrupolar nuclei.

Electric multipole moments arise from non-spherical charge distribution resulting in orientation-dependent energies. A body with an electric dipole moment is aligned by an electric field ($E = -\frac{dV}{dz}$); however, one with an electric quadrupole moment interacts with the gradient of an inhomogeneous electric field

$$(E = -\frac{d^2V}{dz^2}).$$

This is quantified by the quadrupole moment of the nucleus, Q, with units of m^2. The sign of Q depends on the distribution of the positive charge which can be either in a cigar-shape (+ve) or a discus-shape (-ve) around the symmetry axis.

The electric field in a molecule or ion arises from the nuclei and electrons. A value of zero is necessarily found at the equilibrium position of each nucleus. If a nucleus is not in a highly symmetrical position (sites of tetrahedral, octahedral, cubic or spherical symmetry, e.g. $[NH_4]^+$, $[VO_4]^{3-}$) there is, however, a finite electric field gradient. In solution rapid isotropic molecular tumbling will tend to average the quadrupolar energy so the

quadrupolar fine structure found in solid state experiments is not observed. Consequently, a single absorption is usually detected (ignoring scalar couplings). This averaging can be sufficiently effective to give a sharp resonance, hence line widths can range from a few Hz to tens of KHz when observing quadrupolar nuclei.

Alternatively, this effect can be considered as causing relaxation. The direction of the electric field gradient affects the quadrupolar interaction and is fixed in the molecular framework. So when the molecule tumbles at the appropriate rate (approx. the transition frequency) the quadrupolar energy is modulated and spin-lattice relaxation induced. Hence, this relaxation mechanism depends on electrical interactions rather than magnetic ones.

In the case of ^{51}V n.m.r. a wide variation of linewidths at half height ($\Delta\nu_{\frac{1}{2}}$) have been observed ranging from < 5 Hz for $[VO_4]^{3-}$[25] to 1 KHz for the $[VO_2]^+$ complex with $[H_2edta]^{2-}$[38]. Broad resonances allow the undetectable overlap of peaks, whilst a shoulder would probably be observed for the narrower ones. Generally for vanadates[25] $\Delta\nu_{\frac{1}{2}}$ is approximately 100-200 Hz and slightly larger for peroxovanadates[38], 150-300 Hz. As for ^{17}O n.m.r. the linewidths are expected to be larger due to lower symmetry, however, the large chemical shift dispersion should allow

information to be gained by observing this nucleus.

2.2.2 Referencing

Reference compounds should give a sharp single line spectrum, provide an intense signal when only a small amount is present, be in the area of the spectrum away from other signals and be chemically inert. The reference for ^{51}V n.m.r., $VOCl_3$, satisfies all these criteria apart from the last as it hydrolyses in the presence of atmospheric moisture. However, it can be used when inside a sealed capillary tube and placed concentrically in the n.m.r. tube. The effect of moisture requires that both H_3PO_4 and $P(OCH_3)_3$ be used in sealed capillary tubes.

Due to the extensive use of capillary references the effect of their employment is described. Heath and Howarth[25] noted that there is a difference of approximately -1 p.p.m. between the neat and capillary $VOCl_3$ references when observing ^{51}V n.m.r. due to different magnetic susceptibilities. This is mainly attributed to the change in shielding of the bulk diamagnetism of the sample with and without the capillary. It also depends on the shape and orientation of the container, namely the capillary. The local magnetic field, H, acting on the molecules can be related to the external field, H_{mag}, Eqn. 2.2 for a capillary.

$$H = H_{mag} \left(1-\frac{2\pi}{3}\chi_v\right) \qquad (2.2)$$

χ_v = bulk susceptibility

The true chemical shift differs from the apparent observed one by $\frac{2\pi}{3}\chi_v$, given by Eqn. 2.3.

$$\sigma - \sigma_{obs} = \frac{2\pi}{3}\chi_v \qquad (2.3)$$

Therefore, a slight shift is expected when using capillary references.

2.2.3 Even Excitation Over Large Sweepwidths[150]

As has been stated earlier (Sections 1.2.1.1 and 2.2.1) a large chemical shift dispersion has been observed for ^{17}O n.m.r. spectra of polyoxoanions. In addition, initial work[151] on the sulphide complexes shows a ^{51}V chemical shift range of +1500 to -600 p.p.m. For quantitative data all resonances must be stimulated equally or alternatively a large range of frequencies must be evenly excited at the same time.

As the pulse length, at radiofrequency ν, approaches infinity the signal becomes pure sinusoidal at this frequency and gives an infinitely narrow contribution at ν on Fourier transformation. If the pulse length is shortened although the source is monochromatic the frequency spectrum is no longer thus allowing excitation over a range of frequencies. This

$$H = H_{mag} \left(1-\frac{2\pi}{3}\chi_v\right) \qquad (2.2)$$

χ_v = bulk susceptibility

The true chemical shift differs from the apparent observed one by $\frac{2\pi}{3}\chi_v$, given by Eqn. 2.3.

$$\sigma - \sigma_{obs} = \frac{2\pi}{3}\chi_v \qquad (2.3)$$

Therefore, a slight shift is expected when using capillary references.

2.2.3 Even Excitation Over Large Sweepwidths[150]

As has been stated earlier (Sections 1.2.1.1 and 2.2.1) a large chemical shift dispersion has been observed for ^{17}O n.m.r. spectra of polyoxoanions. In addition, initial work[151] on the sulphide complexes shows a ^{51}V chemical shift range of +1500 to -600 p.p.m. For quantitative data all resonances must be stimulated equally or alternatively a large range of frequencies must be evenly excited at the same time.

As the pulse length, at radiofrequency ν, approaches infinity the signal becomes pure sinusoidal at this frequency and gives an infinitely narrow contribution at ν on Fourier transformation. If the pulse length is shortened although the source is monochromatic the frequency spectrum is no longer thus allowing excitation over a range of frequencies. This

is due to many different frequencies that have to be combined in order to form the rising and falling edges of the rectangular pulse. Hence, to stimulate all resonances equally a pulse much shorter than that giving a 90^{o} flip angle is applied. To cover the frequency range required to observe the sulphide complexes a series of three overlapping spectra were acquired.

2.3 THE SPECTROMETERS AND THEIR USE

Most n.m.r. data in this study have been obtained using a Bruker WH400 n.m.r. spectrometer. However, some ^{31}P data and initial ^{51}V data were acquired using a Bruker WH90 spectrometer. Details of both spectrometers are given here, but the mode of operation of the WH90 is not included as it is analogous to the WH400.

2.3.1 The Spectrometers

2.3.1.1 Bruker WH400 N.M.R. Spectrometer

This spectrometer is equipped with a 9.4 T Oxford Instruments superconducting magnet, operating at 400 MHz for ^{1}H n.m.r. (Table 2.1 gives the frequency data and standards for the various nuclei used in this study). The instrument has quadrature detection and a ^{2}H field/frequency lock. In addition to the pretuned 400 MHz probehead for ^{1}H n.m.r., a range of

TABLE 2.1 Resonance frequencies and standards used in this study

Nucleus	Standard	Freq. at B_0 = 9.4 T[a] /MHz	Freq. at B_0 = 2.1 T[b] /MHz
^{1}H	TSS	400.0	90.0
^{13}C	TSS	100.5	22.6
^{51}V	$VOCl_3$	105.2	22.6[c]
^{17}O	Solvent Water	54.2	-
^{31}P	H_3PO_4 or $P(OCH_3)_3$	162.0	36.4

[a] Bruker WH400

[b] Bruker WH90

[c] Using the ^{13}C probehead and reducing the magnetic field proportionately

TSS = 3(trimethylsilyl)-1-propanesulphonic acid sodium salt hydrate

nuclei can be detected using a tuneable broadband probehead operating between 162 MHz (for ^{31}P) and 15 MHz (for ^{39}K). An Aspect 3000 computer is used to acquire and process all data. Storage of free induction decays (F.I.D.s) and spectra is possible with either a Control Data Corporation Winchester hard disk system or a Bruker floppy disk unit.

Independent temperature calibration was carried out using a Comark digital thermometer after a suitable period for equilibration. Temperature control was effected by passing gas over a heater coil and then onto the sample. To increase the temperature above ambient air was used, whilst a decrease in temperature was achieved by using nitrogen just above its boiling point, with further heating as necessary.

2.3.1.2 Bruker WH90 N.M.R. Spectrometer

This spectrometer is equipped with a 2.1 T electromagnet and pretuned probeheads for the following nuclei: ^{1}H, ^{13}C, ^{19}F, ^{31}P and ^{11}B. It has a ^{2}H lock for field/frequency stability. A Nicolet BNC-12 computer is used for spectral acquisition and processing, linked to a DRI hard disk for data storage. Temperature control was accomplished in an analogous manner to that used for the WH400 spectrometer.

Observation of ^{51}V n.m.r. on this

spectrometer was achieved by fitting the ^{13}C probehead tuned to 22.6 MHz and decreasing the magnetic field proportionately, as predicted using the equation (2.4).

$$\nu = \frac{\gamma B}{2\pi} \qquad (2.4)$$

ν = frequency
γ = gyromagnetic ratio
B = magnetic field

No field/frequency lock was available using this method, so the number of transients accumulated was low, and repeatedly rereferenced.

2.3.2 Operation of the Bruker WH400 Spectrometer

All spectrometer operations were carried out according to the manufacturer's instructions.

For nuclei other than proton, a suitable tuneable broadband probehead was mounted in the magnetic field. Tuning to the correct radiofrequency (rf) was achieved by pulsing quickly and matching the rf at the probehead to that desired. All tuning operations were undertaken after equilibration at the chosen temperature. The magnetic field was homogenised as far as possible by shimming.

Suitable parameters were chosen for the nucleus under observation (described in the experimental section of each chapter) such as sweep width, pulse length,

number of scans and delay times. After accumulation of the F.I.D. using these parameters an appropriate Lorentzian-to-Gaussian line broadening[152] was applied before Fourier transform.

2.4 PREPARATIVE METHODS

An outline of the main preparative methods used in this project are given in this section. Any changes from these methods will be described in the relevant chapter.

2.4.1 Polyanions

2.4.1.1 Decavanadate (6-)

V_{10} is the only vanadate species that exists in aqueous solution between pH 2 and 6.5 (see Section 1.2.1.1). Preparation of decavanadate is possible by dissolution of a solid vanadate, e.g. $NaVO_3$, $[NH_4]VO_3$ (Fisons) and adjusting the pH to between 2 and 6. Addition of a few drops of acetone starts precipitation.

^{17}O enrichment is undertaken by dissolving the vanadate in ^{17}O enriched H_2O (M.S.D. Isotopes) and leaving overnight to allow oxygen exchange before pH adjustment.

2.4.1.2 Tetradecavanadophosphate (9-)

An analogous preparation was used as that earlier used for the crystal structure[53].

$Na_8H[PV_{14}O_{42}]$ was prepared by the stoicheiometric addition of phosphoric acid and vanadate solution with a V:P ratio of > 2 and < 12. The pH was adjusted to 2.5 ± 0.3, giving a red solution. Cooling overnight yielded the dark red solid $Na_8H[PV_{14}O_{42}].9H_2O$.

For complete ^{17}O enrichment the above preparation was used except that the vanadate was dissolved in ^{17}O enriched H_2O and $POCl_3$ was hydrolysed with the enriched water to give enriched phosphoric acid (warming removed Cl^- as HCl vapour).

2.4.2 Peroxovanadates

The decomposition of H_2O_2 in aqueous solution has been studied[153] and hence these complexes were prepared when required for n.m.r. analysis and the H_2O_2 used repeatedly standardised by literature methods[154]. Solutions containing peroxovanadate complexes were prepared by stoicheiometric addition of approximately 8.9 mol dm^{-3} H_2O_2 to vanadate solution. The overall vanadium concentration was varied between 0.01 and 2 mol dm^{-3}, mainly in the lower part of the range for quantitative measurements and the upper to record the ^{17}O spectra. All measurements were made in the presence of 2 mol dm^{-3} $Na[ClO_4]$ to control ionic strength unless otherwise stated.

2.4.3 Sulphidovanadates

Preparation of sulphidovanadates is possible

both in solution and by solid state reactions. All methods will be described in this section.

2.4.3.1 Preparations in Solution

2.4.3.1.1 In Aqueous Solution

The method is based on that used by Busine and Tridot[155] for the preparation of the tetrathio anion, $[VS_4]^{3-}$, by bubbling H_2S into ammonia solution to form ammonium hydrogen sulphide and then reacting this with aqueous vanadate solution.

In this study 100 cm^3 of an aqueous solution containing 0.05 mol dm^{-3} Na_2HPO_4 for pH determination (see Section 2.5), 10% ^2H_2O for field/frequency lock and 10 cm^3 0.88 NH_3 solution was saturated with H_2S by bubbling for approximately 2 hours at 273 K. On addition of vanadate solution a brown colour was observed which turned purple within 1s. Overall vanadium concentrations of between 3 x 10^{-3} and 0.01 mol dm^{-3} were used. No chemical interactions between the V^V species and NH_3, phosphate ion or 2 mol dm^{-3} $Na[ClO_4]$ to control ionic strength were observed.

2.4.3.1.2 In the Presence of Methanol

Mixing of solid sodium orthovanadate (Fisons) and sodium sulphide (Fisons) followed by addition of methanol with gentle shaking gave a yellow solution of a monosulphide complex within approximately 2 minutes.

Ranade, *et al.*[80] undertook the above

preparation but added only a few drops of methanol followed by sodium hydroxide solution. No sulphidovanadate species were found using their method in this study.

2.4.3.2 Solid State Reactions

2.4.3.2.1 Preparation of Na_3VS_4

Previously the copper[77] and potassium[78] salts have been prepared using this method.

Stoicheiometric amounts of elemental sodium, vanadium (Johnson-Matthey) and sulphur sealed under vacuum in a thick-walled glass tube gave Na_3VS_4 after heating at 500°C for 1-2 hours.

2.4.3.2.2 Preparation of the Tri-, Di- and Monothio Anions[81]

Gentle heating of a finely ground mixture of sulphur, V^V oxide (V_2O_5) and anhydrous sodium carbonate, with V:S ratios between 1:4 and 1:1, formed a melt and gave a mixture of the thioanions and vanadate species.

2.5 pH MEASUREMENTS

All pH measurements except those in the sulphidovanadate study were made using a Radiometer PHM 84 Research pH meter and a Radiometer GK2401C glass electrode containing an internal $AgCl/Ag^+$ reference. Calibration and pH measurements were performed according to the manufacturer's instructions. All pH readings were corrected[156] for extremes of acid or alkali

and the $[Na]^+$ ion effect.

Values of pD given in the study of ADP and ATP are obtained[157] by the addition of 0.4 to the pH reading, Eqn. 2.5.

$$pD = 0.4 + pH_{read} \qquad (2.5)$$

After measuring the pH of some solutions containing sulphidovanadates, a small amount of a black precipitate appeared in the electrode probably due to Ag_2S. Direct measurement of the pH using a hydrogen electrode would not be feasible due to contamination of the pure H_2 required[156] by H_2S from the solution and the length of time required to equilibrate the electrode. In this case the pH was monitored indirectly by the ^{31}P n.m.r. chemical shift of the phosphate ion present, calibrated by a sulphide-free titration in the same medium between pH 7 and 13. The inflexion in the pH titration curve is due to the first protonation of the phosphate ion which occurs in this pH region, Eqn. 2.6.

$$H^+ + PO_4^{3-} \rightleftharpoons HPO_4^{2-} \qquad (2.6)$$

The pH cell contents[158] has been measured in an analogous manner previously.

3. POLYOXOMETALLATE ANIONS V_{10} AND PV_{14}

The structures of these polyanions are shown in Figs. 1.1, 1.2 and 1.3. The nomenclature used in this chapter is consistent with that found in these figures.

3.1 EXPERIMENTAL

The preparation of both of these species has been described in Section 2.4.1. The V_{10} anion was not isolated as a solid but employed directly on lowering the pH to approximately 6.5. ^{51}V n.m.r. was used to check its presence. Solid PV_{14} was dissolved to give a concentration between 0.06 and 10^{-3} mol dm^{-3}. A 2 mol dm^{-3} $Na[ClO_4]$ medium was used to minimise ionic strength variations. However, for ^{17}O measurements solid $Na[ClO_4]$ was added to the $H_2{}^{17}O$ to give this concentration.

$^{31}P-\{^1H\}$ n.m.r. spectra were recorded at 162 and 36.4 MHz using Bruker WH400 and WH90 spectrometers respectively, and referenced to capillary trimethyl phosphite at 140.2 p.p.m. (298 K). This reference was used as an earlier work[53] reported the pH dependence of the ^{31}P resonance of the PV_{14} anion around δ_P = 0 p.p.m. which could be obscured by

the peak from the reactant phosphate ion in the system. Between 50 and 1000 transients were accumulated at a rate of approximately one per second using 16 K and 8 K data points for the WH400 and WH90 respectively, and a flip angle of $\sim 45^{\circ}$. ^{31}P Shifts were reproducible to within $\pm$ 0.01 p.p.m.

^{51}V n.m.r. spectra at 105.2 MHz required the accumulation of up to 3000 transients with 8 K data points. A spectral width of 20 KHz and a pulse length of 12 μs ($\sim 45^{\circ}$ flip angle) were used. ^{51}V chemical shifts could be measured reproducibly within $\pm$ 1 p.p.m.

Similarly for ^{17}O spectra, n.m.r. data obtained required up to 100 000 transients at approximately 100 per second, with a spectral width of 100 KHz and a pulse length of 8 μs ($\sim 30^{\circ}$ flip angle) to allow uniform stimulation over the whole spectral range. ^{17}O chemical shifts were measured to an accuracy of $\pm$ 2 p.p.m.

Kinetics of oxygen exchange of PV_{14} with solvent water were measured by dissolving ^{17}O enriched PV_{14} (Section 2.4.1.2) in distilled water and observing the decrease in intensities of ^{17}O resonances with time. Baseline roll and poor sensitivity resulted in errors in the integration of ^{17}O spectra and in the most favourable cases integrals could be measured to within $\pm$ 20%. The ^{17}O data were recorded during 30 minute periods for up to 8 hours at 295 K. All

rate constants were determined using linear least squares analyses.

3.2 RESULTS AND DISCUSSION

Figs. 3.1 and 3.2 show typical ^{17}O n.m.r. spectra of V_{10} and PV_{14}. The resonance due to O_a in V_{10} has been omitted as has that of O_I for PV_{14} (which could only be easily observed when prepared using ^{17}O enriched phosphate). Figs. 3.3 and 3.4 show the titration curves for the two anions. The ^{51}V titration curve for V_{10} has already been reported[14].

The pKa values for V_{10} found in this study from ^{17}O data are 5.2 and 3.0, which are slightly lower than those found earlier[14], 5.5 and 3.6, due to the change in ionic strength of the medium. The present study uses 2 mol dm^{-3} $Na[ClO_4]$, compared with no added salt previously[14] and this increase in ionic strength presumably favours the higher charged species. The pKa values for PV_{14} are 4.7 and 1.3. All pKa values were obtained by computer fitting of titration curves using non-linear regression analysis, with errors of $\pm$ 0.05 for pKa_1 and $\pm$ 0.01 for pKa_2. Examples of the fits are given in Figs. 3.5 and 3.6 for V_{10} and PV_{14}, respectively.

The assignment of the resonances (given in Fig. 3.3) in the ^{17}O spectra of V_{10} was in agreement with earlier work[15]. However, recently the resonances

Fig. 3.1 A typical ^{17}O n.m.r. spectrum of V_{10} (omitting O_a), at pH 3.49. O_f and O_g were assigned by $^{17}O\{^{51}V\}$ n.m.r. experiments[9].

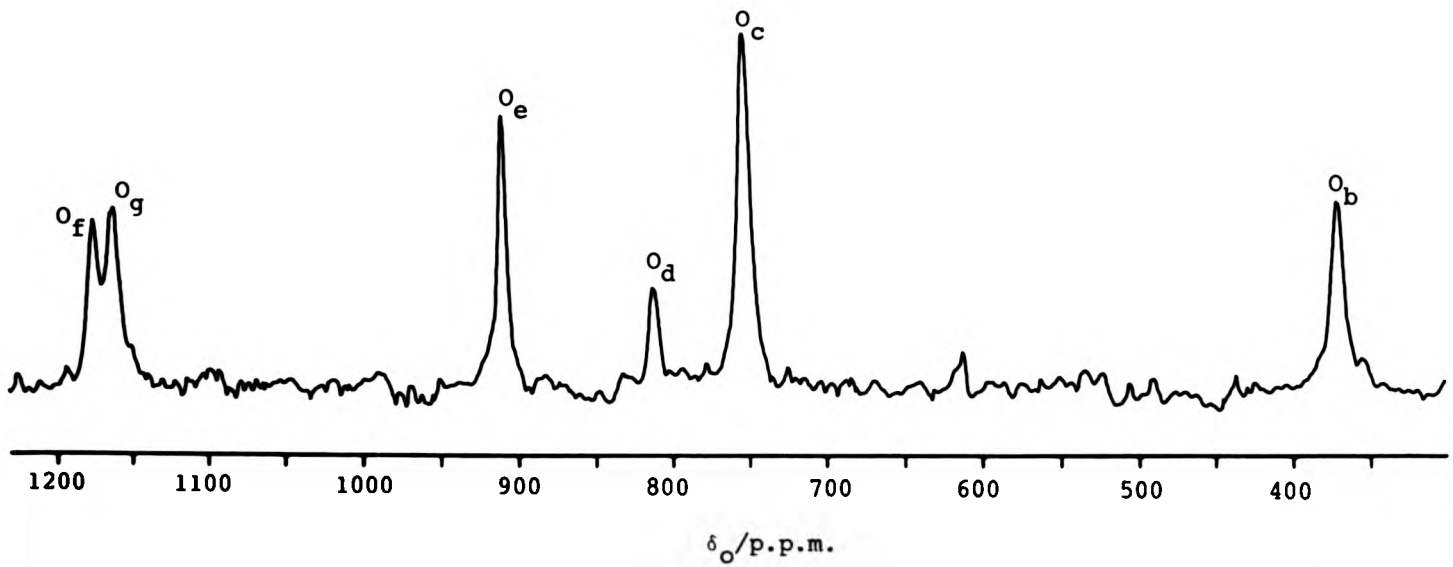

Fig. 3.2 A typical ^{17}O n.m.r. spectrum of PV_{14} (omitting $O_{(I)}$), at pH 2.16.

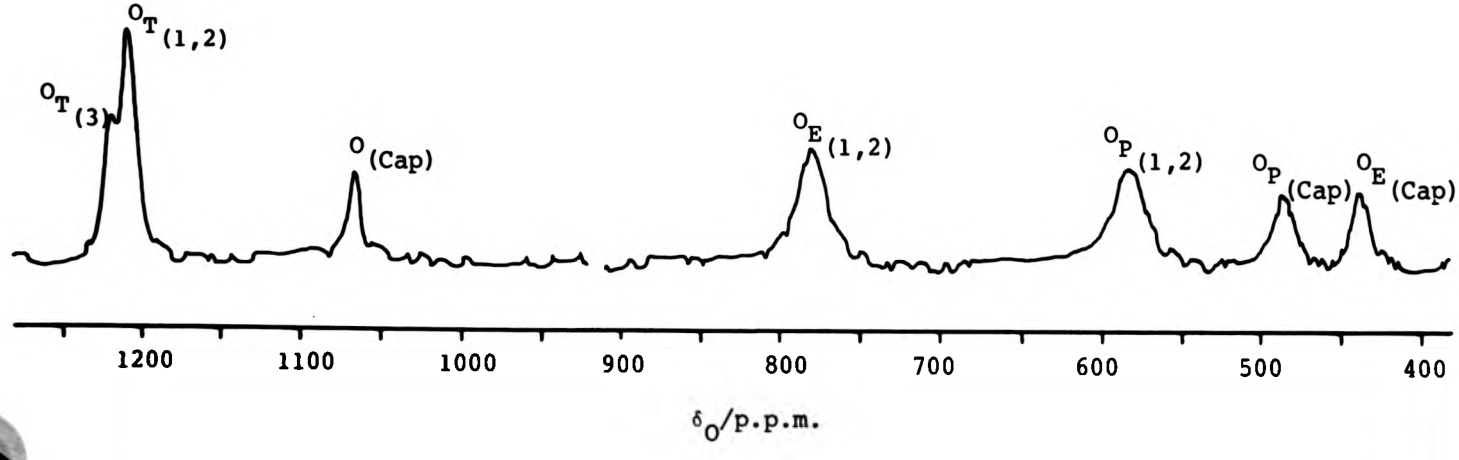

Fig. 3.3 ^{17}O n.m.r. chemical shift *versus* pH for V_{10}.

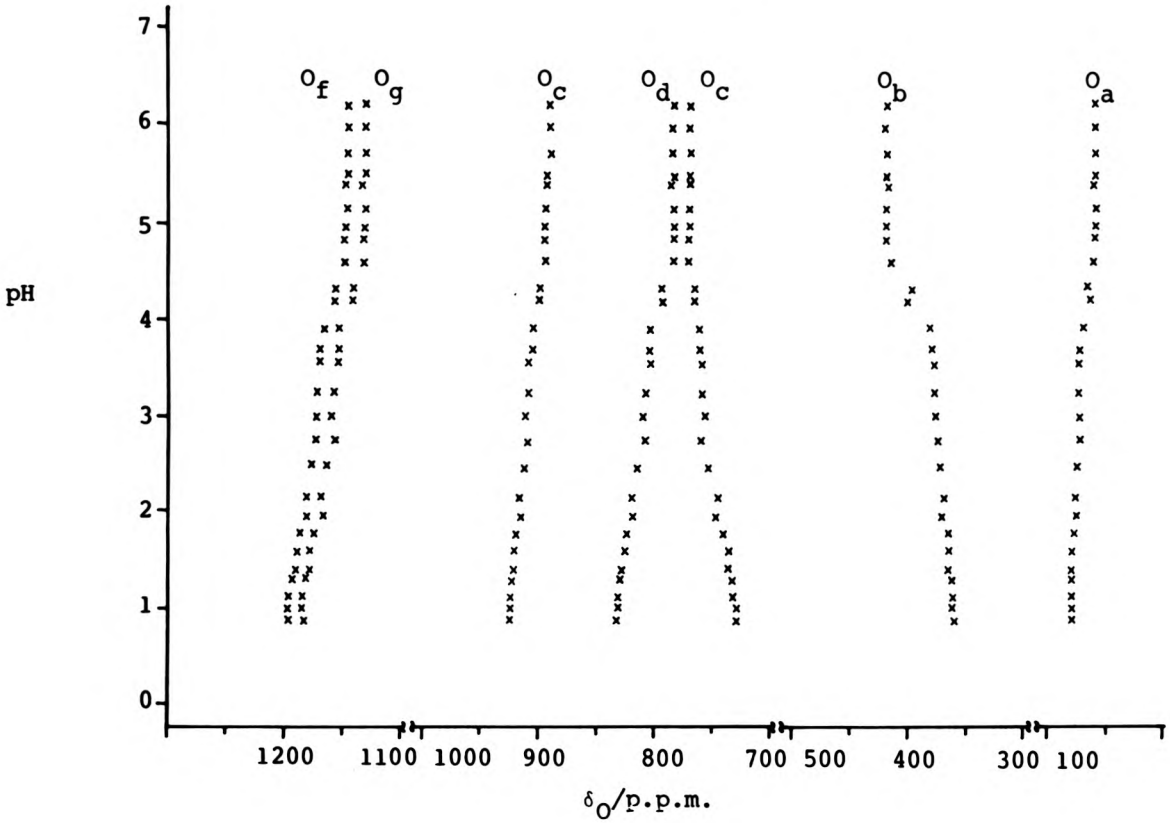

Fig. 3.4 Chemical shift *versus* pH for the PV_{14} ^{17}O, ^{51}V and ^{31}P nuclei. At pH > 5 $O_{P(1,2)}$ and $O_{E(1,2)}$ merge.

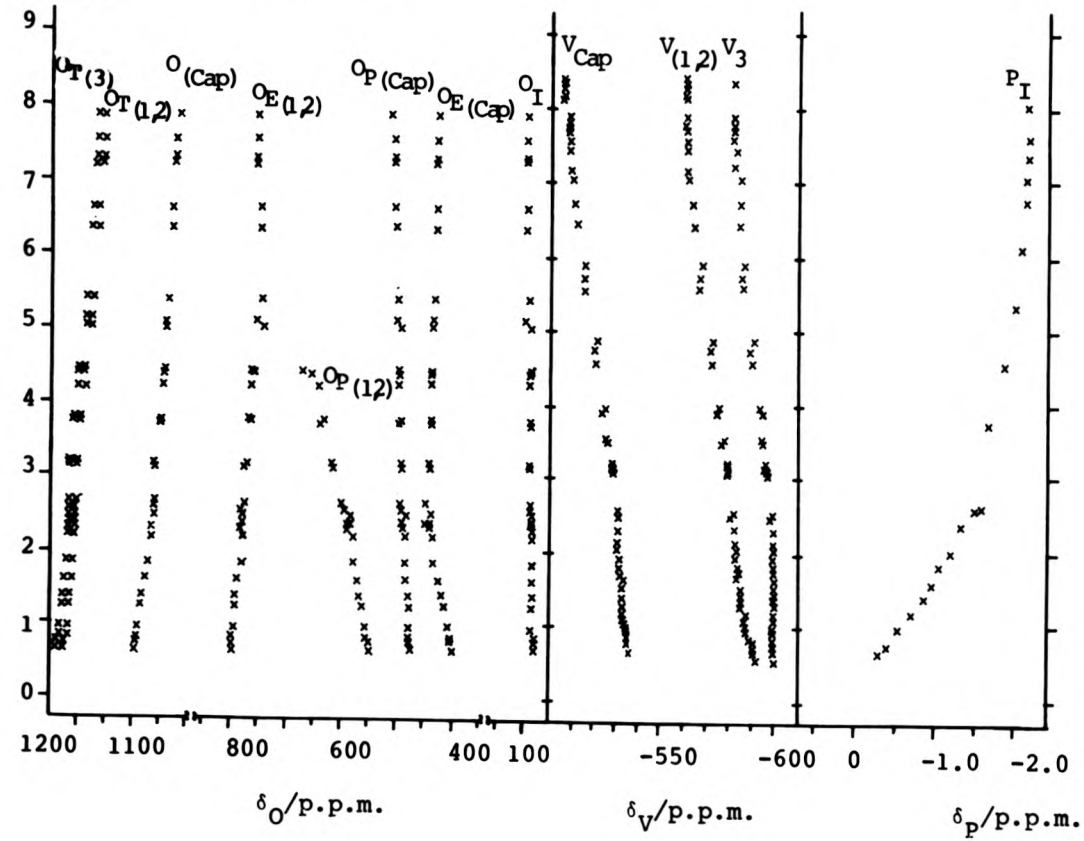

Fig. 3.5 Example fit of experimental ^{17}O n.m.r. chemical shift for V_{10}, O_C, (X) with the calculated chemical shift (solid line) *versus* pH. Non-linear regression analysis allowed values for pKa_1 and pKa_2 to be obtained.

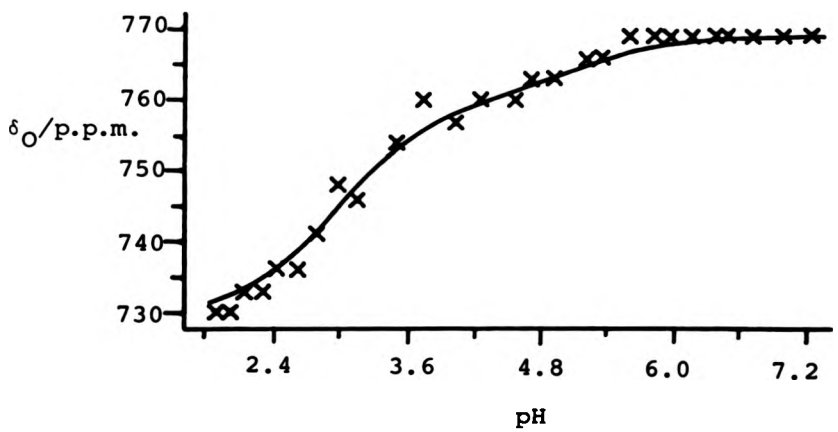

Fig. 3.6 Example fit of experimental ^{17}O n.m.r. chemical shift for PV_{14}, $^{O}E_{(Cap)}$, (X) with the calculated chemical shift (solid line) *versus* pH. Non-linear regression analysis allowed values for pKa_1 and pKa_2 to be obtained.

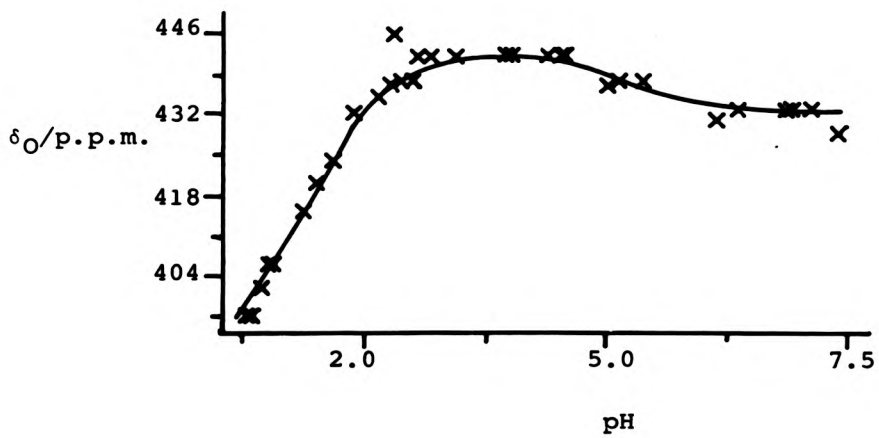

due to terminal oxygen atoms O_f and O_g have been distinguished by ^{17}O-{^{51}V} n.m.r. experiments[9]. The ^{17}O spectra of PV_{14} can be interpreted using peak area and co-ordination number[56], except for the two pairs $O_{E(1,2)}/O_{P(1,2)}$ and $O_{E(cap)}/O_{P(cap)}$. The assignment of these resonances is required for the explanation of the kinetic data, so an extension of ^{17}O n.m.r. shift theory of oxo-ligands is necessary.

3.2.1 ^{17}O Chemical Shift Theory

The inverse dependence of the ^{17}O shift with co-ordination number[56] and metal oxygen distance[57] has already been noted (Section 1.2.1.1). In the latter case this was mainly from data for monoco-ordinate terminal oxygen ligands, e.g. $O_{T(1,2,3)}$ and $O_{(cap)}$ in Fig. 3.4, with much less success observed when applied to multico-ordinate oxygens. In the polyoxometallates under study, the ^{17}O shift of a multico-ordinate oxygen is affected by all the co-ordinated metal ions since these have similar M-O bond lengths. For instance in V_{10}[7], the multico-ordinate oxygen ligands O_b, O_c and O_e have average M-O bond lengths $V_{(1)}$-O_b 1.97 Å, $V_{(3)}$-O_b 1.95 Å, $V_{(1)}$-O_c 1.84 Å, $V_{(2)}$-O_c 1.85 Å, $V_{(2)}$-O_e 2.04 Å and $V_{(1)}$-O_e 1.93 Å; and in PV_{14}[53] $V_{(1)}$-$O_{E(cap)}$ 1.92 Å, $V_{(cap)}$-$O_{E(cap)}$ 2.00 Å, $V_{(1)}$-$O_{E(1,2)}$ 1.83 Å and $V_{(3)}$-$O_{E(1,2)}$ 1.94 Å. Despite the similar V-O bond

lengths about a given oxygen the ^{17}O chemical shifts can be noticeably different, e.g. bidentate oxo ligands O_c and O_e in V_{10} have ^{17}O shifts of 722 and 918 p.p.m., respectively at pH 2. Hence, another factor (or factors) further determines the ^{17}O shift with approximately the same effect as a small variation in M-O bond length.

This factor could be the MÔM bond angle. In a recent review of nitrogen n.m.r. by Mason[159] a change of bond angle about nitrogen, in metal complexes with polyatomic ligands, from linear to bent was shown to increase the chemical shift by up to 500 p.p.m. On bending N_α in metal dinitrogen complexes the resonance undergoes a downfield shift of approximately 350 p.p.m. from the position of that of the linear moiety. Similar observations hold for the nitroso complexes M-NO. The deshielding is caused by paramagnetic circulation involving the lone pair of electrons on the nitrogen between the highest occupied molecular orbital (HOMO) and the lowest unoccupied molecular orbital (LUMO), Fig. 3.7. This is an $n \rightarrow \pi^*$ excitation causing a rotation of charge and hence a local current around nitrogen. These excitations originate from the polarisation of electrons in the magnetic field. Since the effect is normally to reinforce the applied field the circulations are described as 'paramagnetic', with larger downfield

Fig. 3.7 A diagramatical representation of the p_x (horizontal) → p_y (vertical) component of the $n_N \rightarrow \pi^*$ transition showing rotation of charge in a metal nitroso group.

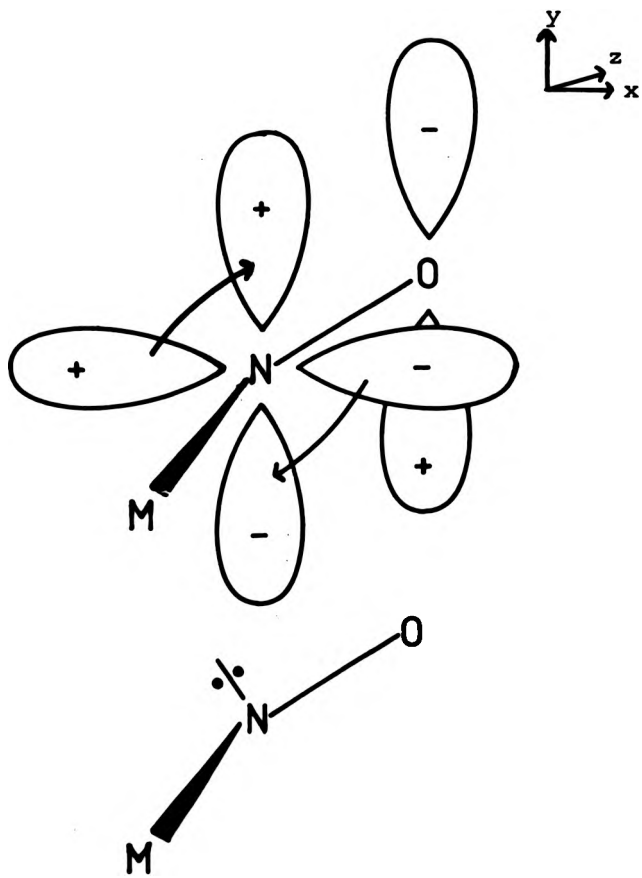

shifts when lower excitation energies separate HOMO and LUMO. On bending the excitation energy required for the circulation is reduced due to the increased availability of the lone pair of electrons and, hence, a large increase in chemical shift is observed.

As oxo ligands contain lone pairs of electrons the same effect may obtain in ^{17}O n.m.r. The $V\hat{O}V$ bond angles for the three bidentate oxygen ligands in V_{10}[7] are $V_{(1)}\hat{O}_cV_{(2)}$ 115.5°, $V_{(2)}\hat{O}_dV_{(2)}$ 114.7° and $V_{(2)}O_eV_{(3)}$ 108.6° with their ^{17}O shifts in the order $O_e > O_d > O_c$. This shows an inverse correlation between ^{17}O chemical shift and $V\hat{O}V$ bond angle for bidentate oxygen in V_{10} as expected from the above argument, despite small differences in V-O bond length and uncertainties of bond angle in solution. The bidentate oxygen ligands in PV_{14}[53], have $V\hat{O}V$ angles of 122.3° ($V_{(1)}\hat{O}_{E(1,2)}V_{(3)}$) and 147.8° ($V_{(1)}\hat{O}_{P(1,2)}V_{(3)}$) which were measured in the crystal structure of the mono-protonated species. Hence, $O_{P(1,2)}$ can be assigned to the resonance with lower ^{17}O shift. On plotting $V\hat{O}V$ and $Mo\hat{O}Mo$ angles against $\delta_{(O)}$, Fig. 3.8, this correlation is further observed even allowing for possible errors in bond lengths and angles. In the case of the Mo data the chemical shift was scaled by a factor of 1.24, calculated from comparison of terminal oxygen resonances[55], to allow for the

Fig. 3.8 Plot of ^{17}O chemical shift *versus* angle $\hat{VOV}$ or $\hat{MoOMo}$ (shift scaled x 1.24) for two co-ordinate oxygen atoms. Points: ●, V_{10} (O_c, O_d and O_e); O, PV_{14} ($O_{E(1,2)}$ and $O_{P(1,2)}$); X, $[Mo_6O_{19}]^{2-}$ and $[Mo_7O_{24}]^{6-}$ refs. 55 and 56 (reassigned to fit published integrals); □, $[V_2O_7]^{4-}$; *, $[Mo_2O_7]^{2-}$; and ◊, $[HV_4O_{12}]^{3-}$. For the latter three compounds the relevant angle has been assumed to reach its maximum possible value in solution.

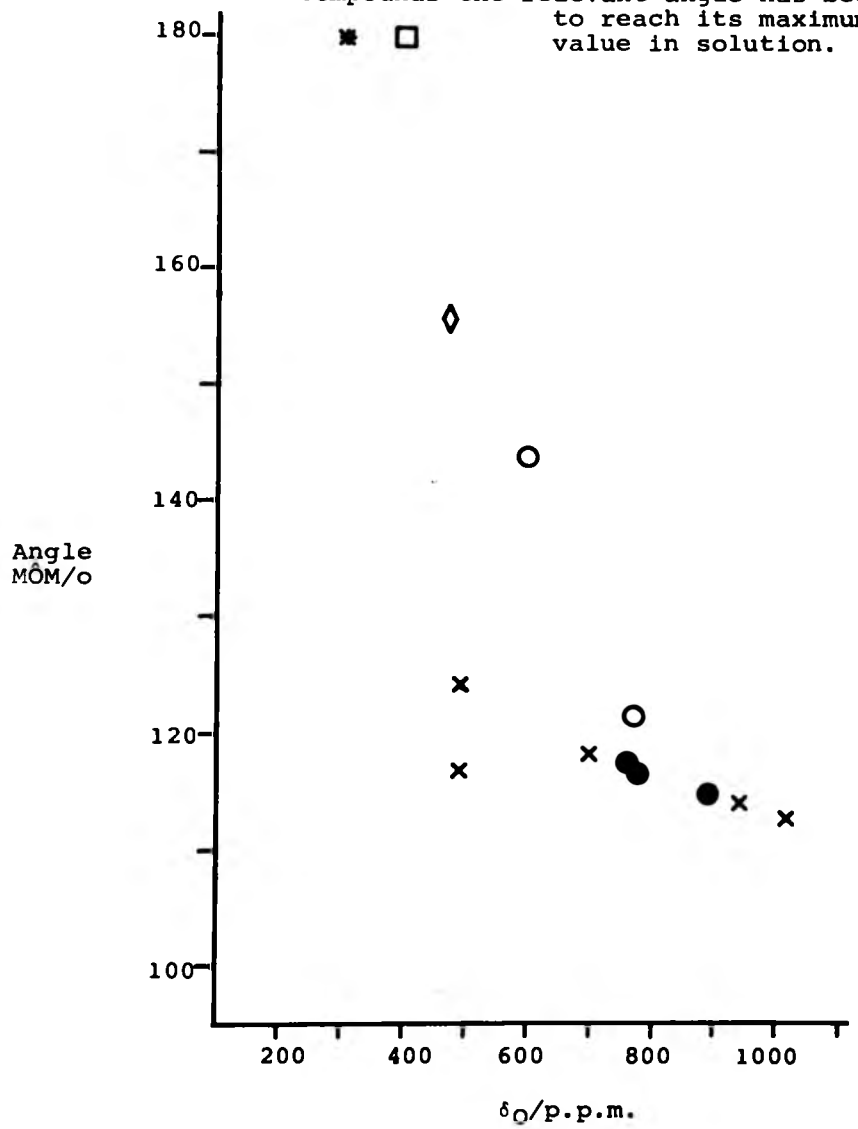

fundamental difference in orbital energies between the Mo and the V atom.

The trico-ordinate oxygen ligands $O_{E(cap)}$ and $O_{P(cap)}$ in PV_{14} were assigned from the significant difference in $V_{(cap)}$-O bond lengths[53] of $V_{(cap)}-O_{E(cap)}$ 2.0 Å, and $V_{(cap)}-O_{P(cap)}$, 1.83 Å. Using the inverse correlation between bond length and ^{17}O shift $O_{P(cap)}$ was assigned to the resonance at higher frequency.

3.2.2 Protonation and pH Dependence

Fig.s 3.3 and 3.4 show a balance of positive and negative shifts in the ^{17}O spectra on protonation, whilst negative shifts are observed for the ^{51}V spectra and a positive shift in the ^{31}P resonance.

The ^{51}V spectrum of PV_{14} can be easily assigned by relative peak areas as shown in Fig. 3.4. The titration curves are similar to those observed for V_{10}[14] which show protonation, but were inconclusive as to the exact sites. The ^{17}O results are of more interest because the reasons for the balance of shifts are not clearly understood.

The ^{17}O titres show that protonation shifts, averaged over all available sites, are too large to be due solely to variations in bond lengths and changes in co-ordination. For instance, in V_{10} the first protonation lowers the ^{17}O shift of each

of the four O_b ligands by 47 p.p.m., which is the equivalent of -188 p.p.m. for protonation at a single oxygen before exchange-averaging. Larger shifts were observed for the PV_{14} anion, e.g. the resonance due to $O_{P(1,2)}$ was shifted by -160 p.p.m. for each of the eight ligands, a total of -1280 p.p.m. for a single site protonation. In addition, some large positive shifts were observed.

Kato, *et al.*[53] suggested that the pentaco-ordinate caps on PV_{14} can be thought of as cationic elements present to reduce the overall negative charge and hence stabilise the Keggin structure. On protonation of the anion the need for these caps would be reduced and a slight increase in length along the 'polar' axis between the two caps may occur. For the bidentate oxygen ligands $O_{P(1,2)}$ this would cause a net increase in the $V_{(1)}\hat{O}_{P(1,2)}V_{(3)}$ angle and, from the ^{17}O theory already described, a negative shift in the resonance. Similarly, if the four $V_{(1)}$-O_g units were to be considered as caps in V_{10}, protonation would cause a lengthening in the $V_{(1)}$-$V_{(1)}$ axis with an increase in $V_{(2)}\hat{O}_cV_{(1)}$ and therefore a decrease in the chemical shift of O_c.

Increases in the ^{17}O shift on protonation were observed mainly for the terminal oxygen ligands, although some positive shifts were found for some multico-ordinate oxygen ligands. This was probably due to a decrease in the V-$O_{(terminal)}$ bond length

with an extension of the other V-O bonds in the co-ordination sphere, and would be expected from the inverse-dependence of ^{17}O chemical shifts with M-O bond length[57]. Competition between these oxygen ligands for the d orbitals on V^{160}, in a given co-ordination sphere would then also give rise to the shifts in the spectrum.

Thus, protonation almost certainly results in slight changes in the structure of these anions, with an extension along their polar axes. These structural modifications alter the bond lengths and bond angles which, in turn, cause both positive and negative shifts in the ^{17}O spectra.

3.2.3 Protonation Sites

The exact sites of protonation in V_{10} and PV_{14} are not clear. $O_{P(1,2)}$ would seem to be the most likely in PV_{14} as it is remote from the V-O cationic caps, thus minimising electrostatic repulsion. The difference between the two pKa values is indicative of the two protonation sites being diagonally opposite each other on the equatorial belt on electrostatic grounds. This reinforces the reasoning for the choice of $O_{P(1,2)}$ as protonation sites, allowing the maximum possible distance between the first and second protonation sites as well as between the protonation sites and

VO caps.

For V_{10}, O_c is indicated as these allow the maximum possible distance between the two protonation sites and have been shown to be one of the most basic oxygen ligands[15]. This is in agreement with earlier work from limited ^{17}O data[15], x-ray crystallographic data used in empirical bond length/bond number calculations[8] and ^{51}V n.m.r. measurements[14]. From the evidence obtained in the present work a better description of protonation and protonation sites would be based on changes in the hydrogen-bonding network around the anion, averaged on the n.m.r. timescale, with the sites being those oxo ligands most favoured to form these bonds.

3.2.4 Oxygen-Exchange Kinetics

Fig. 3.9 shows the pH dependence of the pseudo-first-order rate constant for oxygen exchange between solvent $H_2{}^{16}O$ and the ^{17}O enriched PV_{14} anion. As the twenty eight oxygen ligands in the V_{10} anion exchange at a single rate[15,16] only PV_{14} is considered in this section.

All the data from these experiments can be interpreted in terms of regional stability in the anion and of electrostatics. Only at pH > 6.5 can a rate constant for $O_{(cap)}$ be measured. This is readily explained by the cationic V-O caps being

Fig. 3.9 pH dependence of pseudo-first-order rate constant for ^{17}O exchange with solvent $H_2\,^{16}O$ for PV_{14}: ◊, $O_{P(1,2)}$; □, $O_{P(Cap)}$; O, $O_{T(1,2)}$; X, $O_{E(1,2)}$; ■, $O_{T(3)}$; ●, $O_{E(Cap)}$; ♦, O_{Cap}.

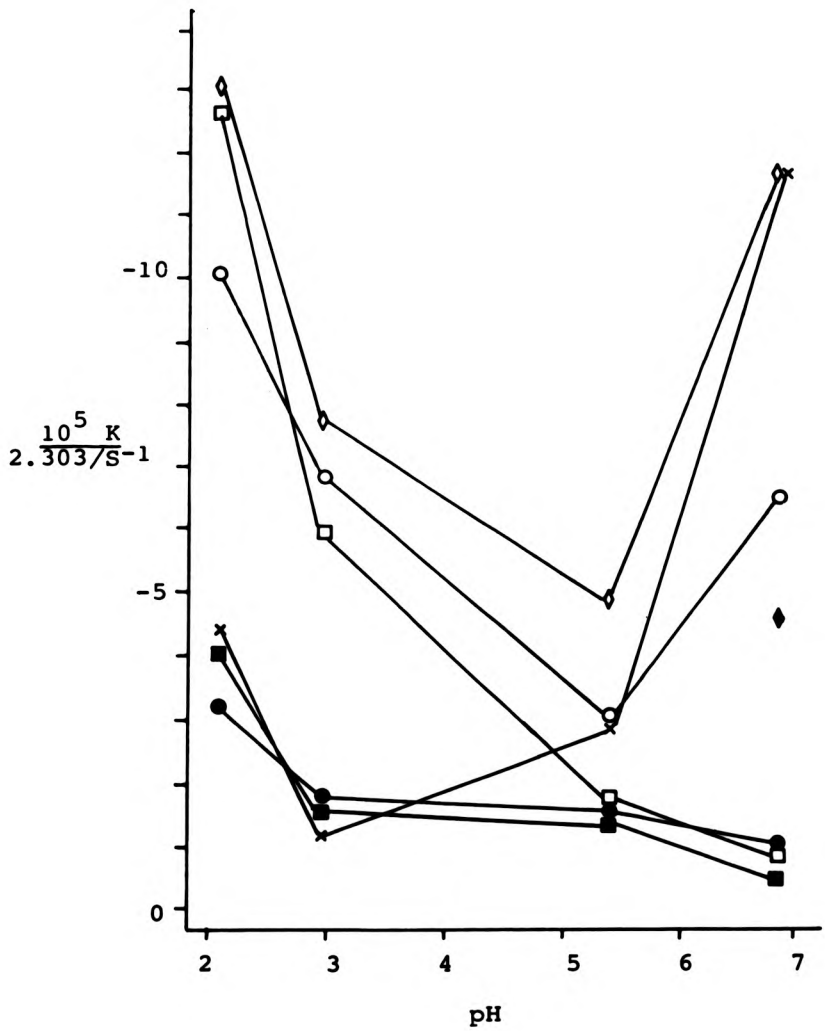

more tightly bound than at lower pH because of the higher negative charge of the species. Thus, the kinetic data confirms the role of the "$[VO]^{3+}$" caps and is in agreement with the conclusions concerning protonation drawn from the titration curves.

As the caps are required by the anion at this pH then the oxo ligands around them, $O_{P(cap)}$ and $O_{E(cap)}$, should also be thermodynamically and kinetically stabilised. Evidence for this was shown by their low rate constants, Fig. 3.8. In addition, $O_{T(3)}$ shows residual stability at high pH. This may be because any distortion of the anion which could detach $O_{T(3)}$ results in the preferential exchange of a neighbouring oxygen ligand. The lability of other oxygen ligands at this pH is expected because the removal of protons from the equatorial belt lowers the stability in this region.

On lowering the pH to between 4 and 5 the oxygen ligands in the equatorial belt of the anion ($O_{P(1,2)}$, $O_{E(1,2)}$ and $O_{T(1,2)}$), have greater stability due to the first protonation step. However, the V-O caps are still required to reduce the overall negative charge with the oxo ligands around them resisting exchange.

On decreasing the pH to approximately 2 an additional change in regional stability was observed. The second inflexion in the titration

curve due to protonation was beginning at this pH and hence the need for the V-O caps was reduced even further. All oxygen ligands were labilised but $O_{E(cap)}$, $O_{E(1,2)}$ and $O_{T(3)}$ apparently have some residual stability. This is indicative of the persistence of the four half-hemisphere units comprising the $V_{(1)}$, $V_{(2)}$ and $V_{(3)}$ octahedra.

3.3 CONCLUSIONS

The effect of varying pH on V_{10} and PV_{14} is not only to protonate but also to slightly modify the structures of these anions. Changes in bond lengths and angles were indicated from the ^{17}O titration curves, giving a semiquantitative insight into the reasons for variations in chemical shifts. The kinetic stability of the PV_{14} anion shows its sensitivity to pH and indicates the need for the presence of cationic V-O caps to reduce its overall negative charge.

4. OXOPEROXOVANADIUM (V) COMPLEXES

4.1 EXPERIMENTAL

The preparative procedures and standardisation methods used in this chapter have been described in Section 2.4.2. All pH variations were undertaken by addition of concentrated NaOH and $HClO_4$ solutions.

Vanadium-51 n.m.r. spectra at 105.2 MHz were acquired by accumulation of between 100 and 1000 transients at a rate of approximately 5 per second. A spectral width of 40 KHz was used to observe the region from -470 to -850 p.p.m. which includes most vanadate resonances[25] (when V_{10} was present the range was extended to start at -400 p.p.m.[14]), and a pulse width of between 12 and 15 μs (a flip angle of ∿ 45-60°).

Oxygen-17 spectra at 54.2 MHz were obtained in an analogous manner but required up to 100 000 transients; a spectral width of 100 KHz was used and an 8 μs pulse length (∿ 35° flip angle) for equal excitation over the whole spectral range.

Linewidths are larger than for vanadates[25], thus ^{51}V and ^{17}O chemical shifts were reproducible to within ± 1 p.p.m. and ± 2 p.p.m. respectively, except for some minor components (± 3 p.p.m.). The accuracy of the ^{51}V integrals were found to depend on the relative size and overlap of resonances, with an

uncertainty of ± 5% in favourable cases. The ^{17}O n.m.r. spectra could not be integrated accurately because of baseline roll and poor sensitivity. Thus, these integrals were not used for calculating equilibrium constants.

All n.m.r. measurements were carried out in the presence of 2 mol dm^{-3} $Na[ClO_4]$ to minimise ionic strength changes and at 273 K except where noted.

4.2 RESULTS

Table 4.1 contains a list of species observed in this study with their n.m.r. data and pKa values. Throughout the results and discussion these species will be referred to by the notation in this table. Figs. 4.1 and 4.2 show the ^{51}V and ^{17}O chemical shifts, respectively, as a function of pH. To give an indication of the relative proportions of the major species, Fig. 4.3 shows a plot of %V *versus* pH at various [V]:[OO] ratios. Typical ^{51}V and ^{17}O spectra obtained in this study can be found in Fig. 4.4.

4.2.1 pH < 5

On addition of two equivalents of H_2O_2 solution to a vanadate solution the pH decreased from ∿6.5-7.0 to ∿ 4.5, suggesting the monomeric peroxovanadate formed was in the same protonation

Table 4.1 Peroxovanadate species identified in this study with their chemical shifts and pKa's (Note: Vanadate data can be found in Table 1.1.)

(a) Monomers

No peroxo ligands per V	1	2	3	4
#	(*P2*)	(*P8*)	(*P12*)	
Formula	$[VO_3(OO)]^{3-}$	$[VO_2(OO)_2]^{3-}$	$[VO(OO)_3]^{3-}$	$[V(OO)_4]^{3-}$
δ_V/p.p.m.	-769.3	-769.3	<-830	-737.6
$\Delta\nu_{\frac{1}{2}}$/Hz				480
δ_O/p.p.m.	568	602	< 990	a
#	(*P3*)	(*P9*)	(*P13*)	
Formula	$[VO_2(OH)(OO)(OH_2)_2]^{2-}$	$[VO(OH)(OO)_2(OH_2)_2]^{2-}$	$[V(OH)(OO)_3]^{2-}$	
δ_V/p.p.m.	-627.6	-770.6	-737.2	
$\Delta\nu_{\frac{1}{2}}$/Hz	75	230	220	
δ_O/p.p.m.	1041[b], <75	1021[b], 83	1014	
pKa	>14	>14	>14	
#		(*P10*)		
Formula		$[V(OH)_2(OO)_2(OH_2)_2]^{-}$		
δ_V/p.p.m.		-699.9		
$\Delta\nu_{\frac{1}{2}}$/Hz		270		
δ_O/p.p.m.		1057, <75		
pKa[c]		6.98 ± 0.25		
#	(*P1*)	(*P14*)		
Formula	$[VO(OO)]^{+d}$	$[HV(OH)_2(OO)_2(OH_2)_2]$		
δ_V/p.p.m.	-549.3	<-705		
$\Delta\nu_{\frac{1}{2}}$/Hz	350			
δ_O/p.p.m.	1240, <75	< 1065, <75		

(b) Dimers

#	(*P4*)			
Formula	$[\{VO_2(OO)\}_2O]^{4-}$			
δ_V/p.p.m.	-636.3			
$\Delta\nu_{\frac{1}{2}}$/Hz				
δ_O/p.p.m.	a			
#	(*P5*)	(*P6*)	(*P11*)	
Formula	$[HO_2VOVO(OO)_2]^{3-}$	$[HO_2(OO)VOVO(OO)_2]^{3-}$	$[\{VO(OO)_2\}OH]^{3-}$	
δ_V/p.p.m.	-556.2, -742.8	-624.3, -742.8	-766.5	
$\Delta\nu_{\frac{1}{2}}$/Hz	100		650	
δ_O/p.p.m.	a	a	1057	
#	(*P7*)			
Formula	$[H_4\{(OO)_2OVOVO_2(OO)\}]$			
δ_V/p.p.m.	-670.6, -674.0			
$\Delta\nu_{\frac{1}{2}}$/Hz				
δ_O/p.p.m.	1208, 924?			

[a] Not observed

[b] Average due to H transfer

[c] For loss of one H, in 2 mol dm^{-3} $Na[ClO_4]$

[d] Species probably also has co-ordinated H_2O

Fig. 4.1 Plot of ^{51}V chemical shift of peroxovanadates *versus* pH. Typical conditions were [OO]:V = 2:1, 0.1 mol dm^{-3} in vanadium. Species are numbered as in Table 4.1.

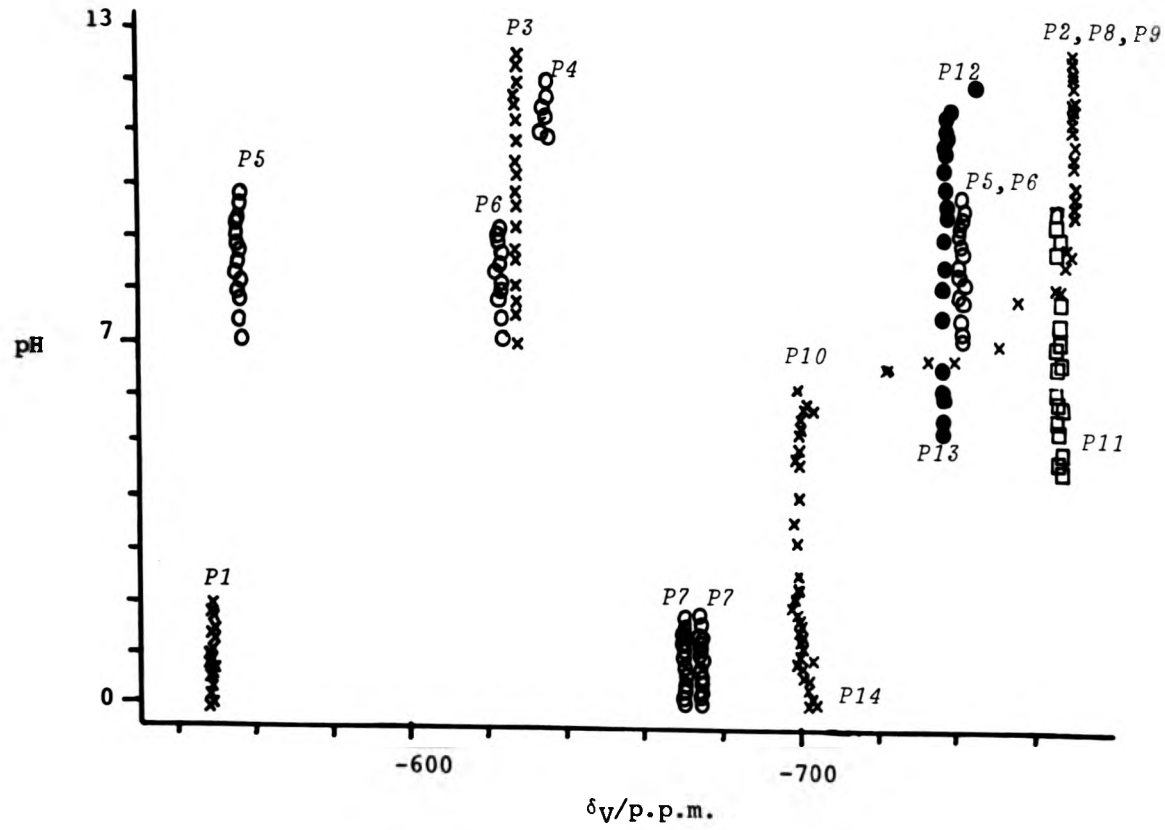

Fig. 4.2 Plot of ^{17}O chemical shifts of peroxovanadates *versus* pH. Typical conditions were [OO]:V = 2:1, 1.5 mol dm^{-3} in vanadium. Species are numbered as in Table 4.1.

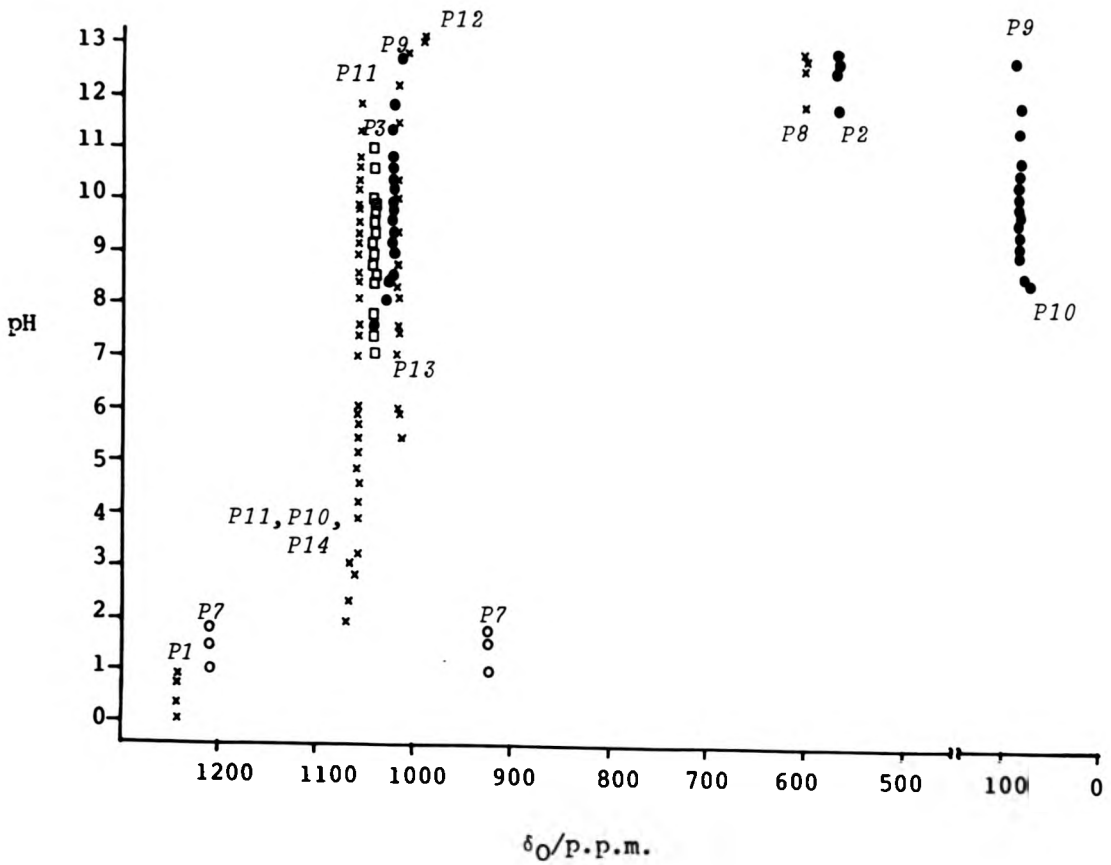

Fig. 4.3 pH dependence of the concentrations of the major species from n.m.r. integrals. All solutions contain 0.07 mol dm^{-3} vanadium. [OO] = 0.14 (——), 0.42 (---) and 0.07 mol dm^{-3} (- - -); in the latter two cases the concentrations of the other species are reduced in appropriate proportion.

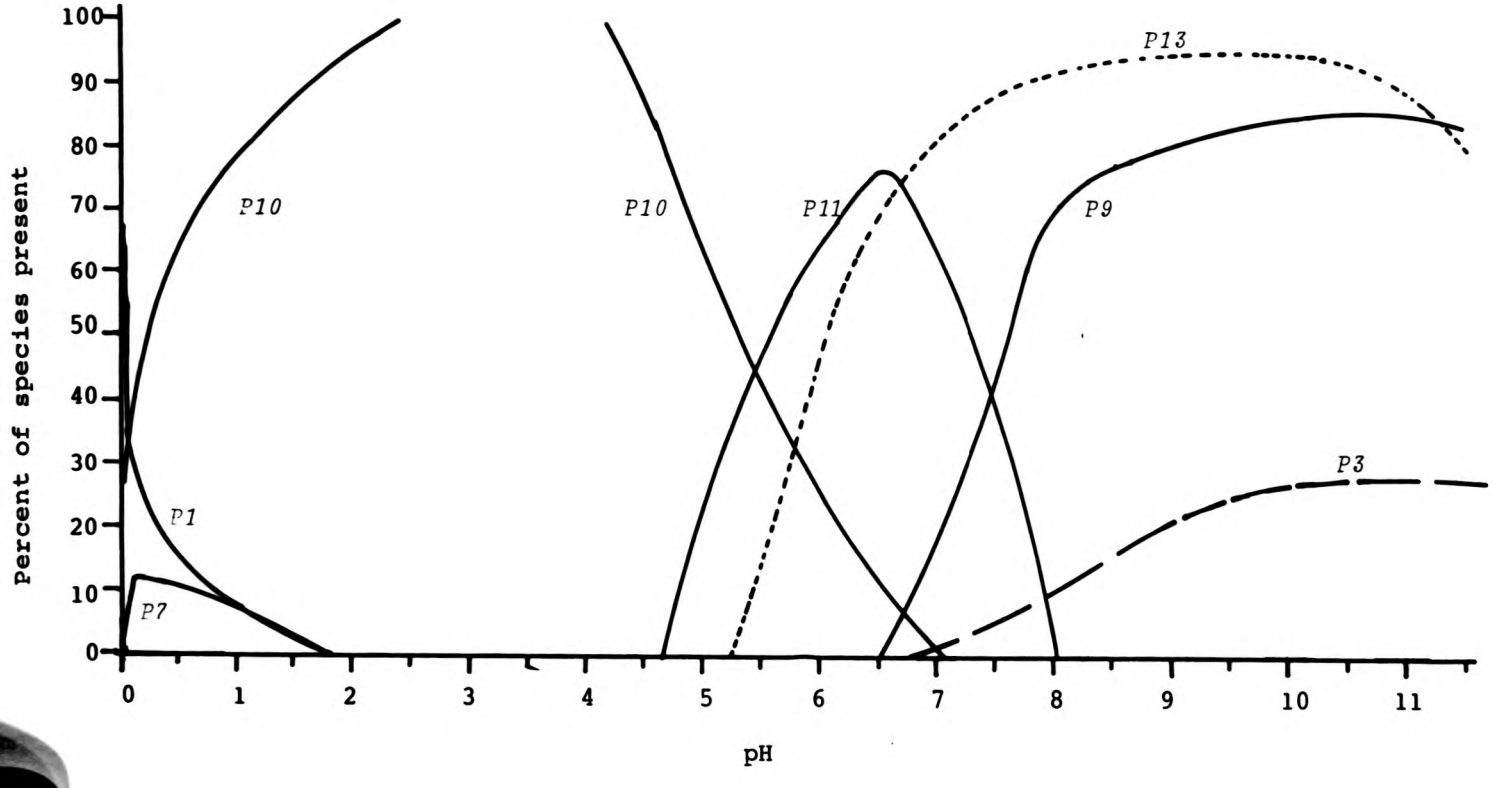

Fig. 4.4 Typical peroxovanadate spectra: (a) ^{17}O ([V] = 1.4 mol dm^{-3}, pH 9.79, [OO]:V = 2:1); (b) ^{51}V ([V] = 0.07 mol dm^{-3}, pH 0.45, [OO]:V = 2:1), with resolution enhancement to show both resonances due to (*P7*). Species are numbered as in Table 4.1.

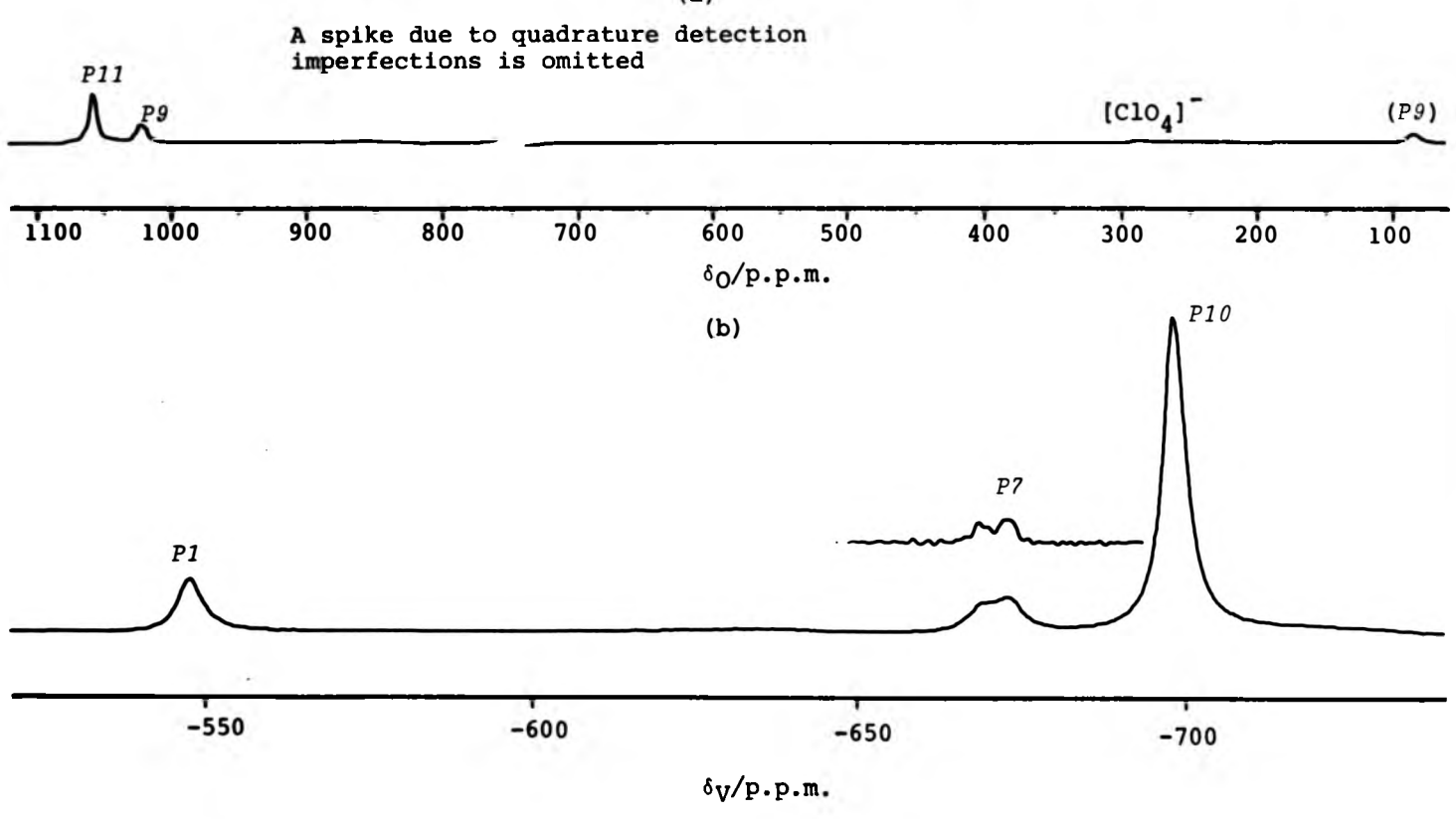

state as the monomeric vanadate, $[H_2VO_4]^-$, but with a lower pKa. Only one resonance was found in the ^{51}V n.m.r. spectrum, at -699.9 p.p.m. This resonance was assigned to $[H_2VO_2(OO)_2]^-$, (*P10*) in agreement with Howarth and Hunt[38], and Chauveau[36,37]. The ^{17}O spectra at this pH exhibited one peak at δ_O = +1057 p.p.m., which is a significantly higher shift than those resonances observed for tetrahedral monomeric vanadates[25] (δ_O = +565 p.p.m. for $[VO_4]^{3-}$ and +573 p.p.m. for $[HVO_4]^{2-}$). This intimates that the vanadium is octahedrally co-ordinated with a more accurate formula being $[V(OH)_2(OO)_2(OH_2)_2]^-$ and could have a shorter V-O bond length than in the monomeric vanadates. Further evidence will be presented later regarding the co-ordination sphere.

On addition of very small amounts of perchloric acid to this solution, the pH decreased to approximately 3 with no change in colour, ^{51}V spectra or ^{17}O spectra.

Below this pH additional resonances at δ_V = -549.3, -670.6 and -674.0 p.p.m. were observed, Fig. 4.1. After a further decrease to below pH 0.1, only the resonance at δ_V = -549.3 p.p.m. was found. Over this pH range the resonance due to (*P10*) shifted to lower frequency by up to 4 p.p.m. In the ^{17}O spectra, Fig. 4.2, the peak at δ_O = +1057 p.p.m. (*P10*) shifted to +1065 p.p.m. and a new resonance appeared at +1240 p.p.m. Below pH 0.1 only the latter resonance

was observed.

The peaks at δ_V = -670.6 and -674.0 p.p.m., Figs. 4.1 and 4.4, have equal areas, were observed over the same pH range, and had a concentration dependence; indicating the species to be an unsymmetrical dimer. On varying the V:(OO) ratio the maximum proportion of this species was found at a ratio of 1:1.5. From the stoicheiometry of its formation it would be uncharged and was thus tentatively assigned as $[H_4\{O(OO)_2VOV(OO)O_2\}]$, (*P7*), with the sites of protonation uncertain. The equilibrium constant, pKc, in 2 mol dm^{-3} $Na[ClO_4]$ was found to be -0.97 ± 0.27 (23 observations), with an identical value in the absence of perchlorate (27 observations).

$$(P10) + (P1) \rightleftharpoons (P7) + H_2O \qquad (4.1)$$

The shift in resonance of (*P10*) from δ_V = -699.9 to -703 p.p.m. coupled with broadening was due to protonation to form $[HV(OH)_2(OO)_2(OH_2)_2]$, (*P14*), with an average signal observed because of fast exchange between (*P10*) and (*P14*). This is the only aqueous species where protonation occurs at (OO). When no $Na[ClO_4]$ was present a shift to -711 p.p.m. was observed presumably due to the presence of $Na[ClO_4]$ favouring the species of higher charge. Recently[161], a proton bound to a (OO) ligand *via* a hydrogen bond was shown to be present in $(Hbipy)[H\{VO(OO)_2bipy\}_2].xH_2O_2.(6-x)H_2O$ (where x ≈ 0.5). This crystal structure analysis

showed the complex to contain a proton bridge between two peroxide ligands, one bound to each vanadium.

Below pH 0.1, one species gave the resonances at δ_V = -549.3 p.p.m. and at δ_O = +1240 p.p.m. When one equivalent of H_2O_2 was added to vanadate this species was formed quantitatively. These observations are consistent with the species $[VO(OO)]^+$, (*P1*). This may be better formulated as $[VO(OO)(OH_2)_4]^+$. A short V-O bond was indicated from the ^{17}O shift, whilst fast exchange between the co-ordinated and bulk water caused the ^{17}O resonance for the co-ordinated water to be indistinguishable from that of the solvent.

When less than two equivalents of H_2O_2 were added to a vanadate solution appropriate amounts of V_{10} or $[VO_2]^+$ were also formed in this pH region. Addition of larger amounts of H_2O_2 favoured (*P10*) rather than (*P7*) and (*P1*).

4.2.2 pH > 5

Note: In this section each species will be discussed in turn together with its role in the equilibria.

On increasing the pH of a solution containing peroxovanadate species prepared with two equivalents of H_2O_2, the peak at δ_V = -699.9 p.p.m. due to (*P10*) gradually shifted to -770.6 p.p.m. with a pKa of 6.98, Fig. 4.1. The ^{17}O spectra show a shift from

+1057 p.p.m. to +1021 p.p.m. and a new resonance of equal area (within the accuracy of measurement) at +83 p.p.m. appeared from beneath the water peak, Fig. 4.4. The peak at +1021 p.p.m. was assigned to the oxo ligands and that at +83 p.p.m. to the oxygen of co-ordinated water in $[VO(OH)(OO)_2(OH_2)_2]^{2-}$, (*P9*) which is formed by deprotonation of (*P10*). After further increase to pH > 13 a slight shift in the (*P9*) resonance to δ_V = -769.3 p.p.m. was observed. In the ^{17}O spectra, the resonances at +1021 p.p.m. and +83 p.p.m. broadened and decreased in proportion as a new peak at +602 p.p.m. appeared, Fig. 4.2. This was due to the final deprotonation and a change in co-ordination around vanadium from octahedral to tetrahedral with loss of co-ordinated water to form $[VO_2(OO)_2]^{3-}$, (*P8*).

Between pH 5 and 11 a relatively broad resonance ($\Delta\nu_{\frac{1}{2}}$ = 650 Hz) at δ_V = -766.5 p.p.m. was observed. The dependence of its intensity upon vanadium concentration suggested a dimer. Also, this species is found in maximum proportion in the presence of two equivalents of H_2O_2. Thus, the formula $[\{VO(OO)_2\}_2OH]^{3-}$, (*P11*), is entirely consistent with the data and is in agreement with earlier work[36,37,38]. The ^{17}O resonance due to the terminal oxo ligands was found at +1057 p.p.m. (co-incident with that from (*P10*)) as; (i) this was the only oxygen resonance at pH 6, and; (ii) when (*P9*) was formed its resonance

shifted to +1021 p.p.m. whilst a peak remained at +1057 p.p.m. until approximately pH 11. The equilibrium constant (pKc) for the formation of this dimer was found to be -10.1 $\pm$ 0.33 (27 observations) for the nominal reaction 4.2, whilst in the absence of $Na[ClO_4]$ this decreased to approximately -9.9.

$$2(P9) + H^+ \rightleftarrows (P11) + 5H_2O \qquad (4.2)$$

In the absence of 2 mol dm^{-3} $Na[ClO_4]$ the dimer resonance was observed at δ_V = -762.4 p.p.m., a 4 p.p.m. shift to higher frequency, probably due to a slight change in the angle of the VÔV bridge.

A small peak at δ_V = -737.2 p.p.m. was observed above pH 6 under the same preparative conditions with an increase in relative intensity at higher H_2O_2 concentrations. At pH > 13 the resonance shifted to lower frequency, Fig. 4.1, by up to 96 p.p.m. (an even lower frequency may be detected at higher pH). However, Howarth and Hunt[38] reported a shift to -845 p.p.m. This peak can be assigned to $[V(OH)(OO)_3]^{2-}$, (*P13*), and the shift in δ_V to deprotonation forming $[VO(OO)_3]^{3-}$, (*P12*), with an average signal being observed from fast exchange. The ^{17}O resonance of (*P13*) is at +1014 p.p.m. which shifts to lower frequency on deprotonation, Fig. 4.2. Addition of more than three equivalents of H_2O_2 followed by NaOH gave a purple/black coloured solution of $[V(OO)_4]^{3-}$, δ_V = -737.6 p.p.m.,

as observed previously[38].

Above pH 10 in solutions containing two equivalents of H_2O_2 (*P9*) becomes slightly less favoured forming vanadate and another peroxovanadate species (δ_V = -627.6 p.p.m.). The species has a lower V:(OO) ratio than that intended by this preparation and was also observed in appreciable quantity (up to 25% $[V]_{total}$) when only one equivalent of H_2O_2 was present. Therefore this resonance was assigned as $[VO_2(OH)(OO)]^{2-}$, (*P3*). The ^{17}O data show that the oxo ligands have a shift of +1041 p.p.m. At high pH this resonance decreased in intensity and another peak replaced it at +568 p.p.m., Fig. 4.2. This indicates the more correct formula for (*P3*) to be $[VO_2(OH)(OO)(OH_2)_2]^{2-}$ and is evidence for deprotonation and a change in co-ordination from octahedral (*P3*) to tetrahedral $[VO_3(OO)]^{3-}$, (*P2*). The major resonance in the ^{51}V spectra was δ_V = -769.3 p.p.m., hence this species must have a ^{51}V resonance which is co-incident with that of (*P8*).

If less than two equivalents of H_2O_2 were added (*P3*) was found together with various vanadate species[25] and (*P10*) or (*P9*) dependent upon pH. In addition four new resonances were detected in the ^{51}V spectra, none of which were more than 5% $[V]_{total}$. A peak at δ_V = -636 p.p.m. appeared between pH 10.5 and 12. The other three resonances at -556, -624 and

-743 p.p.m. were observed between pH 7 and 10 (with -624 p.p.m. having a slightly smaller pH range than the other two), Fig. 4.1. The relative intensities of all four resonances exhibit concentration dependences consistent only with dimeric species, and have maximum intensities at (OO):V ratios between 1:1 and 1.5:1. As resonances at δ_V = -556 and -743 p.p.m. occur over exactly the same pH range, these were assigned to the same species. By analogy with the ^{51}V chemical shifts of the monomers this species is thought to be $[HO_3VOVO(OO)_2]^{3-}$, (*P5*). Monoprotonation is inferred because of the near parallel pH range with the known dimer. However, these peaks do not have the same intensity, but the sum of the intensities of the peaks at -556 and -624 p.p.m. equals that at -743 p.p.m. within the accuracy of measurement. By similar arguments the species $[HO_2(OO)VOVO(OO)_2]^{3-}$, (*P6*), can be assigned from the resonances at -624 and -743 p.p.m. The peak at δ_V = -636 p.p.m. is thought to be due to a symmetrical dimer with a V:(OO) ratio of 1:1, as it is in the region of the spectrum where resonances from monoperoxo species are found. An unprotonated dimer is suggested as all protonated dimers are found in the pH range 6-10.5. Therefore, this resonance was assigned as $[\{VO_2(OO)\}_2O]^{4-}$, (*P4*). The observation of the -556 p.p.m. resonance was fortuitous as the region in the ^{51}V spectrum from -535

to -595 p.p.m. contains the vanadate resonances expected at (OO):V ratios lower than 2:1. In fact resonances from other dimers may be observed by overlap or co-incidence of peaks, and the peak at -636 p.p.m. could be from $[O_3VOVO_2(OO)]^{4-}$ with only one ^{51}V resonance detected.

4.2.3 Equilibria

All equilibria were found to be rapidly reversible with the exception of those involving (*P13*) which were found to take several minutes to equilibrate.

4.2.4 Effect of Temperature on the ^{51}V Spectra

On increasing the temperature by 25°C the ^{51}V chemical shift of $VOCl_3$ was found to be 1.1 p.p.m. to higher frequency, in agreement with earlier work[10].

After making an allowance for the change in $VOCl_3$ chemical shift it was observed that some peroxovanadate resonances shift with increasing temperature whilst others do not. There are four major species whose resonances were affected by temperature change; (i) (*P10*) by +4.5 p.p.m., (ii) (*P9*) by +2.5 p.p.m., (iii) (*P13*) by +1.5 p.p.m. and (iv) (*P1*) by between +2 and +7 p.p.m. over a 25°C increase.

4.3 DISCUSSION

The complexation already described resolves the anomalies shown earlier to exist in this system (Section 1.2.1.2). Although some unsymmetrical dimers have been observed (*P5*, *P6* and *P7*) others may be present but not detected because of their low proportions or co-incidence of peaks. The lack of higher polymers can be rationalised by the inability of the (OO) ligand to catenate. Only one peroxovanadate complex containing a peroxide bridge is known[109,110]; $M_3[HV_2O_2(OO)_3F_4].2H_2O$.

Upon substitution of $(O)^{2-}$ by $(OO)^{2-}$ a decrease in ^{51}V chemical shift is generally seen, with the same observation on deprotonation. For instance, δ_V (*P3*) = -627.6 p.p.m. whilst the ^{51}V shift for (*P9*) was -770.6 p.p.m., and on protonation of the latter an increase of 70.7 p.p.m. to -699.9 p.p.m. occurred. ^{51}V chemical shifts in isopolyvanadates tend to be higher for those with octahedral rather than tetrahedral co-ordination; *cf.* octahedral V in V_{10}[14] at $\delta_V \approx$ -423, -498 and -515 p.p.m. and tetrahedral V in other isopolyvanadates[25] range from -535 to -595 p.p.m.

Protonation causes both increases and decreases in ^{17}O chemical shifts for vanadates[25], V_{10} and PV_{14} (see Chapter 3). These have been demonstrated to be due to the amount of double

bond character in tetrahedral vanadates[25], whilst in other isopoly and heteropolymetallates due to co-ordination number[56], bond length[57] and π bond order[58]. In addition, changes in the MÔM bond angle were shown, in Chapter 3, to affect the oxygen shift of bidentate oxygen signals *via* a paramagnetic shift induced by electron circulation from HOMO to LUMO. However, these correlations are of limited use in predicting ^{17}O chemical shifts; for instance bidentate oxygen resonances in V_{10} and PV_{14} are found over a range of 400 p.p.m., and Klemperer[56] has reported similar observations for isopolymolybdate species.

In the present study, all the ^{51}V spectral assignments are consistent with the limited understanding already described. However, the ^{17}O spectra, which can be thought of as comprising three regions, were not as anticipated, Fig. 4.2. These regions contained resonances from co-ordinated water (0-100 p.p.m.), tetrahedrally co-ordinated $(O)^{2-}$ or $(OH)^{-}$ (550-650 p.p.m.) and octahedrally co-ordinated $(O)^{2-}$ or (OH^{-}) (1000-1250 p.p.m.).

Bonds between the metal ion and co-ordinated water are weak. The use of both remaining *p* orbitals in covalent bonding to hydrogen in water will strongly inhibit ligand-to-metal charge transfer, from which the chemical shift largely arises. Thus, the ^{17}O shift of co-ordinated water would be expected to be extremely close to that observed for bulk solvent

(δ_O = 0), if distinguishable at all. In the octahedral hydrated oxodiperoxopyridine-2,6-dicarboxylate V^V complex, the V-OH_2 bond length is 2.21 Å whilst the V-O length is 1.58 Å showing the inequality of these two ligands. In addition, in V_{10} octahedrally co-ordinated O_a, Fig. 1.1, has a ^{17}O shift of ∿ 70 p.p.m., Fig. 3.3, and V-O_a bond lengths[6] range from 2.12 to 2.32 Å.

In the 550-650 p.p.m. region tetrahedral vanadate species $[VO_4]^{3-}$ and $[HVO_4]^{2-}$ have ^{17}O chemical shifts[25] at +565 and +573 p.p.m. respectively. Whilst for octahedrally co-ordinated V this region lies between those observed for di- and trico-ordinate oxygens, Figs. 3.3 and 3.4. Those ^{17}O shifts from (*P2*) and (*P8*), at +568 and +602 p.p.m. respectively, indicate these to have tetrahedrally co-ordinated V. The small differences on replacing $(O)^{2-}$ for $(OO)^{2-}$ could be due to a slight increase in the multiple-bond character of the V-O bond. In the vanadate species $[VO_4]^{3-}$ each V-O bond has the same formal multiple-bond character. A slight increase in that for V-O bonds in peroxovanadates implies that the V-(OO) bonds also have a bond order > 1 but lower than that in the V-O bond.

The third region in the ^{17}O spectrum, 1000-1250 p.p.m., has been assigned to $(O)^{2-}$ or $(OH)^-$ in octahedral complexes. Previously, resonances from

terminal oxygen ligands bound to octahedral vanadium were found in this range, Figs. 3.3 and 3.4, whilst similar values have been reported for isopolymolybdates and tungstates[56] (after a scaling due to a change of metal). Hence, the resonances from, at least, monomeric mono- and diperoxo species in this region can be attributed to oxo ligands in octahedral complexes.

The large variation in ^{17}O shifts between those for tetrahedral and octahedral complexes is thought to be due to competition between the oxo ligands for vacant *d* orbitals on vanadium[160]. For tetrahedral V, the strongly bound $(O)^{2-}$ or $(OH)^{-}$ ligands often vie for the same *d* orbital. In the octahedral complexes, to maintain the valence of the vanadium, the bond order of the V-O or V-(OO) bonds must be decreased because of the two $V-OH_2$ bonds and the V-O bond length is increased. The ligand *trans* to oxo (and in competition with it for that *d* orbital) could be either OH_2 or $(O)^{2-}$ or $(OH)^{-}$, which have a lower ability to compete for that orbital and the ^{17}O shift increases. In support of this proposal is the observation of a markedly less intense yellow coloured solution when the unprotonated tetrahedral peroxovanadate species are present than the protonated octahedral species.

In the octahedral complex when the solvent exchange is sufficiently slow, a resonance for

co-ordinated water will be observed. This is true for (*P9*) which gives peaks at +1021 and +83 p.p.m. To allow rapid proton exchange between $(O)^{2-}$ and $(OH)^{-}$ in (*P9*) and observe one resonance, the $(O)^{2-}$ and $(OH)^{-}$ must be mutually *cis*, as probably are each other ligand pair. Similar arguments apply for (*P10*) as its exchange with (*P9*) is rapid. Analogous compounds have been shown to prefer $(O)^{2-}$ *trans* to H_2O[131] whilst another[106] favours the oxo ligand *trans* to a long V-O bond to an oxygen in the adjacent anion. Other compounds[106,112,125] contain peroxide ligands *cis* to each other.

On the basis of the above arguments for octahedral co-ordination the protonated monoperoxo species, (*P3*) has the formula $[VO_2(OH)(OO)(OH_2)_2]^{2-}$. Deprotonation changes the co-ordination sphere from octahedral, (*P3*), to tetrahedral, (*P2*) with (*P2*) in slow exchange with the octahedral form, (*P3*), by analogy with (*P9*) and (*P8*).

The co-ordination of (*P13*) and (*P11*) is undetermined from the above discussion. In the case of (*P13*) there are no strongly bound, competing $(O)^{2-}$ or $(OH)^{-}$ ligands, hence the large ^{17}O chemical shift. (*P11*) is known to have tetrahedral co-ordination[39], with the proton bound to the bridging oxygen[41]. The oxo ligand on one V has little competition for *d* orbitals as the bridging oxygen is bound to the other V (with a V-O bond

length of 2.01 Å) and H making it similar to co-ordinated water. Thus, a large ^{17}O shift would be expected.

Further reduction in the number of ligands able to compete with $(O)^{2-}$ in π bonding allows an increase in ^{17}O shift, as observed for (*P1*). Similar observations emphasising this tendency have been made for $VOCl_3$ (δ_O = +1350 p.p.m., neat liquid) and $VO(NO_3)_3$ (δ_O = +1398 p.p.m., in CH_3CN)[162]. All attempts made to detect a resonance for $[VO_2]^+$ were unsuccessful presumably because of rapid oxygen-exchange with the solvent.

4.4 CONCLUSIONS

The use of ^{17}O n.m.r. has increased the understanding of the peroxovanadate complexation, yielding information on their co-ordination spheres and resolving the previous anomaly of the unprotonated monoperoxo species. Also high-field ^{51}V n.m.r. has facilitated the detection of previously unknown unsymmetrical dimers.

length of 2.01 Å) and H making it similar to co-ordinated water. Thus, a large ^{17}O shift would be expected.

Further reduction in the number of ligands able to compete with $(O)^{2-}$ in π bonding allows an increase in ^{17}O shift, as observed for (*P1*). Similar observations emphasising this tendency have been made for $VOCl_3$ (δ_O = +1350 p.p.m., neat liquid) and $VO(NO_3)_3$ (δ_O = +1398 p.p.m., in CH_3CN)[162]. All attempts made to detect a resonance for $[VO_2]^+$ were unsuccessful presumably because of rapid oxygen-exchange with the solvent.

4.4 CONCLUSIONS

The use of ^{17}O n.m.r. has increased the understanding of the peroxovanadate complexation, yielding information on their co-ordination spheres and resolving the previous anomaly of the unprotonated monoperoxo species. Also high-field ^{51}V n.m.r. has facilitated the detection of previously unknown unsymmetrical dimers.

5. SULPHIDO- AND OXOSULPHIDOVANADIUM(V) SPECIES

5.1 EXPERIMENTAL

The preparation of the sulphido- and oxosulphidovanadium(V) complexes has already been described in Section 2.4.3. U.v./visible spectra, used to check the solid state reaction products, were obtained using a Shimadzo UV-365 spectrophotometer, operated according to the manufacturer's instructions.

Between 1000 and 10000 transients were accumulated to obtain ^{51}V n.m.r. spectra at 105.2 MHz, at a rate of approximately 10 per second. Three overlapping sections were required to cover the whole spectrum due to the large chemical shift range (+1500 to -600 p.p.m.). For each of these three regions a spectral width of 150 KHz and a pulse length of 7 μs ($\sim 30^{o}$ flip angle) were used. ^{51}V shifts were reproducible to within ± 1 p.p.m.

^{31}P n.m.r. spectra at 162 MHz were similarly obtained, but required 32 transients, a spectral width of 10 KHz and a pulse width of 12 μs ($\sim 45^{o}$ flip angle). The ^{31}P chemical shifts could be reproducibly measured to within ± 0.01 p.p.m. From the ^{31}P chemical shift of the phosphate resonance, the pH could be determined, as described earlier (Section 2.5).

5.2 RESULTS AND DISCUSSION

Table 5.1 contains a list of species observed in this work with their n.m.r. data, for comparison vanadate data can be found in Table 1.1. The notation used in Table 5.1 will be employed throughout this chapter. Figs. 5.1 and 5.2 show typical ^{51}V n.m.r. spectra obtained for solutions at high and low pH respectively. Fig. 5.3 indicates the effect of pH on ^{51}V chemical shift for those sulphidovanadate species present at > 5% $[V]_{total}$.

5.2.1 General Observations

The monosulphido species, (*S1*) and (*S2*), in Table 5.1 are previously unreported, as are all the dimeric complexes. No ^{51}V resonances have previously been reported for these species nor their acid dissociation constants measured.

Before the ^{51}V chemical shifts and assignments are discussed, the preparation of these new species are considered as these show a number of significant differences between the sulphidovanadate(V) and oxovanadium(V) species. The main dissimilarity is that vanadate species are all in kinetic equilibrium[25], whilst there are few equilibria involving sulphido-vanadium(V) complexes. At lower pH ($\sim$ 7.4) this is indicated by large variations in peak area for the

5.2 RESULTS AND DISCUSSION

Table 5.1 contains a list of species observed in this work with their n.m.r. data, for comparison vanadate data can be found in Table 1.1. The notation used in Table 5.1 will be employed throughout this chapter. Figs. 5.1 and 5.2 show typical ^{51}V n.m.r. spectra obtained for solutions at high and low pH respectively. Fig. 5.3 indicates the effect of pH on ^{51}V chemical shift for those sulphidovanadate species present at > 5% $[V]_{total}$.

5.2.1 General Observations

The monosulphido species, (*S1*) and (*S2*), in Table 5.1 are previously unreported, as are all the dimeric complexes. No ^{51}V resonances have previously been reported for these species nor their acid dissociation constants measured.

Before the ^{51}V chemical shifts and assignments are discussed, the preparation of these new species are considered as these show a number of significant differences between the sulphidovanadate(V) and oxovanadium(V) species. The main dissimilarity is that vanadate species are all in kinetic equilibrium[25], whilst there are few equilibria involving sulphido-vanadium(V) complexes. At lower pH ($\sim$ 7.4) this is indicated by large variations in peak area for the

Table 5.1 Sulphidovanadate Species Identified in this Study

Number of S around one V atom	1	2	3	4
(a) Monomers				
#	*S1*	*S3*	*S5*	*S7*
Formula	$[VO_3S]^{3-}$	$[VO_2S_2]^{3-}$	$[VOS_3]^{3-}$	$[VS_4]^{3-}$
δ_V/p.p.m.	-250	+184	+740	+1395
$\Delta\nu_{\frac{1}{2}}$/Hz	130	90	60	< 40
Colour in solution	Yellow	Brown	Magenta	Magenta
#	*S2*	*S4*	*S6*	*S8*
Formula	$[HVO_3S]^{2-}$	$[HVO_2S_2]^{2-}$	$[HVOS_3]^{2-}$	$[HVS_4]^{2-}$
δ_V/p.p.m.	-121	> +230	+748	+1392
$\Delta\nu_{\frac{1}{2}}$/Hz	160		80	40
pKa[a]	10.5	~9.8	9.8	7.3
(b) Dimers				
#	*S9*	*S10*	*S11*	
Formula	$[V_2O_6S]^{4-}$	$[V_2O_4S_3]^{4-}$	$[V_2S_7]^{4-}$	
δ_V/p.p.m.	~198	~220	+1457	
pKc[b]			-4.8 ± 0.4	

a for loss of one proton

b for *S1* + *S8* ⇌ *S11* + $[HS]^-$

Fig. 5.1 Typical ^{51}V n.m.r. spectrum of sulphidovanadates (pH > 13, 3.2×10^{-3} mol dm^{-3} in vanadium).

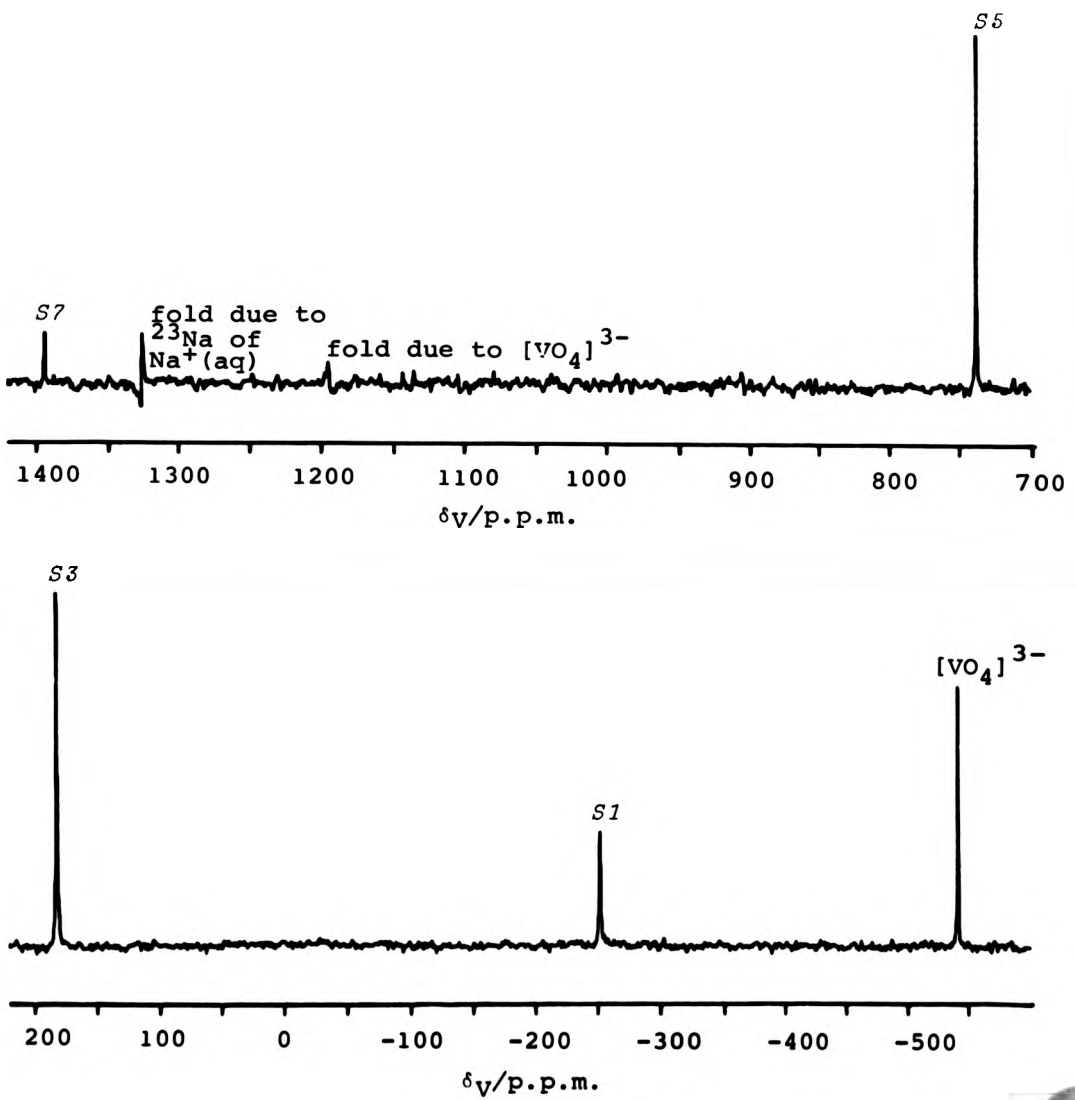

Fig. 5.2 Typical ^{51}V n.m.r. spectrum of sulphidovanadates (pH 7.25, 0.012 mol dm^{-3} in vanadium).

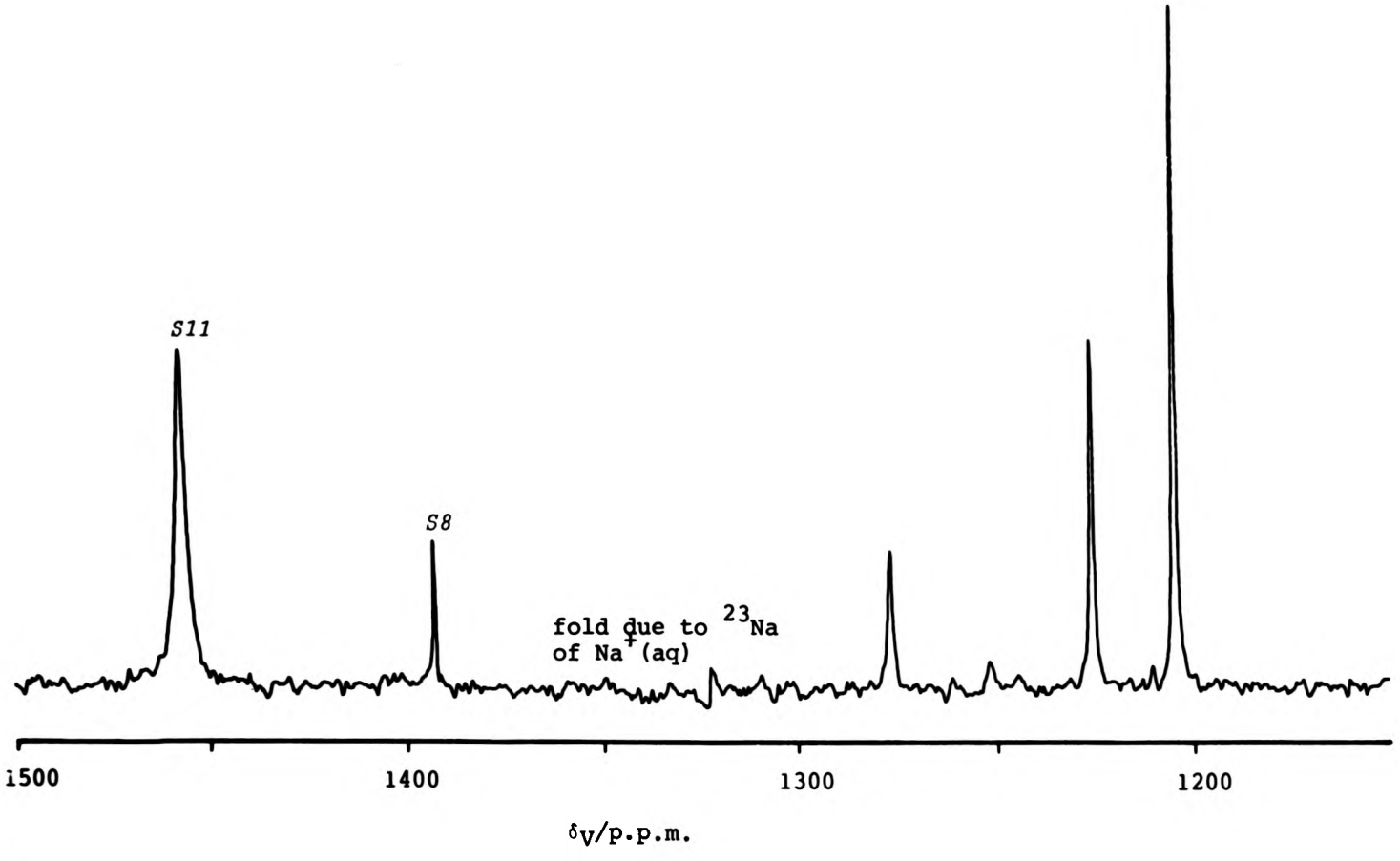

Fig. 5.3 Plot of ^{51}V chemical shifts of sulphidovanadates *versus* pH. Species are numbered as in Table 5.1.

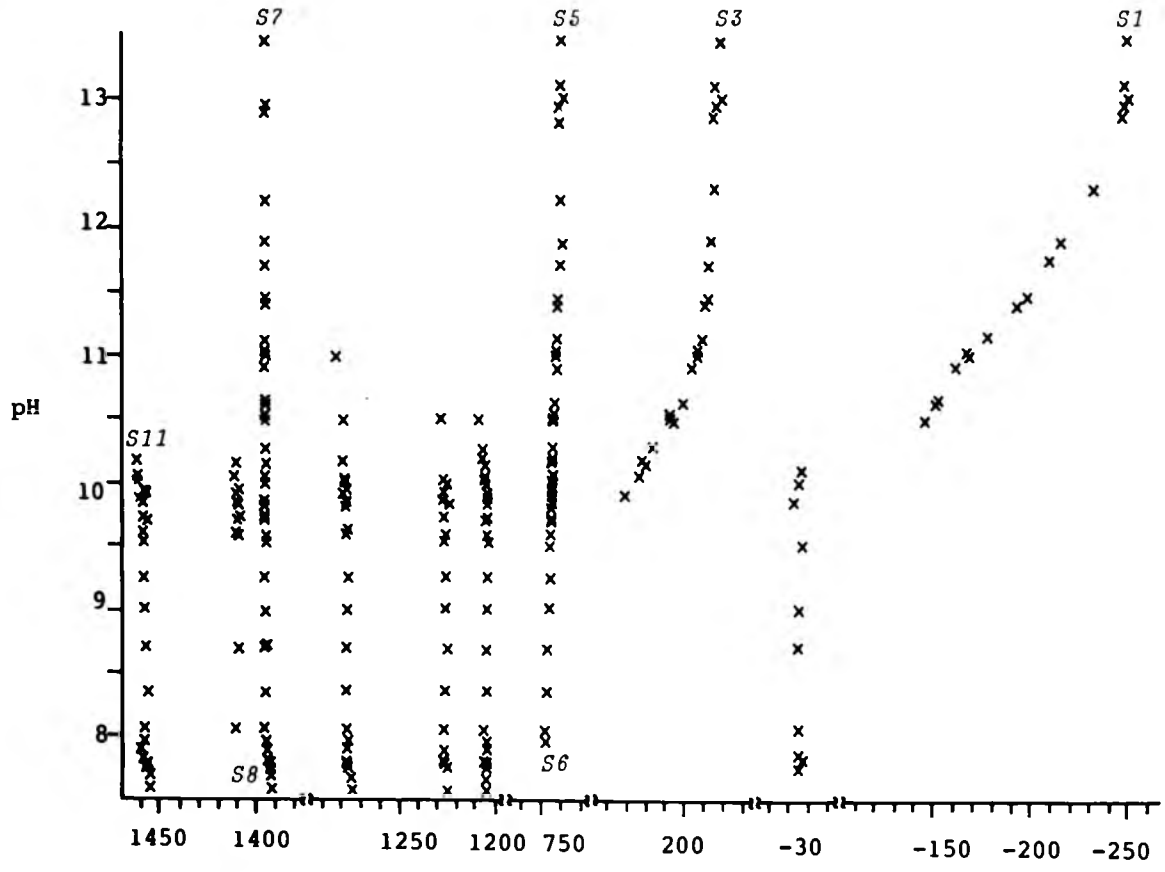

Fig. 5.3 Plot of ^{51}V chemical shifts of sulphidovanadates *versus* pH. Species are numbered as in Table 5.1.

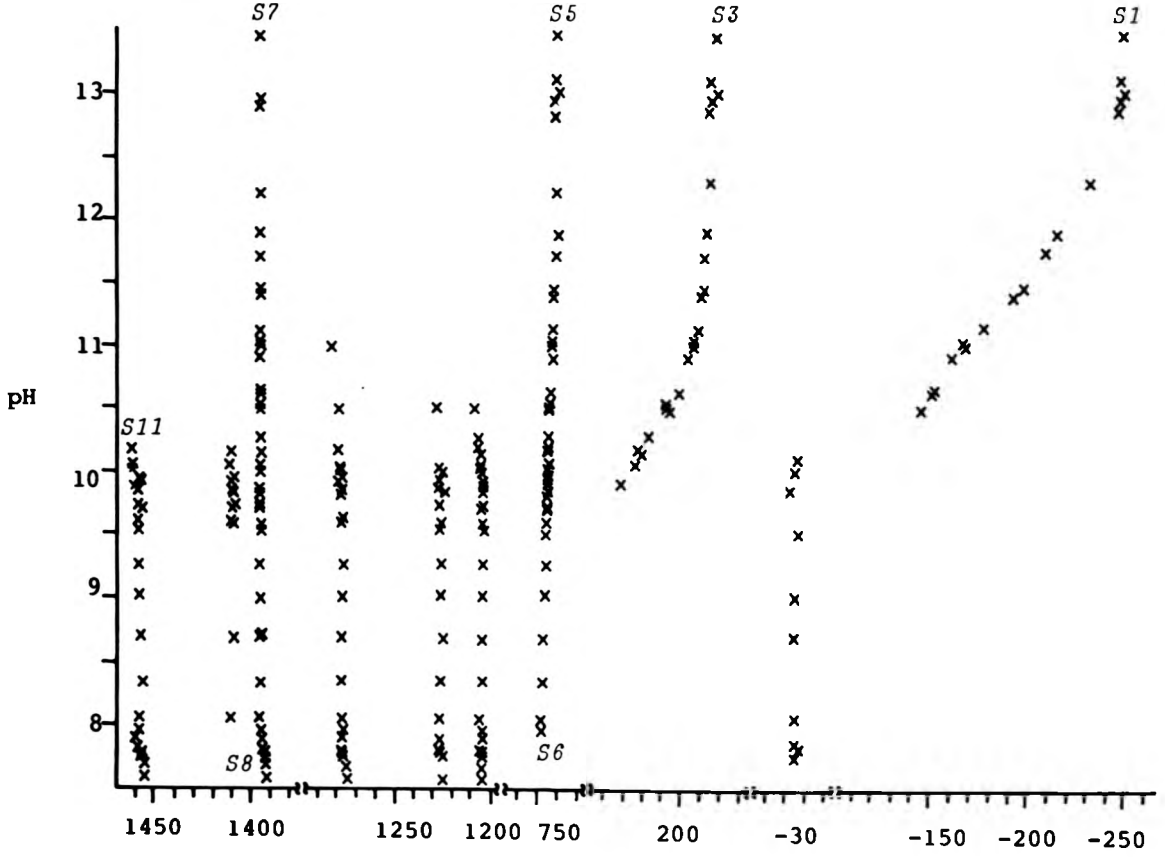

resonances between +1200 and +1500 p.p.m., using near-identical pH, $[V]_{total}$, $[HS]^-$, but different preparative methods. These peak areas remained constant, within the accuracy of measurement, for several hours.
Above pH 10, Fig. 5.3, the species with resonances at lower frequency steadily increased in proportion until the resonance from monomeric vanadate at $\delta_V \approx -540$ p.p.m. was the largest peak. At even higher pH all the vanadium appeared as $[VO_4]^{3-}$. A slow relative increase in the intensity of these peaks was also found with time. Earlier work[83,163] reported a slow decrease in the uv/vis absorption of (*S?*) with time (approx. ½ to 1 hour) when dissolved in 1 mol dm^{-3} NaOH. From these two observations it can be deduced that slow hydrolysis of V-S bonds occurs with $[OH]^-$ but not H_2O. Also they suggested from the inertness at pH 7.4 that $[HS]^-$ cannot attack V-O or V-OH bonds. Further evidence for the latter conclusion is the lack of reaction of sodium sulphide with vanadate to form sulphido complexes over the pH range 7-13, even in the presence of buffer to control pH. These observations indicate that the formation of sulphidovanadates described in Section 2.4.3.1.1 must be able to take place either because H_2O is available as the leaving group at pH < 7[25], equation 5.1, or by concerted reactions with an initial

$$[HVO_4]^{2-} + H^+ \rightleftharpoons [H_2VO_4]^- \qquad (5.1)$$

pKa = 7.1[25]

proton transfer taking place, e.g. equation 5.2.

$$H_2S + [HVO_4]^{2-} \rightarrow \{[HS]^- + [H_2VO_4]^-\} \rightarrow S2 + H_2O \qquad (5.2)$$

The titration curves in Fig. 5.3 for (*S1*) and (*S3*) end at just below their pKa values. Acidification by H_2S in an attempt to extend these curves led to the formation of (*S5*) and (*S7*), confirming that reactions such as 5.2 lead to the appearance of species with higher S:V ratios.

However, attack on V-S bonds must take place to form the dimeric species (*S11*), (evidence for this complex is presented later), by equilibria such as that in equation 5.3. Thus, the nucleophile in these equilibria could be either $[HS]^-$ or $[VO_nS_{4-n}]^{3-}$

$$S7 + S8 \rightleftharpoons S11 + [HS]^- \qquad (5.3)$$

(n = 0 to 4) or their protonated forms. In earlier work[25], $[HVO_4]^{2-}$ was shown to be the principal nucleophile in vanadate equilibria.

Unlike vanadate, which forms V_{10} below pH 7, the presence of sulphide causes reduction of V^V to V^{III} at this pH. Raising $[V]_{total}$ or lowering $[HS]^-$increases the rate of reduction as effectively as lowering the pH, perhaps by polymerisation assisting reduction. This means that $[V]_{total}$ has

to be limited to a maximum of approximately 0.01 mol dm^{-3} which considerably limits the extent to which any polymerisation equilibria can be studied.

5.2.2 Complexation and Assignment of Resonances

5.2.2.1 Monomers

At pH 13 four resonances at δ_V = +1395, +740, +184 and -251 p.p.m. are observed in addition to the vanadate resonance. The predominant vanadate species[25] at this pH is monomeric, thus by analogy, these peaks are assigned to *(S7)*, *(S5)*, *(S3)* and *(S1)* respectively. Two other observations support this assignment. Firstly, $Na_3[VOS_3]$ has been claimed[81], from u.v./visible spectra, to be the major product formed by reaction of V_2O_5, Na_2CO_3 and S in a melt containing the reactants in the correct stoicheiometric ratio (Section 2.4.3.2.2). This reaction was undertaken, the solid from the cooled melt extracted with a saturated solution of Na_2S, and resonances at δ_V = +733 (> 75% $[V]_{total}$), +184 and -253 p.p.m. were found. This indicated the formation of $Na_3[VOS_3]$ (major product), $Na[VO_2S_2]$ and $Na_3[VO_3S]$ respectively. The u.v./vis spectrum showed peaks at 521, 456, 326 and 295 nm in agreement with the literature spectrum. On increasing the V_2O_5:S ratio a higher proportion of $Na_3[VO_2S_2]$ and $Na_3[VO_3S]$ can be observed. In each case a resonance

due to some unreacted vanadate is detected, with its relative intensity increasing with lower V_2O_5:S ratios in the reaction. Various solid salts containing (*S7*) have been prepared by the reaction of the elements[75,77,78]. The sodium salt was prepared by this method (Section 2.4.3.2.1), extracted with a saturated Na_2S solution and a resonance at δ_V = +1390 p.p.m. detected. The u.v./vis spectrum of (*S7*), recorded immediately after dissolving, gave absorbances at 539 (ε_1 = 5720 mol^{-1} cm^{-1}), 393, 350 and 266 nm in agreement with the reported spectrum[71,163]. Secondly, when the ^{51}V chemical shift is plotted against the number of sulphur atoms per vanadium, Fig. 5.4, the expected trend for replacement of oxo ligands at vanadium is found. Recently, the molybdenum -95 chemical shifts, for the analogous molybdenum complexes, have been published, and they exhibit the same trend (also plotted in Fig. 5.4).

As the pH is lowered the chemical shifts of the monomers, apart from (*S7*), increase in frequency due to protonation. In the case of (*S7*), sulphur must be protonated whilst in the oxosulphido species the site is probably oxygen. Computer fitting of the data to the curve predicted by the Henderson-Hasselbach equation, 5.4, gave pKa values of

$$pH = pKa + \log \frac{[salt]}{[acid]} \qquad (5.4)$$

due to some unreacted vanadate is detected, with its relative intensity increasing with lower V_2O_5:S ratios in the reaction. Various solid salts containing (*S7*) have been prepared by the reaction of the elements[75,77,78]. The sodium salt was prepared by this method (Section 2.4.3.2.1), extracted with a saturated Na_2S solution and a resonance at δ_V = +1390 p.p.m. detected. The u.v./vis spectrum of (*S7*), recorded immediately after dissolving, gave absorbances at 539 (ε_1 = 5720 mol^{-1} cm^{-1}), 393, 350 and 266 nm in agreement with the reported spectrum[71,163]. Secondly, when the ^{51}V chemical shift is plotted against the number of sulphur atoms per vanadium, Fig. 5.4, the expected trend for replacement of oxo ligands at vanadium is found. Recently, the molybdenum -95 chemical shifts, for the analogous molybdenum complexes, have been published, and they exhibit the same trend (also plotted in Fig. 5.4).

As the pH is lowered the chemical shifts of the monomers, apart from (*S7*), increase in frequency due to protonation. In the case of (*S7*), sulphur must be protonated whilst in the oxosulphido species the site is probably oxygen. Computer fitting of the data to the curve predicted by the Henderson-Hasselbach equation, 5.4, gave pKa values of

$$pH = pKa + \log \frac{[salt]}{[acid]} \qquad (5.4)$$

Fig. 5.4 Comparison of chemical shifts of (X) monomeric sulphidovanadate(V) and (O) sulphidomolybdate(VI) species[85].

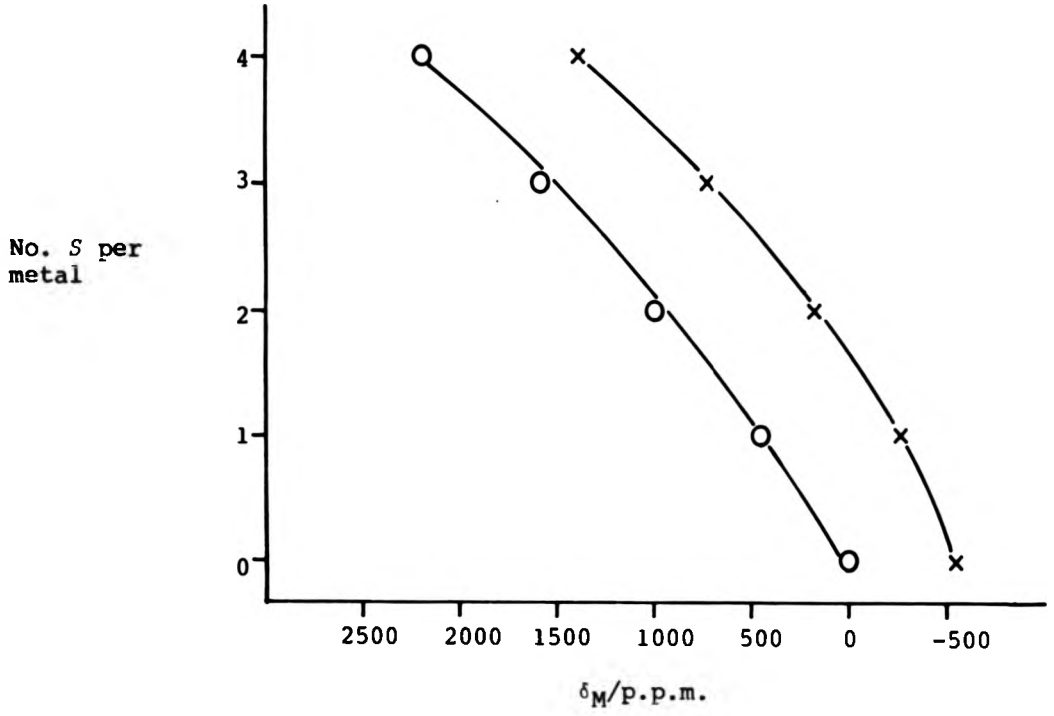

7.3, 9.4, ∿9.8 and 10.5 for the protonation of (*S7*), (*S5*), (*S3*), and (*S1*) respectively in 2 mol dm^{-3} $Na[ClO_4]$. In other studies of vanadium(V) complexes[25] (see also Chapter 4) the pKa values have been measured with and without the presence of $Na[ClO_4]$. Similar results were found in this study to those observed earlier. The pKa values were 0.5 to 1.5 units lower when 2 mol dm^{-3} $Na[ClO_4]$ was present. Throughout this project this has been attributed to the presence of the salt favouring species with higher negative charge. In this study the first protonation of the phosphate ion, equation 5.5, was used to determine

$$[PO_4]^{3-} + H^+ \rightleftharpoons [HPO_4]^{2-} \qquad (5.5)$$

the pH of the solutions (Section 2.5). The pKa of this equilibrium was observed to decrease from 12.12 to 10.7 on a change of medium from no added salt to 2 mol dm^{-3} $Na[ClO_4]$.

In Fig. 5.3 it can be seen that the titration curves for (*S1*) and (*S3*) are incomplete, whilst an accurate value for the pKa for protonation of (*S1*) and the ^{51}V chemical shift of its protonated form, (*S2*), are quoted, Table 5.1. Ranade, *et al.*[80] suggested, from u.v./visible spectroscopy, that (*S1*) is formed by the reaction of $Na_3[VO_4]$ and Na_2S in methanol. When the ^{51}V spectrum of $Na_3[VO_4]$ was recorded it was

found to contain three resonances at -531.2, -546.4 and -566.5 p.p.m. These are assigned to $[VO_3(OMe)]^{2-}$, $[HVO_4]^{2-}$ and $[V_2O_7]^{4-}$ respectively, by comparison with vanadate data, Table 1.1. On addition of Na_2S, with gentle shaking, a yellow colour appeared (within approximately 1 minute) together with another resonance at -120.0 p.p.m. This resonance was assigned to either $[VO_2S(OMe)]^{2-}$ or (*S2*), which is in agreement with the data gained from the aqueous preparation (Section 2.4.3.1.1).

Earlier in the chapter it was noted that the substitution of S for O occurs only as the pH approaches the pKa for the deprotonation of the species with higher S:V ratio. (The solutions initially contained (*S7*) and its oligomers at approximately pH 7 to 7.5, and with addition of alkaline $[HS]^-$, as "sodium sulphide solution", the pH was increased.) This indicates that hydrolysis should involve the deprotonated species with reactions of type $[VS_nO_{4-n}]^{3-} + [OH]^- \rightarrow [VS_{n-1}O_{5-n}]^{3-} + [HS]^-$. This observation further supports the assignment of the resonances of the monomeric species.

5.2.2.2 Oligomers

The few equilibria involving sulphido-vanadates involve the formation of oligomeric species. In Fig. 5.3 a number of resonances are observed

between δ_V = +1200 and +1500 p.p.m. from pH 7 to 10. At this pH most vanadate species are polymeric. By analogy some new polysulphidovanadate species were expected to be found in low proportion because of the limit imposed on $[V]_{total}$ due to reduction of V^V by sulphide. In this study three dimeric species were observed.

In an attempt to find possible equilibria between species giving resonances in the δ_V = +1200 to +1500 p.p.m. region, a selective excitation experiment[164] (DANTE) was employed. The aim was to observe transfer of excitation *via* complex equilibria to other resonances. The initial excitation was undertaken using a long, soft pulse, but as vanadium is a quadrupolar nucleus the relaxation time and speed of the equilibria were the determining factors in the experiment. If the equilibria are slow, very little excitation is transferred for observation during the acquisition of the FID. If a delay to allow transfer is used, quadrupolar relaxation will occur and no signal will be observed. In each experiment only one resonance was detected with a slightly lower signal-to-noise ratio for a given number of accumulated transients in comparison with a normal spectrum. This indicates that any equilibria are relatively slow.

Only one resonance (δ_V = +1457 p.p.m.) exhibited a consistent intensity relationship with $[V]_{total}$, and this showed it to be dimeric. The best fit for the equilibrium

constant suggests that the resonance at δ_V = +1457 p.p.m. is due to $[V_2S_7]^{4-}$, (*S11*). Equation 5.3 describes the formation of (*S11*) with a pKc = -4.8 ± 0.4 (the amounts of (*S7*) and (*S8*) were calculated using the theoretical Henderson-Hasselbach relationship, equation 5.4). The other peaks in the +1200 - +1500 p.p.m. region may be due either to other symmetrical higher polymers (e.g. $[V_5S_{15}]^{5-}$, $[V_4S_{12}]^{4-}$, $[V_4S_{13}]^{6-}$) or to complexes containing persulphide or catenated sulphide ligands (see next section).

At higher pH, as the resonances due to the (*S3*)/(*S4*) and (*S1*)/(*S2*) species pass through their pH inflexion, broadening is observed, Fig. 5.5. In the latter case another resonance is found at approximately -198 p.p.m. over a narrow pH range about 11.0. Each observation showed a peak located at this frequency. On increasing $[V]_{total}$ the integral of this component varied in a manner consistent with it being the dimeric anion $[O_3VSVO_3]^{4-}$, (*S9*). The equilibrium, equation 5.6, is postulated

$$S1 + S2 \rightleftharpoons S9 + [HS]^- \qquad (5.6)$$

to be analogous to that forming (*S11*), equation 5.3. The data obtained do not allow the calculation of an equilibrium constant as there are few observations

Fig. 5.5 ^{51}V n.m.r. spectra showing equilibrium between *(S1)*, *(S2)* and *(S9)*.

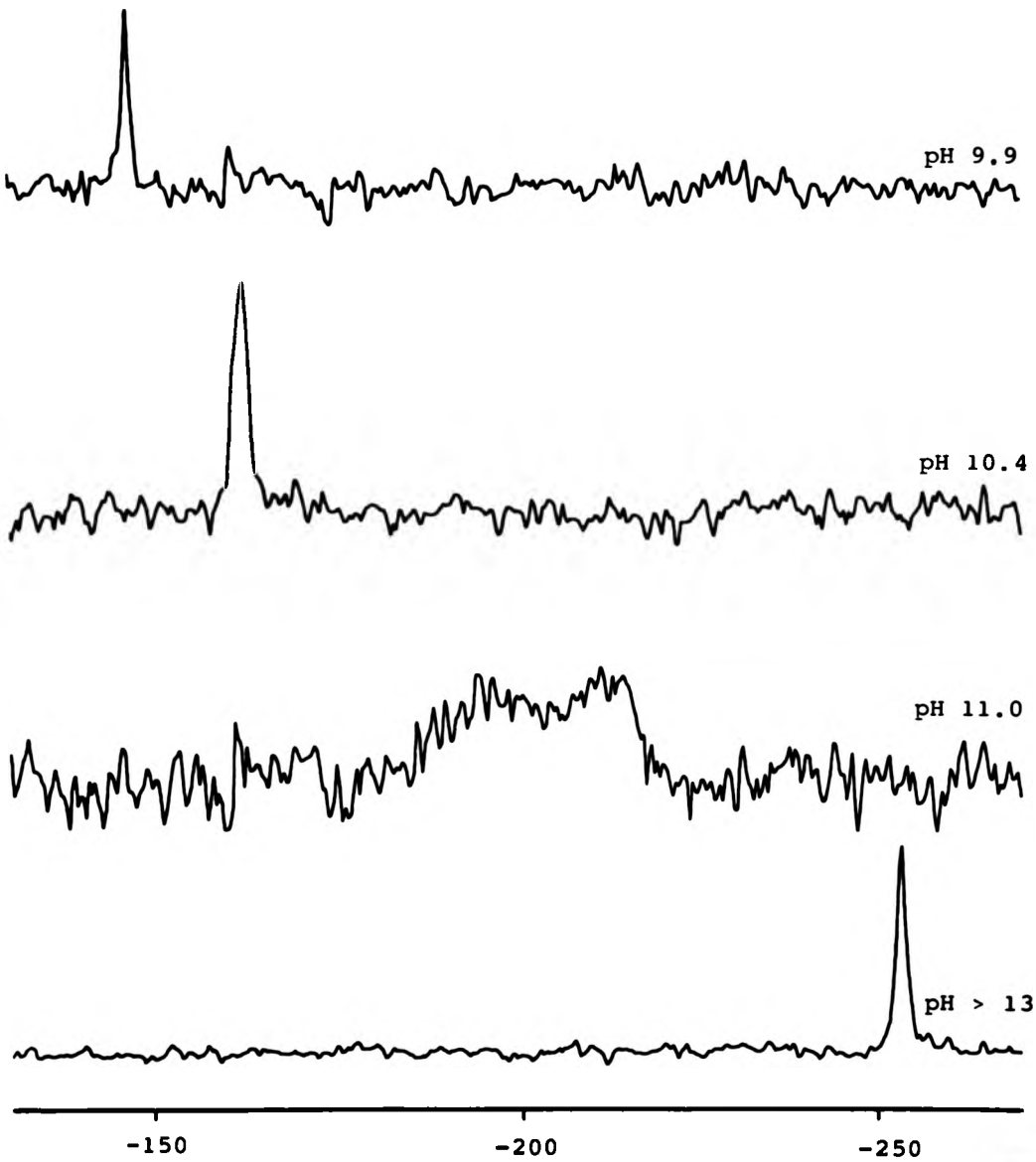

of the resonance from (*S9*). However, qualitatively a lower pKc should be found for equilibrium 5.6 than for that forming (*S11*) because the polymer is less favoured.

As no splitting of resonances is observed at the disulphido pH inflexion, by implication the broadening is assigned to the formation of $[O_2SVSVO_2S]^{4-}$, (*S10*), at approximately pH 9.6. The equilibrium is described by equation 5.7.

$$S3 + S4 \rightleftharpoons S10 + [HS]^- \qquad (5.7)$$

5.2.2.3 Catenated Sulphide Species

As described above, only the resonance at δ_V = +1457 p.p.m. in the +1200 to +1500 p.p.m. region can be assigned to a polymeric species from its concentration dependence. None of the peaks in this region of the spectrum have constant integral ratios, indicating no unsymmetrical polymers to be present, apart from any obscured by accidental coincidence of resonances. This leaves the possibility of catenated sulphur ligands[165] complexing with vanadium. Catenated sulphide complexes of molybdenum have been found previously, for instance $[Mo(S)(S_4)_2]^{2-}$, ref. 166, $[Mo_2S_2(\mu\text{-}S)_2(S_2)(S_4)]^{2-}$, ref. 167, $[Mo_2(S_2)_6]^{2-}$, ref. 167 and $[Mo_3S_{13}]^{2-}$, ref. 168.

It is feasible that catenated sulphide

ligands could complex with vanadium and form monomeric or symmetrical polymeric species giving rise to the, as yet, unassigned resonances in the +1200 to +1500 p.p.m. region of the spectrum.

5.2.3 Chemical Shifts

The ^{51}V chemical shifts found in this study exhibit the same trend as the ^{95}Mo shifts[85] on replacement of oxygen by sulphur, Fig. 5.4. In addition, the same trend is observed on increasing the number of chloride ligands attached to vanadium[87]; $\delta_V([VO_2Cl_2]^-)$ = -364 p.p.m., δ_V ($[VOCl_3]$) = 0 p.p.m. and δ_V ($[VOCl_4]^-$) = +43 p.p.m. Thus, vanadium shows the common feature of transition metal complexes containing the metal in the d^0 configuration, an increase in nuclear shielding with increasing electronegativity, or 'hardness', of the attached ligands[169].

Recently, ^{51}V chemical shift calculations have been undertaken by Becker and Berlage[75], and Howarth[151] for a number of tetrahedral vanadium(V) species. These were based on proposals made by Jameson and Gutowsky[170]. The diamagnetic contribution to the chemical shift of the core electrons on vanadium (effectively the "V^{5+}" ion) and the paramagnetic contribution from the valence electrons in the molecular orbitals were quantified to give a ^{51}V shift. Howarth's[151]

calculations, including those for the monomers found in this study, showed a correlation between calculated and observed chemical shift, Fig. 5.6. Thus, the chemical shifts found in this study are consistent with the formulae proposed for the sulphonovanadate species.

5.3 CONCLUSIONS

The chemistry and physical properties of sulphidovanadate species show large differences to the vanadate complexes. The differences in chemical shift almost certainly arise from the lower orbital energies and larger radii of the sulphur orbitals.

The lowering of the pKa on replacement of oxygen by sulphur can be rationalised in terms of the V-O bond strength. The strength of the short V-O bond is increased because of secondary $p \rightarrow d$ π-bonding, unlike the V-S bond. On replacement of O by S the strength of a given π-bond is increased. A similar observation is found for Mo^{VI} complexes[85]. Gradual replacement of O by S in $[MoO_4]^{2-}$ results in an increase in the ^{17}O chemical shift; $\delta_O([MoO_4])^{2-}$ = 544 p.p.m., $\delta_O([MoO_3S]^{2}$ 624 p.p.m., $\delta_O([MoO_2S_2]^{2-})$ = 696 p.p.m. and $\delta_O([MoOS_3]^{2-})$ = 759 p.p.m. Miller and Wentworth[57] showed an inverse correlation between the ^{17}O chemical shift of an oxometallate anion and the M-O bond length.

Fig. 5.6 Calculated *versus* observed chemical shift of vanadium(V) species[151]. In ascending observed shift order, VOF_3 (in THF and $CHCl_3$), $[VO_4]^{3-}$, (*S1*), $VOCl_3$, (*S3*), $VOBr_3$, (*S5*), (*S7*) and $Tl[VSe_4]$ (solid state).

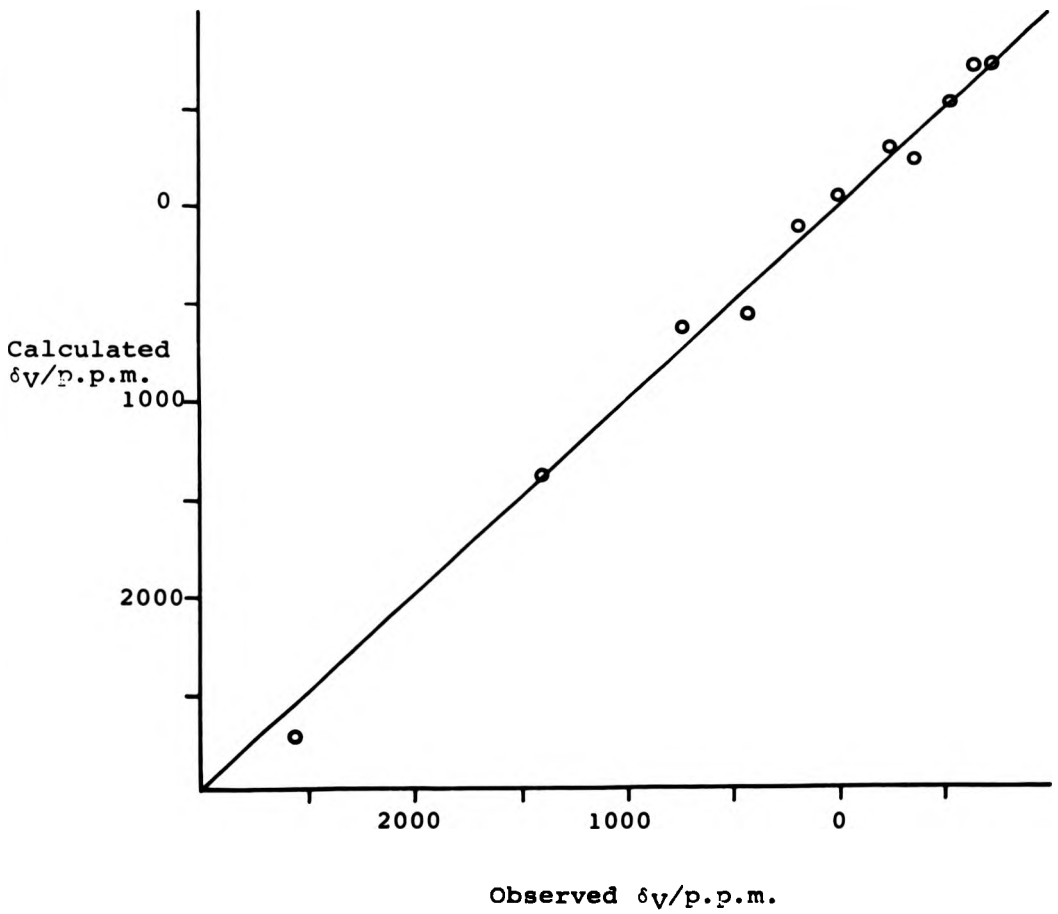

The replacement of O by S in Mo^{VI} complexes shows a shortening of the Mo-O bond length and thus the oxygen is more tightly bound to Mo. As the V-O bond strength is increased, it will be harder to protonate the oxygen, and this explains the observed trend of a lower pKa for those species with more S ligands. This argument also implies that the V-S bond is relatively long in comparison to the V-O bond, and is much weaker.

The lack of potency of $[HS]^-$ as a nucleophile towards vanadate may be partially due to the weak V-S bond, as it seems to attack only $V\text{-}OH_2$ bonds. However, the relatively rapid monomer-dimer equilibria forming (*S9*) and (*S10*) is surprising in view of this observation. Thus, an alternative equilibrium can be suggested, equation 5.8, which is similar to that found previously for vanadates[25].

$$[V^*O_3S]^{3-} + [O_3VSVO_3]^{4-} \rightleftharpoons [O_3V^*SVO_3]^{4-} + [VO_3S]^{3-} \quad (5.8)$$

The sulphidovanadates tend to form dimers, but not higher oligomers. In each case the bridging ion is sulphide which reduces steric and electrostatic repulsion and also minimises any effects on the strong V-O bond.

6. INTERACTION OF VANADATE WITH ATP AND ADP

6.1 INTRODUCTION

The object of this study was to elucidate the complexation of vanadate with ATP and ADP. Vanadate has been shown to catalyse the hydrolysis of the polyphosphate chain of these nucleotides at low pH (see Sections 1.2.2.2 and 1.2.2.3), however little is known about the structure of any complexes or intermediates. A number of PPPi complexes with vanadate have been postulated, Fig. 1.4, which could feasibly be formed by vanadate and ATP or ADP.

Fig. 6.1 shows a labelled diagram of adenosine-5'-polyphosphate. Throughout this Chapter the notation in the diagram will be used.

6.1.1 Conformation of ATP and ADP in Solution

Although the known chemistry of the interaction of V^V with ATP and ADP was discussed in the introductory chapter (see Section 1.2.2.3), no mention was made of the nucleotide structure in solution. Nearly all studies which have been undertaken use ATP or AMP and suggest nucleotide aggregation in solution.

In ATP, self-association is pH-dependent, with protonation of the adenine ring stabilising the aggregate[171]. The aggregate is a dimer at low pH,

Fig. 6.1 The structure of ATP. The notation used in this diagram is used throughout this chapter.

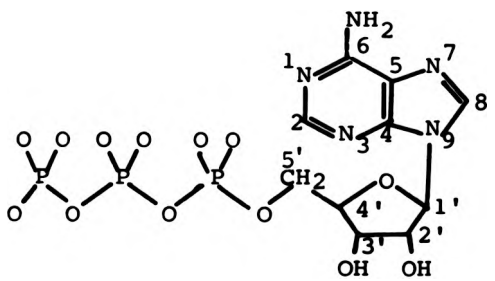

with head-to-tail base stacking. It is a relatively rigid complex, where the negatively charged phosphate of one ATP molecule interacts electrostatically with the positively charged adenine ring (from protonation) of the other ATP, Fig. 6.2. However, it has been noted that highly charged counter ions and ionic strength changes can affect the association of ATP in solution. The X-ray crystal structure[172] of the disodium salt of ATP shows an *anti* configuration along the glycosidic bond with the triphosphate group folded back towards the adenine. This crystal structure also suggests that the dimer that exists in solution also persists in the solid.

A monomer-dimer-trimer equilibrium model for base association in basic solutions has been suggested[173], but models including higher oligomers also fit the data, indicating that ATP molecules in solution can undergo indefinite linear association. The spin-lattice relaxation time, T_1, of the protons H_8, H_1' and H_2 in ATP was found to be dependent on the nucleotide concentration. This was attributed to base stacking and a value for an association constant of 5.3 ± 1.3 $dm^3\ mol^{-1}$ was obtained using the data (corrected for viscosity changes) for H_2.

Studies of AMP aggregation suggest species of higher order than a dimer[171].

Fig. 6.2 A diagramatic representation of a pair of ATP molecules showing head-to-tail base stacking of the adenine ring.

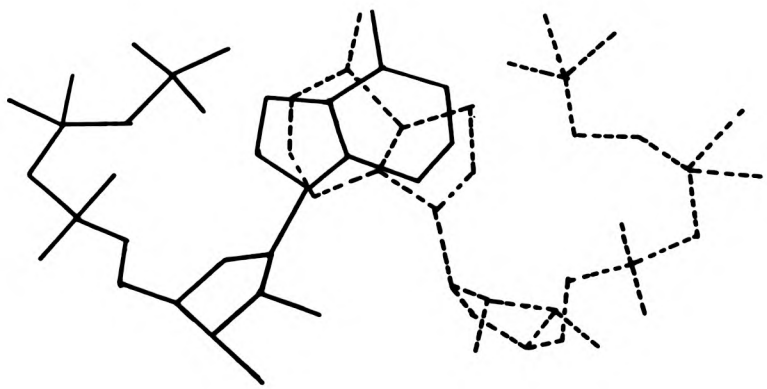

6.1.2 Interaction of Metal Ions with ATP and ADP

Throughout the study of metal-ion interactions with ATP or ADP, the phosphate groups have been suggested to be the prime site for complexation[63,66,67,174]. This probably implies the formation of a chelate with divalent cations. Although a macrochelate between the metal ion, polyphosphate group and N(7) has been postulated[174] for the species formed by ATP and Zn^{2+}. Similar observations have been made for ADP[174] and to a lesser extent AMP[175].

6.2 RESULTS AND DISCUSSION

Figs. 6.3 and 6.4 show the ^{31}P titration curves of both ATP and V^V ATP with and without 2 mol dm^{-3} $Na[ClO_4]$ present respectively. Although a change in ^{31}P chemical shift was observed at neutral pH on addition of vanadate, the largest changes were found at low pH. The size of these changes are much larger than could be due to experimental error. Therefore, V^V must be associating with ATP around the polyphosphate chain.

The curves show a smaller effect on the ^{31}P resonances from vanadate above pH 3.5 when 2 mol dm^{-3} $Na[ClO_4]$ is present. This indicates that the vanadate is probably complexing with the ATP dimer, as such an association is known to be less favoured with increasing ionic strength[171]. Hydrolysis of polyphosphate,

Fig. 6.3 ^{31}P n.m.r. (at 36.4 MHz) *versus* pH for ATP(X) and V^{V} ATP(O) in 2 mol dm^{-3} $NaClO_4$.

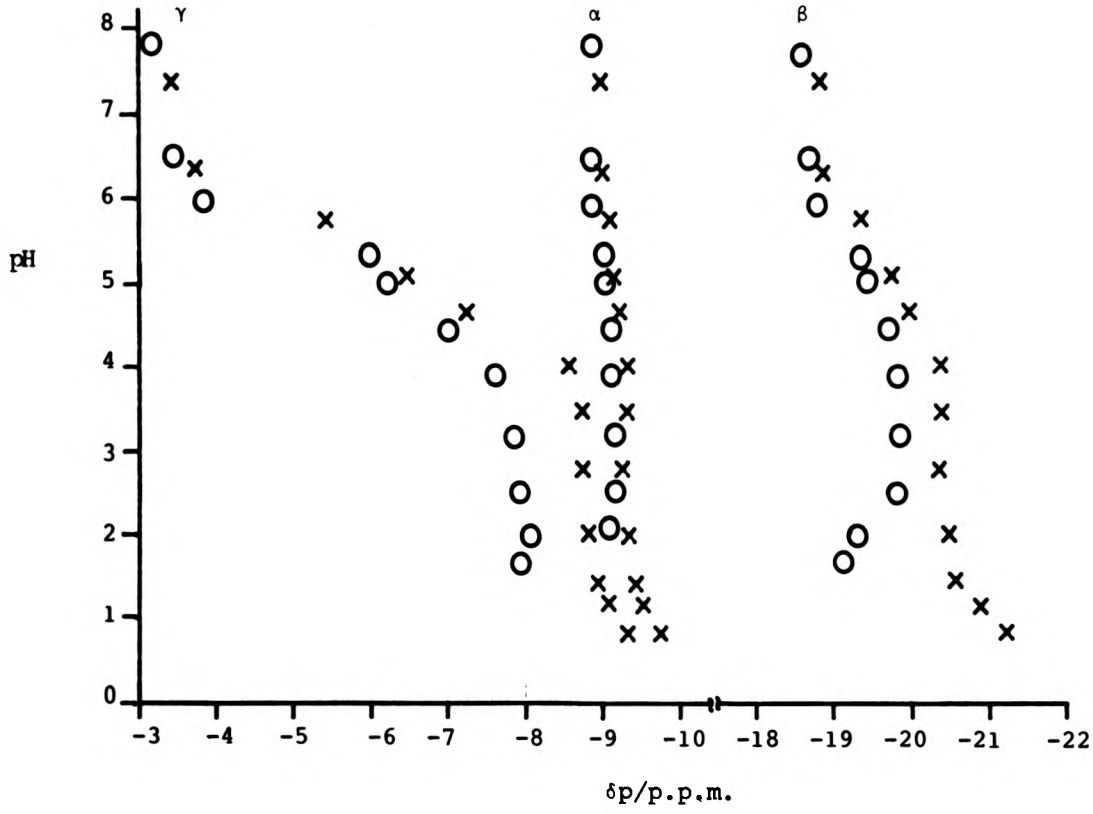

Fig. 6.4 ^{31}P n.m.r. (at 162 MHz) chemical shift *versus* pH for ATP(X), V^V ATP(O) and V^V ADP (●). No added $NaClO_4$.

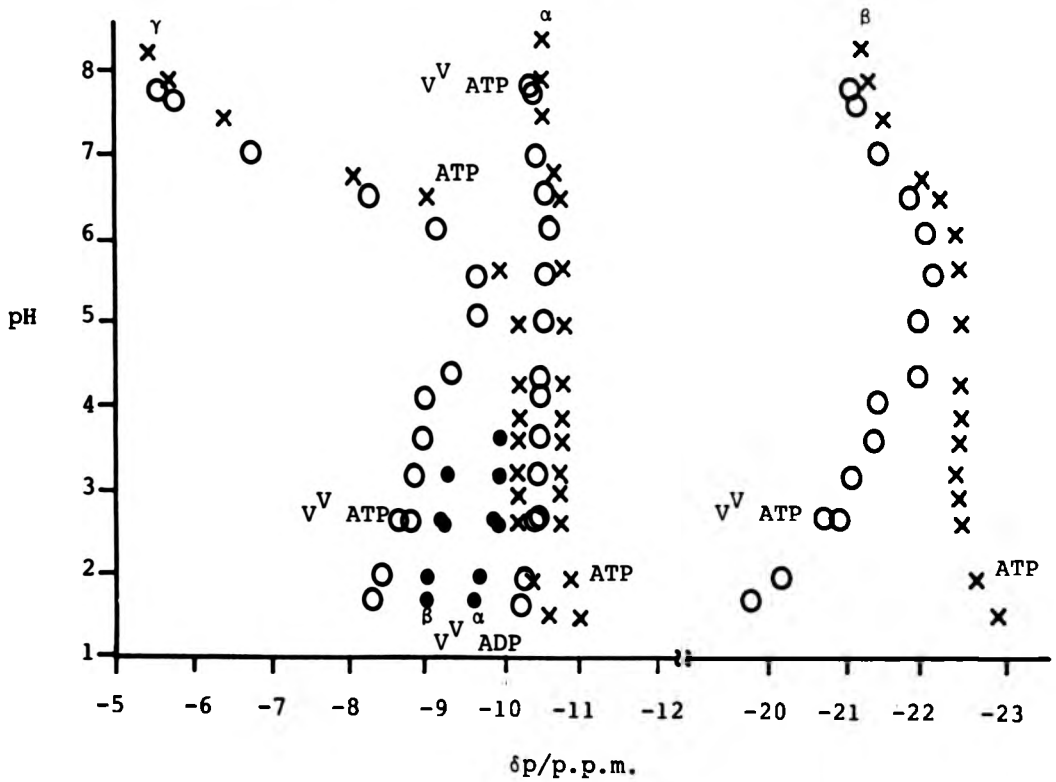

releasing $[PO_4]^{3-}$, by vanadate is known to occur at low pH[63]. Woltermann, *et al.*[63] noted that $t_{\frac{1}{2}} \approx 2$ hours for the phosphate hydrolysis at pH 2, whilst after mixing ATP or PPPi and vanadate at pH 8 no $[PO_4]^{3-}$ is found in the first 50 minutes. Thus larger effects on the ^{51}V or ^{31}P chemical shifts are expected at low pH. Over the pH range 6.5 to 2 the only vanadate species present in aqueous solution is V_{10} (Chapter 3 and refs. 14 and 25) with pKa values of 5.5 and 3.6 or 5.2 and 3.0 on the addition of 2 mol dm^{-3} $Na[ClO_4]$. An increase in the relative integral of the ^{51}V resonance from the complexed vanadate is observed on lowering the pH, Fig. 6.5. Thus, it would appear that the ATP is complexing with V^V originating from the H_2V_{10} species. This would not be expected on electrostatic grounds as both ATP and V_{10} are negatively charged (HATP has a 3- charge and HV_{10} a 4- charge). However, V_{10} is found in aqueous solution until pH 2 when it breaks down to form $[VO_2]^+$, which could complex more readily. The increase in proportion of V^V complexed to ATP between pH 2 and 3.5 coincides with an increase in V_{10} oxygen exchange rate noted by Murmann and Geise[16]. This may be due to the same breakdown mechanism that allows oxygen exchange facilitating the release of V^V from V_{10} to complex with ATP.

In addition to the titration curves for the V^V ATP complex, Fig. 6.3 indicates that ADP (and in

Fig. 6.5 Percent vanadium as the V^V ATP complex *versus* pH, from the relative integrals in ^{51}V n.m.r. spectra (no added $NaClO_4$).

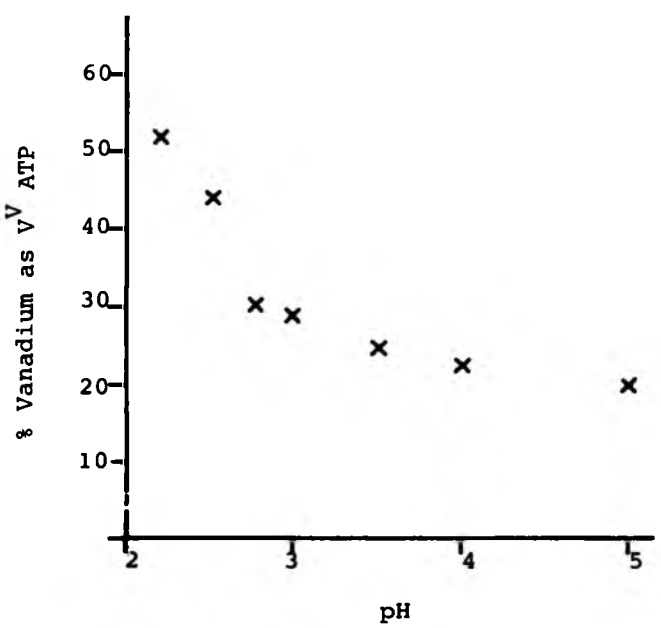

turn V^V ADP complex) and $[PO_4]^{3-}$ are formed below pH 4. From the integrals of the ^{31}P resonances a ratio of up to 1:4 of $[PO_4]^{3-}$:ATP β phosphorus can be found by the end of the titration. This ratio is in the correct range of V:P ratios where PV_{14} would be expected to be formed. However, no PV_{14} has been found during the titrations, from ^{51}V or ^{31}P n.m.r. spectra. Only when leaving a solution containing ATP and vanadate overnight was the distinctive colour of PV_{14} observed, after ATP phosphate hydrolysis. This indicated that vanadate favours complexing with the polyphosphate of ATP rather than with $[PO_4]^{3-}$.

The ^{31}P resonance of PV_{14} is sharp ($\nu_{\frac{1}{2}}$ = 5 Hz). However, on complexation with vanadate all the ^{31}P resonances from both ATP and ADP broaden excessively (e.g. each resonance of the γP doublet in ATP has a width at half height of 5 Hz, whilst the resonance from the V^V ATP complex has a width at half height of 100 Hz at pH 2.6). This suggests that a dynamic process could be taking place. Woltermann, *et al.*[63] have suggested two complexes are present when V^V hydrolyses PPPi; (i) "$[VO]^{3+}$" bound to each phosphorus *via* an oxygen bridge and (ii) $[VO_2]^+$ bound to two adjacent phosphorus. Imamura, *et al.*[64] have postulated that hydrolysis of PPPi by V^V occurs with a pentaco-ordinate terminal phosphorus intermediate bound to $[HVO_4]^-$ *via* an oxygen bridge. All three of these V^V:

polyphosphate complexes could be in equilibrium, or the vanadate moiety could be in equilibrium between the two polyphosphate chains of the dimerised ATP, or simply between bound and complexed vanadate. The first possibility would seem to be the most likely from the observed initial formation of the complex and the known conformation of the dimer.

These two observations indicate, qualitatively, that the formation constant of the V^V ATP complex is extremely large as both the V_{10} and PV_{14} polyanions are the favoured species under the similar conditions with no ATP present. The stability constants of three V^V:PPP_i complexes have been measured[62]; $[VO_2(H_2PPP_i)]^{2-}$ $(3.59 \pm 1.09) \times 10^4$ dm^3 mol^{-1}, $[VO_2(HPPP_i)]^{3-}$ $(1.34 \pm 0.49) \times 10^8$ dm^3 mol^{-1} and $[VO_2(HPPP_i)_2]^{7-}$ $(8.05 \pm 1.13) \times 10^{12}$ dm^6 mol^{-2}.

Similar observations can be made from ADP ^{31}P n.m.r. titrations, Fig. 6.6, and the increase in complexed vanadium with pH Fig. 6.7. Although AMP is not observed (the ^{31}P resonance of AMP:V is probably coincident with the α resonance of ADP).

In order to investigate the possibility of a macrochelate with vanadate bound to the polyphosphate chain and an adenine ring nitrogen, both ^{13}C and ^{1}H n.m.r. titrations were undertaken.

The ^{13}C titration curve shows no effect when vanadate is added to both ATP and ADP. However, in the case of ATP, the analogous ^{1}H n.m.r. curve, Fig. 6.8,

polyphosphate complexes could be in equilibrium, or the vanadate moiety could be in equilibrium between the two polyphosphate chains of the dimerised ATP, or simply between bound and complexed vanadate. The first possibility would seem to be the most likely from the observed initial formation of the complex and the known conformation of the dimer.

These two observations indicate, qualitatively, that the formation constant of the V^V ATP complex is extremely large as both the V_{10} and PV_{14} polyanions are the favoured species under the similar conditions with no ATP present. The stability constants of three V^V:PPP_i complexes have been measured[62]; $[VO_2(H_2PPP_i)]^{2-}$ $(3.59 \pm 1.09) \times 10^4$ dm^3 mol^{-1}, $[VO_2(HPPP_i)]^{3-}$ $(1.34 \pm 0.49) \times 10^8$ dm^3 mol^{-1} and $[VO_2(HPPP_i)_2]^{7-}$ $(8.05 \pm 1.13) \times 10^{12}$ dm^6 mol^{-2}.

Similar observations can be made from ADP ^{31}P n.m.r. titrations, Fig. 6.6, and the increase in complexed vanadium with pH Fig. 6.7. Although AMP is not observed (the ^{31}P resonance of AMP: V is probably coincident with the α resonance of ADP).

In order to investigate the possibility of a macrochelate with vanadate bound to the polyphosphate chain and an adenine ring nitrogen, both ^{13}C and ^{1}H n.m.r. titrations were undertaken.

The ^{13}C titration curve shows no effect when vanadate is added to both ATP and ADP. However, in the case of ATP, the analogous ^{1}H n.m.r. curve, Fig. 6.8,

Fig. 6.6 ^{31}P n.m.r. (at 162 MHz) chemical shift *versus* pH for ADP(X) and V^V ADP(O). No added $NaClO_4$.

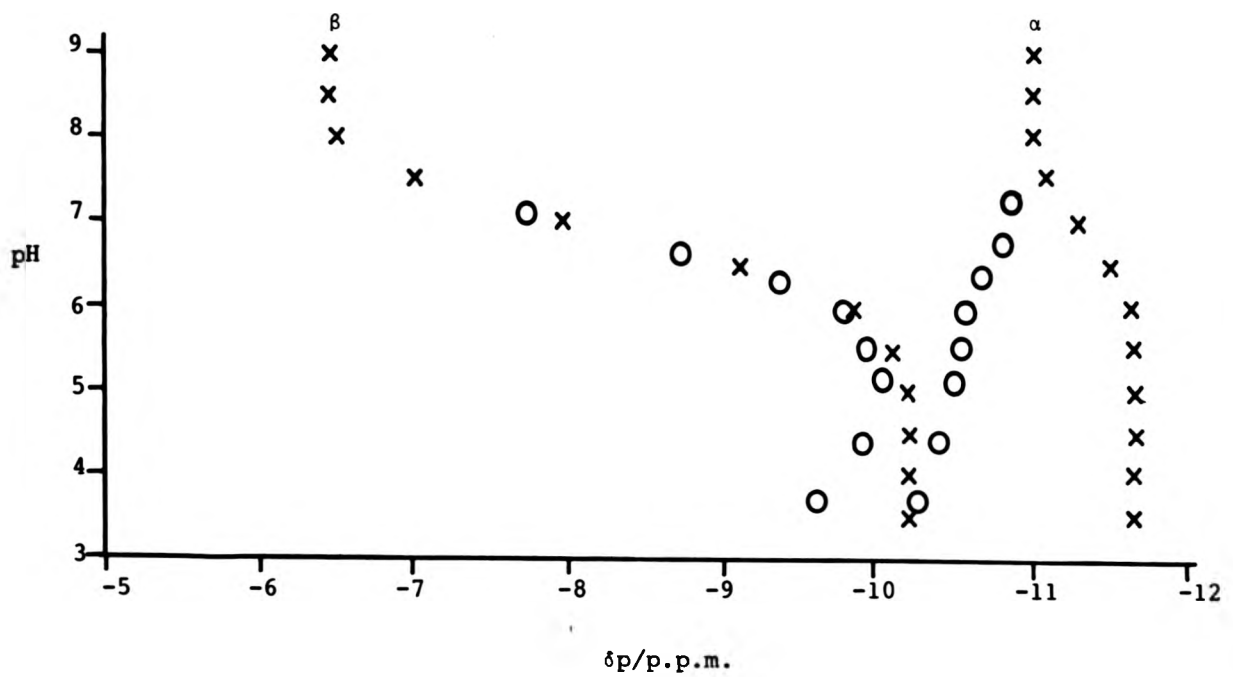

Fig. 6.7 Percent vanadium as V^V ADP *versus* pH, from the relative integrals in ^{51}V n.m.r. spectra (no added $NaClO_4$).

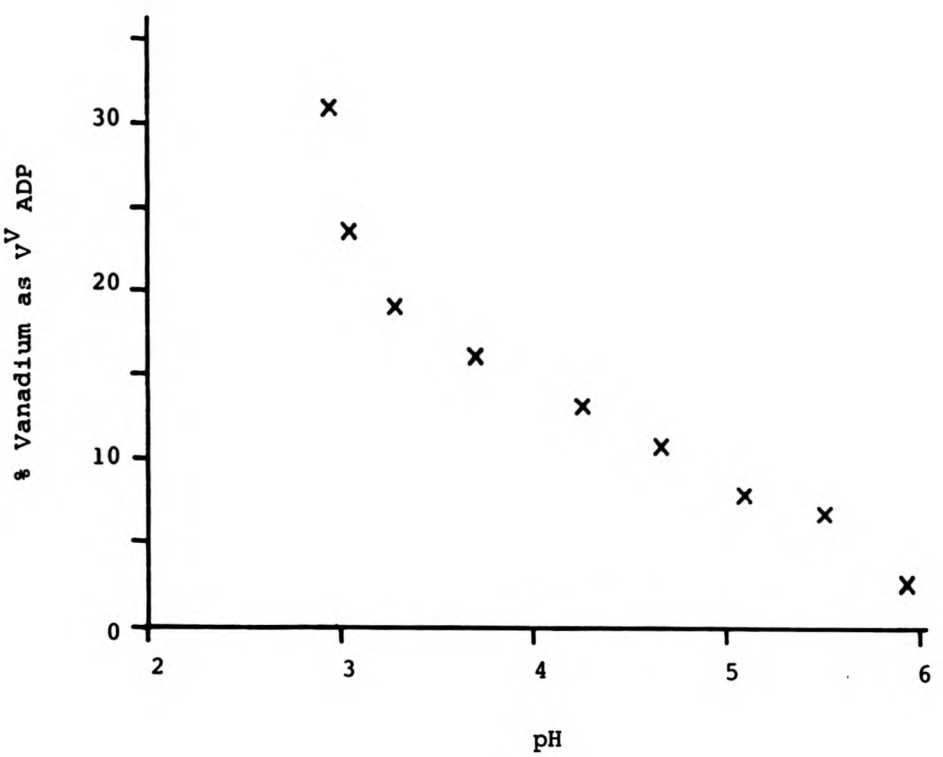

Fig. 6.8 ^{1}H n.m.r. chemical shift *versus* pD for ATP(O) and V^{V}ATP(X). No added $NaClO_4$.

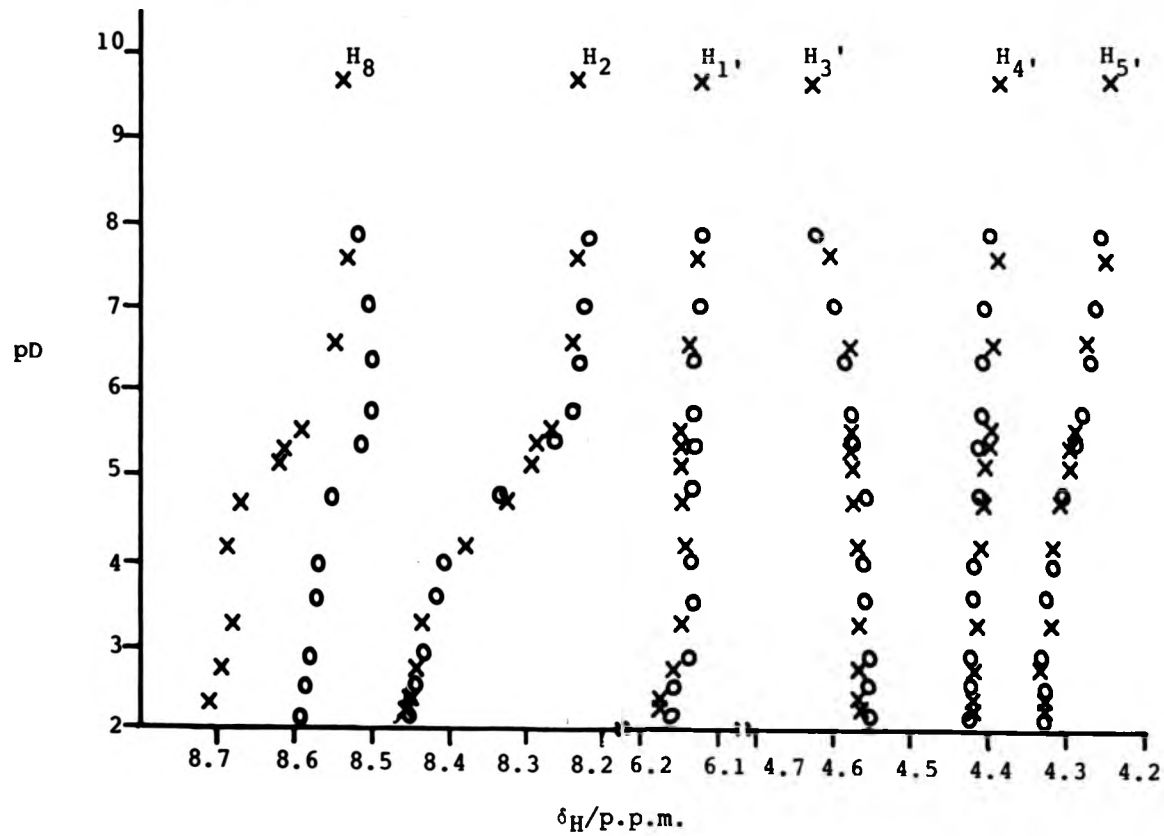

shows a broadening of the resonance due to H_8 below pD 5.3 and a shift in δ_H of $\sim$ 0.1 p.p.m. at pD 2. The electrostatic interaction between the polyphosphate chain and adenine, in the dimer (see Section 6.1.1) brings the complexed vanadate into the proximity of H_8.

In the ^{51}V spectra, above pH 5 a signal can be seen for the complexed vanadate at δ_V = -560 p.p.m., which shifts to high frequency, -543 p.p.m., on lowering the pH (coincident with the $[VO_2]^+$ resonance). The resonance due to the V^V ATP complex is broad with a width at half height of 1250 Hz. This suggests a $[VO_2]^+$ moiety may be the V^V group in the complex at low pH.

In the range pH 6-7 in the ^{31}P n.m.r. titration of ADP, two doublets of low but equal intensity (no more than 10% of either of the ADP resonances) were observed at -9.27 (pH dependent) and -9.95 (pH independent) at pH 6. These may be due to a complex between ADP and a polyvanadate species or monomeric vanadate and more than one ADP molecule. Due to overlap in the ^{31}P spectra the study of these resonances was limited, but their presence was noted.

6.3 CONCLUSIONS

V^V readily complexes with ATP and ADP, binding to the polyphosphate chain probably as $[VO_2]^+$ bridging

two terminal phosphates and forming a weak hydrogen bond with H_8 on the adenine ring in ATP. Exchange between three possible complexes, Fig. 1.4, (with one an intermediate in phosphate hydrolysis) may be taking place.

6.4 EXPERIMENTAL

Biochemical grade ATP and ADP were dissolved in solution without further purification. Throughout the study the concentration of either ATP or ADP did not exceed 0.07 mol dm^{-3} due (i) to their known interaction with sodium 2,2-dimethyl-2-silapentane-5-sulphate (DSS) added as a reference for ^{1}H and ^{13}C n.m.r.[176]; and (ii) to limit aggregation *via* base stacking[171,173]. Up to two equivalents of vanadate solution were added to ATP and ADP solutions. To minimise ionic strength variations all measurements were performed in the presence of 2 mol dm^{-3} $Na[ClO_4]$ unless otherwise noted. All pH variation was undertaken using concentrated NaOH and $HClO_4$ except for measurement of ^{1}H n.m.r. spectra, when concentrated DCl and Na[OD] in D_2O were used. All n.m.r. measurements were made at 295 K.

^{1}H n.m.r. spectra were obtained at 400 MHz by accumulation of 32 transients, with a sweep width of 6 KHz and a pulse length of 4 μs ($\sim 45^{o}$ flip angle).

^{13}C spectra at 105.2 MHz were similarly recorded but required the accumulation of 2000 transients, a sweep width of 25 KHz and a pulse length of 12 μs (∿ 40^{o} flip angle). In both cases 32 K data points were used to record the FID.

^{51}V n.m.r. spectra at 105.2 MHz required the accumulation of between 200 and 2000 transients, with a sweep width of 40 KHz and a pulse length of 12 μs (∿ 45^{o} flip angle).

^{31}P n.m.r. spectra were obtained at both 162 and 36.4 MHz using Bruker WH400 and WH90 n.m.r. spectrometers respectively. When using the WH400 a sweep width of 10 KHz and a pulse length of 15 μs (∿ 55^{o} flip angle) were employed, and analogous parameters for the WH90.

SOME CONSIDERATIONS FOR FURTHER WORK

(a) Polyanions

The assignment of the three ^{51}V resonances from the V_{10} anions was accomplished by ^{17}O $\{^{51}V\}$ n.m.r. experiments[9]. However, recording ^{17}O n.m.r. spectra with ^{51}V decoupling for PV_{14} would be of little value in confirming the assignment of $O_{E(1,2)}/O_{P(1,2)}$ and $O_{E(Cap)}/O_{P(Cap)}$ as (i) $V_{(3)}$ is bound to both $O_{E(1,2)}$ and $O_{P(1,2)}$, (ii) $V_{(1)}$ and $V_{(2)}$ (both of which give the same ^{51}V resonance) are bound to both $O_{E(1,2)}$ and $O_{P(1,2)}$, and (iii) $V_{(1)}$ and $V_{(2)}$ are each bound to $O_{E(Cap)}$ and $O_{P(Cap)}$.

Further evidence of change of the MÔM bond angle and pH on ^{17}O chemical shift could be obtained by recording the ^{17}O spectra (and ^{17}O n.m.r. pH titrations) of isopoly and heteropolymolybdates and tungstates.

(b) Peroxide Complexes

The work undertaken in this project yielded information to allow the elucidation of the peroxovanadate equilibria. However, few of these species have been isolated. Confirmation of the octahedral configuration around V^V would be possible by X-ray crystallography if a suitable sample could be prepared.

(c) Sulphide Complexes

Further work on V^V sulphide complexes could

be undertaken to isolate the (*S11*) dimer or to find specific preparation of V^V species with catenated sulphide ligands. Mo complexes with polysulphide ligands[85] have been prepared by various reactions, e.g. (i) $[MoS_4]^{2-}$ with sulphur, (ii) $[MoS_4]^{2-}$ with organic disulphides or (iii) by reaction of $[MoO_4]^{2-}$ with $[NH_4]_2\ S_x$. As $[MoS_4]^{2-}$ can be prepared from $[MoO_4]^{2-}$ and H_2S[177] (in a similar manner to preparing (*S7*), from vanadate, Section 2.4.3.1.1), polysulphide V^V species may possibly be found in an analogous manner.

(d) ADP and ATP Complexes with V^V

From the data obtained in this project it seems likely $[VO_2]^+$ bound to two adjacent phosphorus atoms *via* oxygen bridges is the preferred complex with polyphosphates. However, this species is in equilibrium with the two other possible complexes, Fig. 1.4. If the linewidth of the ^{31}P resonances of the preferred complex were found (by reducing the exchange on cooling), then the exchange between the three complexes could be studied from the excess linewidth.

REFERENCES

1. F. A. Cotton and G. Wilkinson, "Advanced Inorganic Chemistry. A Comprehensive Text", p689, 4th Edition John Wiley, 1980

2. D. A. Rice, *Coord. Chem. Rev.*, 1982, 45, 67

3. E. M. Page, *Coord. Chem. Rev.*, 1984, 57, 237

4. H. T. Evans, Jr., *Inorg. Chem.*, 1966, 5, 967

5. A. G. Swallow, F. R. Ahmed and W. H. Barnes, *Acta Cryst.*, 1966, 21, 397

6. P. A. Durif, M. T. Averbuch-Pouchot and J. C. Guitel, *Acta Cryst.*, 1980, 36B, 680

7. T. Debaerdemaeker, J. M. Arrieta and J. M. Amigo, *Acta Cryst.*, 1982, 38B, 2465

8. H. T. Evans, Jr., and M. T. Pope, *Inorg. Chem.*, 1984, 23, 501

9. C. J. Besecker, W. G. Klemperer, D. J. Maltbie and D. A. Wright, *Inorg. Chem.*, 1985, 24, 1027

10. O. W. Howarth and R. E. Richards, *J. Chem. Soc.*, 1965, 864

11. N. Ingri and F. Brito, *Acta Chem. Scand.*, 1959, 13, 1971

12. M. T. Pope and B. W. Dale, *Q. Rev. Chem. Soc.*, 1968, 22, 527

13. J. V. Hatton, Y. Saito and G. W. Schneider, *Can. J. Chem.*, 1965, 43, 47

14. O. W. Howarth and M. Jarrold, *J. Chem. Soc., Dalton Trans.*,1978, 503

15. W. G. Klemperer and W. Shum, *J. Amer. Chem. Soc.*, 1977, 99, 3544

16. R. K. Murmann and K. C. Geise, *Inorg. Chem.*, 1978, 17, 1160

17. B. W. Clare, D. L. Kepert and D. W. Watts, *J. Chem. Soc., Dalton Trans.*, 1973, 2479 and 2481

18. F. Corigliano and S. Di Pasquale, *J. Chem. Soc., Dalton Trans.*, 1978, 1329

19. D. M. Druskovitch and D. L. Kepert, *J. Chem. Soc., Dalton Trans.*, 1975, 947

20. S. Ostrowetsky, *Bull. Chim. Soc. France*, 1964, 1018

21. M. T. Pope, "Isopoly and Heteropoly Oxometallates", Chapter 6, p101, Springer-Verlag, 1983

22. E. Sh Ganelina, S. A. Borgoyakov and V. P. Pak, *Russ. J. Inorg. Chem.*, 1984, 29, 51

23. C. Madic, G. M. Begun, R. L. Hahn, J. P. Launey and W. E. Thiesse, *Inorg. Chem.*, 1984, 23, 469

24. M. A. Habayeb and O. E. Hileman, Jr., *Can. J. Chem.*, 1980, 58, 2255

25. E. Heath and O. W. Howarth, *J. Chem. Soc., Dalton Trans.*, 1981, 1105

26. L. Pettersson, B. Hedman, I. Andersson and N. Ingri, *Chem. Scripta*, 1983, 22, 254

27. K. H. Tytko and J. Mehmke, *Z. Anorg. Allg. Chem.*, 1983, 503, 67

28. C. Heitner-Wirguin and J. Selbin, *J. Inorg. Nucl. Chem.*, 1968, 30, 3181

29. A. Bino, S. Cohen and C. Heitner-Wirguin, *Inorg. Chem.*, 1982, 21, 429

30. Y. Kera, *Bull. Chem. Soc. Japan*, 1984, 57, 1478

31. H. Mimoun, *Israel J. Chem.*, 1983, 23, 451

32. F. Di Furia, G. Modena, R. Curci, S. J. Bachofer, J. O. Edwards, and M. Pomerantz, *J. Mol. Catal.*, 1982, 14, 219

33. F. A. Cotton and G. Wilkinson, "Advanced Inorganic Chemistry. A Comprehensive Text", p699, 735, 4th Edition, John Wiley, 1980

34. M. Orhanović and R. G. Wilkins, *J. Amer. Chem. Soc.*, 1967, 89, 278

35. J. A. Connor and E. A. V. Ebsworth, *Adv. Inorg. Chem. Radiochem.*, 1965, 6, 292

36. F. Chauveau, *Bull. Soc. Chim. France*, 1960, 819

37. P. Souchay and F. Chauveau, *Compt. Rend.*, 1957, 245, 1434

38. O. W. Howarth and J. R. Hunt, *J. Chem. Soc., Dalton Trans.*, 1979, 1388

39. I-B. Svensson and R. Stomberg, *Acta Chem. Scand.*, 1971, 25, 898

40. R. Stomberg, S. Olson and I-B. Svensson, *Acta Chem. Scand.*, 1984, 38A, 653

41. K. Wieghardt and U. Quilitzsch, *Z. Naturforsch*, 1979, 34B, 242

42. P. Schwendt, *Coll. Czech. Chem. Comm.*, 1983, 48, 248

43. P. Schwendt, P. Petrovic and D. Úskert, *Z. Anorg. Allg. Chem.*, 1980, 466, 232

44. P. Schwendt and D. Úskert, *Chem. Zvesti.*, 1981, 35, 229

45. F. Secco, *Inorg. Chem.*, 1980, 19, 2722

46. G. A. Dean, *Can. J. Chem.*, 1961, 39, 1174

47. U. Quilitzsch and K. Wieghardt, *Inorg. Chem.*, 1979, 18, 869

48. R. C. Thompson, *Inorg. Chem.*, 1982, 21, 859

49. R. C. Thompson, *Inorg. Chem.*, 1983, 22, 584

50. M. T. Pope,
"Heteropoly and Isopoly Oxometallates", p31, 58
Springer-Verlag, 1983

51. V. W. Day and W. G. Klemperer,
Science, 1985, 228, 533

52. F. Preuss and H. Schug,
Z. Naturforsch., 1976, 31B, 1585 and
references therein

53. R. Kato, A. Kobayashi and Y. Sasaki,
Inorg. Chem., 1982, 21, 240

54. M. A. Fedotov, R. T. Maksimovskaya and
L. P. Kazanskii,
React. Kinet. Catal. Lett., 1981, 16, 185

55. M. Filowitz, R. K. C. Ho, W. G. Klemperer
and W. Shum,
Inorg. Chem., 1979, 18, 93

56. W. G. Klemperer,
Angew Chem. Int. Ed. Engl., 1978, 17, 246

57. K. F. Miller and R. A. D. Wentworth,
Inorg. Chem., 1979, 18, 984

58. R. G. Kidd,
Can. J. Chem., 1967, 45, 605

59. H. R. Tietze,
Aust. J. Chem., 1981, 34, 2035

60. J. W. Johnson, D. C. Johnston, A. J. Jacobson
and J. F. Brody,
J. Amer. Chem. Soc., 1984, 106, 8123
and rererences therein

61. S. P. Moulik, B. N. Ghosh and D. K. Mullick,
J. Ind. Chem. Soc., 1963, 40, 743

62. A. A. Ivakin and L. D. Kurbatova,
Russ. J. Inorg. Chem., 1984, 29, 1450

63. G. M. Woltermann, R. L. Belford and
G. P. Haight,Jr.,
Inorg. Chem., 1977, 16, 2985

64. T. Imamura, D. M. Hinton, R. L. Belford,
R. I. Gumport and G. P. Haight,Jr.,
J. Inorg. Biochem., 1979, 11, 241

65. B. S. Cooperman,
"Metals in Biological Systems", Vol. 5,
Ed. H. Siegel, Marcel Dekker, 1976,
and references therein

66. R. D. Prigodich and P. Haake,
Inorg. Chem., 1985, **24**, 89
and references therein

67. K. V. Vasavada, B. D. Ray and
B. D. Nageswara Rao,
J. Inorg. Biochem., 1984, **21**, 323
and references therein

68. Y.-J. Shyy, T. C. Tsai and M.-D. Tsai,
J. Amer. Chem. Soc.,1985, **107**, 3478
and references therein

69. D. W. Hutchinson, M. Naylor and P. M. Cullis,
Antiviral Research, 1985, **5**, 67

70. N. D. Chasteen,
Struct. Bonding, 1983, **53**, 105

71. A. Müller, E. Diemann, R. Jostes
and H. Bögge,
Angew Chem. Int. Ed. Engl., 1981, **20**, 934

72. A. Müller, A. C. Ranade and V. V. K. Rao,
Spectrochim. Acta, 1971, **27A**, 1973

73. A. Müller and E. Diemann,
Chem. Ber., 1969, **102**, 945

74. C. Crevecoeur,
Acta Cryst., 1964, **17**, 757

75. K. D. Becker and U. Berlage,
J. Mag. Res., 1983, **54**, 272

76. A. Müller, K. H. Schmidt, K. H. Tytko,
J. Bouwma and F. Jellinek,
Spectrochim. Acta, 1972, **28A**, 381

77. F. Hullinger,
Helv. Phys. Acta, 1961, **34**, 379

78. J. M. van den Berg and R. de Vries,
Proc. K. Ned. Akad. Wet., 1964, **67B**, 178

79. H. Schäfer, P. Moritz and A. Weiss,
Z. Naturforsch., 1965, **20B**, 603

80. A. C. Ranade, A. Müller and E. Diemann, *Z. Anorg. Allg. Chem.*, 1970, 373, 258

81. E. Diemann and A. Müller, *Spectrochim. Acta*, 1970, 26A, 215

82. A. Müller and E. Diemann, *Chem. Phys. Lett.*, 1971, 9, 369

83. S. S. L. Surana, S. P. Tandon, W. O. Nolte and A. Müller, *Can. J. Spectrosc.*, 1979, 24, 18

84. E. Diemann and A. Müller, *Z. Anorg. Allg. Chem.*, 1978, 444, 181

85. Y. Do, E. D. Simhon and R. H. Holm, *Inorg. Chem.*, 1985, 24, 1831 and references therein

86. F. A. Cotton and G. Wilkinson, "Advanced Inorganic Chemistry. A Comprehensive Text", p712, 4th Edition, John Wiley, 1980

87. R. C. Hibbert, *J. Chem. Soc., Chem. Comm.*, 1985, 317

88. J. Hanich, M. Krestel, U. Müller, K. Dehnicke and D. Rehder, *Z. Naturforsch.*, 1984, 39B, 1686

89. M. N. Mookerjee, R. V. Singh and J. P. Tandon, *Transition Met. Chem.*, 1985, 10, 66

90. A. A. Konovalova, S. V. Bainova, V. D. Kopanev and Y. A. Buslaev, *Koord. Khim.*, 1982, 8, 1211

91. M. Hoch, D. Rehder and C. Weidemann, *Inorg. Chim. Acta*, 1984, 92, L5

92. A. A. Konovalova, S. V. Bainova, V. D. Kopanev and Y. A. Buslaev, *Koord. Khim.*, 1982, 8, 1364

93. F. Preuss, W. Towae and J. Woitschach, *Z. Naturforsch.*, 1980, 35B, 817

94. W. Priebsch and D. Rehder, *Inorg. Chem.*, 1985, in press

95. A. J. Edwards and P. Taylor,
J. Chem. Soc., Chem. Comm., 1970, 1474

96. A. G. Sharpe and A. A. Woolf,
J. Chem. Soc., 1951, 798

97. J. V. Hatton, Y. Saito and W. G. Schneider,
Can. J. Chem., 1965, 43, 47

98. G. W. Bushnell and K. C. Moss,
Can. J. Chem., 1972, 50, 3700

99. U. R. K. Rao, K. S. Venkateswarh,
B. R. Wani, M. S. Sastry, A. G. I. Dalvi
and B. D. Joshi,
Mol. Phys., 1982, 47, 637

100. R. J. Gillespie and U. R. K. Rao,
J. Chem. Soc., Chem. Comm., 1983, 422

101. G. Pausewang and K. Dehnicke,
Z. Anorg. Allg. Chem., 1969, 369, 265

102. R. R. Ryan, S. H. Mastin and M. J. Reisfeld,
Acta Cryst., 1971, 27B, 1270

103. M. K. Chaudhuri and S. K. Ghosh,
Inorg. Chem., 1984, 23, 534

104. R. Stomberg,
Acta Chem. Scand., 1984, 38A, 223

105. R. Stomberg and S. Olson,
Acta Chem. Scand., 1984, 38A, 821

106. R. Stomberg and S. Olson,
Acta Chem. Scand., 1984, 38A, 801

107. G. V. Jere, M. K. Gupta, L. Surendra
and S. M. Kaushik,
Thermochim. Acta, 1982, 58, 67

108. D. Joniaková and P. Schwendt,
Acta Fac. Rerum. Nat. Univ. Comen.-Chimia,
1984, 32, 93

109. P. Schwendt and D. Joniaková,
Polyhedron, 1984, 3, 287

110. P. Schwendt and D. Joniaková,
Proc. Conf. on Coord. Chem., 9th May 1983,
Smolenice, p367

111. P. Schwendt and D. Joniaková,
Thermochim. Acta, 1983, 68, 297

112. R. Stomberg,
Acta Chem. Scand., 1984, **38A**, 541

113. M. K. Chaudhuri and S. K. Ghosh,
Inorg. Chem., 1982, **21**, 4020

114. E. A. Maatta,
Inorg. Chem., 1984, **23**, 2560

115. F. Preuss, W. Towae, V. Kruppa and E. Fuchslocher,
Z. Naturforsch, 1984, **39B**, 1510

116. W. Witke, A. Lachowicz, W. Brüser and D. Zeigan,
Z. Anorg. Allg. Chem., 1980, **465**, 193

117. F. Preuss, E. Fuchslocher and W. Towae,
Z. Naturforsch., 1984, **39B**, 61

118. G. Gattow and H. Savin,
Z. Anorg. Allg. Chem., 1982, **492**, 69

119. A. V. Korzhak and S. Ya Kuchmii,
Russ. J. Inorg. Chem., 1984, **29**, 402

120. F. Salinas, M. Jiménez-Arrabel and I. Durán,
Bull. Soc. Chim. Belges, 1985, **94**, 101

121. L. Banci, A. Bencini, A. Dei and D. Gatteschi,
Inorg. Chim. Acta, 1984, **84**, L11

122. K. Wieghardt,
Inorg. Chem., 1978, **17**, 57

123. R. Matte, A. Preuss and K.-L. Richter,
Z. Naturforsch., 1984, **39B**, 1331

124. N. Vuletić and C. Djordjević,
J. Chem. Soc., Dalton Trans., 1973, 1137

125. N. J. Campbell, M. V. Cappavelli, W. P. Griffiths and A. C. Skapski,
Inorg. Chim. Acta, 1983, **77**, L215

126. H. Szentivanyi and R. Stomberg,
Acta Chem. Scand., 1983, **37A**, 553

127. R. Stomberg and H. Szentivanyi,
Acta Chem. Scand., 1984, **38A**, 121

128. H. Mimoum, L. Saussune, E. Daire, M. Postel, J. Fischer and R. Weiss,
J. Amer. Chem. Soc., 1983, **105**, 3101

129. S. Funahashi, K. Ishihara and M. Tanaka, *Inorg. Chem.*, 1981, 20, 51

130. S. Funahashi, K. Haraguchi and M. Tanaka, *Inorg. Chem.*, 1977, 16, 1349

131. R. E. Drew and F. W. B. Einstein, *Inorg. Chem.*, 1973, 12, 829

132. C. Djordjevic, S. A. Craig and E. Sinn, *Inorg. Chem.*, 1985, 24, 1283

133. H. Mimoun, P. Chaumette, M. Mignard, L. Saussune, J. Fischer and R. Weiss, *Nouveau J. de Chem.*, 1983, 7, 467

134. P. Kalidoss and V. S. Srinivasan, *J. Chem. Soc., Dalton Trans.*, 1984, 2631

135. R. N. Mehrotra, *Can. J. Chem.*, 1985, 63, 663

136. M. T. Pope, "Isopoly and Heteropolymetallates", p4, Springer-Verlag, 1983

137. G. Jander and K. F. Jahr, *Z. Anorg. Allg. Chem.*, 1933, 212, 1

138. A. W. Naumann and C. J. Hallada, *Inorg. Chem.*, 1964, 3, 70

139. F. J. C. Rossotti and H. Rossotti, *Acta Chem. Scand.*, 1956, 10, 957

140. N. Ingri and F. Brito, *Acta Chem. Scand.*, 1959, 13, 1971

141. F. Brito, N. Ingri and L. Sillen, *Acta Chem. Scand.*, 1964, 18, 1557

142. G. Newmann, *Acta Chem. Scand.*, 1964, 18, 278

143. J. Aveston, E. W. Anacker and L. S. Johnson, *Inorg. Chem.*, 1964, 3, 735

144. L. Newmann, W. J. La Fleur, F. J. Brousaiches and A. M. Ross, *J. Amer. Chem. Soc.*, 1958, 80, 4491

145. K. Schiller and E. Thilo, *Z. Anorg. Allg. Chem.*, 1961, 310, 261

146. W. P. Griffiths and P. J. B. Lesniak,
J. Chem. Soc., A, 1969, 1066

147. A. Carrington and A. D. McLachlan,
"Introduction to Magnetic Resonance",
Harper International Edition, 1967

148. R. M. Lynden-Bell and R. K. Harris,
"Nuclear Magnetic Resonance Spectroscopy",
Nelson, 1969

149. R. K. Harris,
"Nuclear Magnetic Resonance Specqroscopy -
A Physicochemical View", Pitman, 1983

150. E. Fukushima and S. B. W. Roeder,
"Experimental Pulse N.M.R.: A Nuts and
Bolts Approach" p50,
Addison-Wesley, 1981

151. O. W. Howarth,
personal communication

152. A. G. Ferridge and L. C. Linden,
J. Magn. Res., 1978, 31, 337

153. Z. M. Galbács and L. J. Csányi,
J. Chem. Soc., Dalton Trans., 1983, 2353

154. A. I. Vogel,
"Textbook of Quantitative Inorganic Analysis",
4th Edition, 1978, p355
Longman

155. A. Busine and G. Tridot,
Bull. Soc. Chim. France, 1961, 1383

156. R. G. Bates,
"Determination of pH. Theory and Practice"
2nd Edition, 364, 293,
John Wiley, 1973

157. P. K. Glasoe and F. A. Long,
J. Phys. Chem., 1960, 64, 188

158. D. G. Gadian, G. K. Radda, R. E. Richards
and P. J. Seeley,
"Biological Applications of Magnetic
Resonance", p470, Ed. R. G. Shulman,
Academic Press, 1979

159. J. Mason
Chem. Rev., 1981, **81**, 205

160. F. A. Cotton and G. Wilkinson
"Advanced Inorganic Chemistry. A Comprehensive Text", p713, 4th Edition, John Wiley, 1980

161. H. Szentivanyi and R. Stomberg
Acta Chem. Scand., 1984, **38A**, 101

162. A. Moharum, R. C. Hibbert, N. Logan and O. W. Howarth,
J. Chem. Soc., Dalton Trans., in press

163. A. Müller, E. Diemann and A. C. Ranade
Chem. Phys. Lett., 1969, **3**, 467

164. G. A. Morris and R. Freeman
J. Mag. Res., 1978, **29**, 433

165. F. A. Cotton and G. Wilkinson
"Advanced Inorganic Chemistry. A Comprehensive Text", p174-180, 4th Edition
John Wiley, 1980

166. E. D. Simhon, N. C. Baenziger, M. Kanatzidis, M. Draganjac and D. Coucouvanis
J. Amer. Chem. Soc., 1981, **103**, 1218

167. M. Draganjac, E. Simhon, L. T. Chan, M. Kanatzidis, N. C. Baenziger and D. Coucouvanis
Inorg. Chem., 1982, **21**, 3321

168. A. Müller, R. G. Battacharyya and B. Pfefferkorn
Chem. Ber., 1979, **112**, 778

169. D. Rehder
Mag. Res. Rev., 1984, **9**, 125

170. C. J. Jameson and H. S. Gutowsky
J. Chem. Phys., 1964, **40**, 1714

171. T. J. Gilligan III and G. Schwarz
Biophys. Chem., 1976, **4**, 55 and references therein

172. O. Kennard, N. W. Isaacs, J. C. Coppola, A. J. Kirby, S. Warren, W. D. S. Motherwell, D. G. Watson, W. L. Wampler, D. H. Chenery, A. C. Larson, K. A. Kerr and L. Riva di Sansererino
Nature, 1970, **225**, 333

173. Y-F. Lam and G. Kotowycz
Can. J. Chem., 1977, 55, 3620

174. M. Cohn and T. R. Hughes, Jr.
J. Biol. Chem., 1962, 237, 176 and references therein

175. M. Razka
Biochemistry, 1974, 13, 4616 and references therein

176. Y-F. Lam and G. Kotowycz
F.E.B.S. Letters, 1977, 78, 181

177. J. W. McDonald, G. D. Friesen, L. D. Rosenheim and W. E. Newton
Inorg. Chim. Acta, 1983, 72, 205